



universität
wien

DIPLOMARBEIT

Titel der Diplomarbeit

Zelluläre Effekte von Inoloquinolin-Komplexen und
verwandten Verbindungen auf menschliche
Tumorzelllinien

Verfasserin

Simone Göschl

angestrebter akademischer Grad

Magistra der Naturwissenschaften (Mag. rer. nat.)

Wien, 2011

Studienkennzahl lt. Studienblatt:

A 419

Studienrichtung lt. Studienblatt:

Diplomstudium Chemie

Betreuerin / Betreuer:

o. Univ.-Prof. Dr. Dr. Bernhard Keppler



universität
wien

DIPLOMA THESIS

Title

Cellular effects of indoloquinoline complexes and
related compounds in human tumor cell lines

Author

Simone Göschl

Supervisor

o. Univ.-Prof. Dr. Dr. Bernhard Keppler

Vienna 2011

To my family

Acknowledgement

I would like to thank o.Univ.-Prof. Dr. Dr. Keppler for giving me the opportunity to work in this research field and to carry out my diploma thesis.

Dr. Michael Jakupec for his management, support, ideas, critical discussions and the proof reading of this diploma work.

Ao. Univ.-Prof. Dr. Arion for his financial support.

Mag. Elfriede Limberger for her help in all administrative affairs.

My colleagues, Robert, Anton, Maria, Caro, Mahsa, Gerhard, Michaela and Mojtaba for the good atmosphere, conversations, support and offside activities.

Michael and Lukas for the preparation of the substances, the good communication and intensive work, but also for nice evenings.

Verena and Markus for proof reading, the good atmosphere during the whole study, the intensive learning hours in the coffee house, some nice evenings and all the fun we had together.

Prof. Dr. Franz Scherr for arousing my interest in chemistry.

My scout friends, especially Martina and Felicitas, who are showing me again and again a world outside from chemistry.

Klaus, my brother, for nice discussions in chemistry, but even more that he is just my brother and being there for me when I need him.

Alex, for all the years spending together, supporting me and everything else that I cannot mention all.

My parents for supporting me in every situation of my whole life.

Abstract

Cancer diseases causes 7.6 million deaths worldwide per year, and the number of affected persons and deaths are increasing steadily.

Treatment of cancer consists of three mainstays: surgery, radiotherapy and chemotherapy. At the moment, platinum(II) complexes are the only metal-based drugs in cancer chemotherapy, but also other complexes with a different metal center have a high potential as antitumor agents, such as ruthenium that has the ability to mimic iron, as well as osmium or copper that plays an important role in biological systems. The combination of metals with biologically active ligands can improve the cytotoxic profile, e.g. by an increase of drug uptake or a decrease of side effects.

In this work, a range of complexes of copper, ruthenium and osmium with indoloquinolines as biologically active ligands were tested for their cytotoxicity. Indoloquinolines have a planar structure and are known for their high potential to intercalate into DNA. Therefore cell cycle and DNA intercalation studies were performed to obtain information about the behavior of the compounds in biological environment. The aim of this work was to find structure-activity relationships and to gain insight into the mode of action of the examined compounds.

Cytotoxicity was determined by the colorimetric MTT assay in three different cell lines: A549 (non-small cell lung cancer), CH1 (ovarian carcinoma) and SW480 (colon carcinoma). The chosen cell lines have different sensitivities against chemotherapeutics in clinical use. A549 is a multidrug-resistant cell line, whereas CH1 is sensitive to a broad variety of drugs. Comparison with the new complexes enables conclusions about resistance mechanisms.

All tested copper compounds show strong cytotoxic effects in all three cell lines, with some IC_{50} values down to the nM range, whereas ruthenium and osmium compounds were less active.

Cell cycle studies were performed to determine the influence of some copper based compounds of the cell cycle, such as arrest in a defined phase. Due to the planar indoloquinoline moiety, DNA intercalation was studied as a potential mode of action. However, no effects on the cell cycle and no intercalating properties in the methyl green assay were found.

Western blotting was used verify to apoptosis induction by the new copper complexes, by using cleavage of the caspase substrate PARP as an indicator for apoptosis. Indeed, increasing concentrations of the studied compounds resulted in increasing cleavage of PARP.

Zusammenfassung

Krebs ist eine Erkrankung, deren Anzahl an betroffenen Personen und Todesfällen stetig steigt. Mittlerweile sterben weltweit bereits 7,6 Millionen Menschen pro Jahr.

Die Krebstherapie besteht aus drei Hauptsäulen, chirurgisch Therapie, Radiotherapie und Chemotherapie. Metall-Komplexe gehören zu einer der unterschiedlichen Substanzklassen in der Chemotherapie. Zytostatika auf Platinbasis sind bereits in Verwendung, aber auch andere Komplexe mit unterschiedlichen Metallzentren zeigen ein hohes Potential, als tumorhemmende Substanzen eingesetzt zu werden. Als interessante Kandidaten bieten sich zum Beispiel Ruthenium, welches Eisen imitieren kann, sowie Osmium oder Kupfer, das eine große Rolle in biologischen Systemen spielt, an. Die Kombination von Metallen mit biologisch aktiven Liganden kann dieses Potential noch steigern.

In dieser Arbeit wurden Kupfer-Komplexe mit Indoloquinolin Liganden untersucht. Auch einige Ruthenium- und Osmium-Komplexe mit Indoloquinolin Liganden wurden auf ihre Zytotoxizität getestet. Indoloquinoline sind biologisch aktive Liganden und haben wegen ihrer planaren Struktur die Möglichkeit in die DNA zu interkalieren. Das Ziel dieser Arbeit war es, Struktur-Wirkungs-Beziehungen sowie andere zelluläre Effekte festzustellen.

Die Zytotoxizität wurde mittels MTT-Assay ermittelt. Die drei verwendeten Zelllinien, A549 (nicht-kleinzelliges Bronchialkarzinom), CH1 (Ovariakarzinom) und SW480 (Kolonkarzinom), zeigen unterschiedliche Sensitivitäten gegen verschiedene Zytostatika. A549 ist eine multidrug-resistente Zelllinie, wohingegen CH1 auf ein breites Spektrum an Substanzen anspricht.

Alle getesteten Kupferkomplexe zeigten eine sehr hohe Zytotoxizität in allen drei Zelllinien. Es wurden einige IC_{50} -Werte im nanomolaren Bereich gefunden. Die Ruthenium- und Osmium-Verbindungen hingegen waren weniger aktiv als erwartet.

Zellzyklus-Untersuchungen mittels Durchflusszytometrie wurden durchgeführt, um den Einfluss der Kupfer-Komplexe auf den Zellzyklus zu untersuchen. Weiters wurden auf Grund der planaren Struktur der Indoloquinoline DNA-interkalierende Eigenschaften mittels Methylgrün-Assay untersucht, um festzustellen, ob dies einen möglichen Wirkmechanismus darstellt. Es konnten jedoch keine Effekte auf den Zellzyklus und keine Interkalationseigenschaften im Methylgrün-Assay gefunden werden.

Western Blotting wurde als Methode herangezogen, um Apoptoseinduktion durch die neuen Kupfer-Komplexe nachzuweisen. Die Spaltung des Caspase-Substrats PARP wurde als Apoptoseindikator herangezogen. Mit zunehmender Konzentration der zu testenden Substanzen konnte ein Anstieg an gespaltenem PARP festgestellt werden.

Table of Contents

1	Abbreviations	1
2	Introduction	2
2.1	Aspects of cancer	2
2.2	Experimental antitumor compounds	5
2.3	Biological studies of antitumor compounds.....	11
3	Materials and Methods	18
3.1	Cell Lines	18
3.2	Media	19
3.3	Buffer	19
3.4	Diverse Reagents	21
3.5	Cell Culture Conditions	22
3.6	Cytotoxicity Assay	22
3.7	Cell Cycle Analysis	23
3.8	DNA Intercalation Assay	23
3.9	Western Blot	24
4	Results and Discussion	26
4.1	Cytotoxicity Assay	26
4.2	Cell Cycle Analysis	33
4.3	Intercalation	36
4.4	Western Blot	38
5	Conclusions	42
6	References	44
7	Appendix	51
8	Curriculum Vitae	65

1 Abbreviations

BSA	Bovine Serum Albumin
Cdk	Cycline dependent kinase
DMSO	Dimethylsulfoxid
DNA	Desoxiribo Nucleic Acid
dsDNA	double stand DNA
EtBr	Ethidium Bromide
HAS	Human serum albumin
HRP	HorseRadishPeroxidase
KP1019	Indazolium <i>trans</i> -[tetrachlorobis(1 <i>H</i> -indazole)ruthenate(III)]
KP1779	[(η^6 - <i>p</i> -Cymene)Os ^{II} (L ²)Cl]Cl, (η^6 - <i>p</i> -cymene)(κ N'-[11 <i>H</i> - indolo[3,2- <i>c</i>]quinolin-6-ylidene]- κ N,N-dimethylethane- 1,2-diamine)chloridoosmium(II) chloride
MTT	3-(4,5-dimethyl-2-thiazolyl)-2,5-diphenyl-2 <i>H</i> -tetrazolium bromide
NAMI-A	imidazolium <i>trans</i> -[tetrachloro(dimethylsulfoxi- de)(1 <i>H</i> -imidazole)ruthenate(III)]
PBS	Phosphate Buffered Saline
PI	Propidium Iodide
SDS	Sodium Dodecyl Sulfat
TBST	Tris-Buffered Saline + Tween 20
TRIS	2-Amino-2-hydroxymethyl-propane-1,3-diol

2 Introduction

2.1 Aspects of cancer

2.1.1 History

Cancer is not a modern disease. The word cancer is the Latin translation (Celsus 28-50 BC) of the Greek word for crab (Hippocrates 460-370 BC), which was used due to the form of a breast tumor reminding of a crab. Earliest descriptions of cancer, although it was not called cancer back then, were discovered in Egypt about 3000 BC. Other evidences of cancer were found in human mummies and fossilized bones, too. At that time there was no treatment for this disease, though.

In the 18th century when scientists started to use autopsies regularly, John Hunter, a Scottish surgeon, suggested that if a tumor has not invaded the surrounding tissue it should be removed. After the development of anesthesia, cancer operations started to improve. [1]

2.1.2 Epidemiology

Nowadays cancer is one leading cause of death in the world. 7.6 million deaths due to cancer were counted in 2008 (approximately 13% of all deaths), and 70% of them can be found in low- and middle-income countries. The World Health Organization (WHO) predicts that a decrease of cancer incidences is not likely. Quite on the opposite, in the year 2030 it will be responsible for more than 11 million deaths. The most frequent forms of cancer include lung cancer, stomach cancer, liver cancer, colorectal cancer, prostate and breast cancer.

Different risk factors can be linked to increased occurrence of cancer such as consumption of alcohol, use of tobacco and chronic infections with different viruses such as hepatitis B and C, but also genetic factors and external agents such as ultraviolet and other ionizing radiation or chemical agents.

With different strategies avoiding risk factors more than 30% of deaths caused by cancer could be prevented, according to an estimation of the WHO. [2]

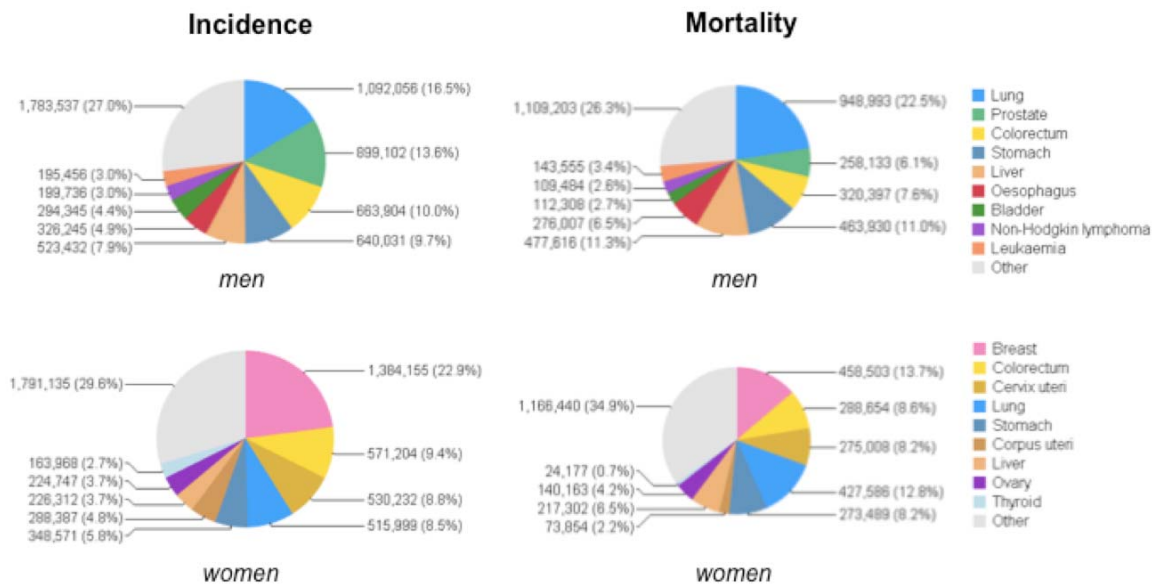


Fig. 1 Incidence and mortality of the most frequent cancers in men and women worldwide. [3]

As shown in **Fig. 1**, different types of cancer affect men and women with different probabilities. Men have a higher risk to die of lung, liver or stomach cancer, whereas women have a higher risk to die of breast, lung or colorectal cancer.

2.1.3 Cancerogenesis

Cancerogenesis is defined as the development of cancer. The two main characteristics of cancer are, firstly, to escape the growth and proliferation controls and, secondly, to invade surrounding tissues. As long as the tumor is not invasive, it is called benign. When it starts to invade other tissues, it is called a malignant tumor. A malignant tumor, spreads through the blood or lymphatic vessels throughout the body and forms secondary tumors (metastases).

Mutations or epigenetic changes can lead to cancer. It should be kept in mind, though, that cancer cannot arise from a single mutation. In fact a larger number of mutations that provide the cell with a growth advantage as compared to the

neighboring cells can lead to cancer. Normally, the cell has checkpoint controls, which will lead to a cell cycle arrest if, for example, DNA has been damaged. This allows the body to initiate repair mechanisms. If it is not possible to restore the DNA in the original form, the cell will undergo apoptosis. Often the response to DNA damage is inactivated; in particular, mutations in the p53 pathway, a tumor suppressor gene, are frequently found that can result in the inactivation of apoptosis. These are just two examples of how cancer cells survive, but there are many possibilities more that are already known. [4]

2.1.4 Treatment

In cancer treatment three mainstays of therapy exist:

- Surgery
- Radiotherapy
- Chemotherapy

Apart from that other methods such as immunotherapy and hormone therapy can also be employed.

Surgical Therapy: Surgery is the oldest method to fight cancer. Already in the 19th century J. Abernethy described such a method for cancer treatment. At that time, the main problem was that anesthesia and antisepsis were not yet developed. Nowadays solid malignant tumors are removed completely with some of their surrounding tissue as far as possible. Surgery is also used for palliation of advanced cancer that e.g. has already metastasized and cannot be cured by surgery.

Radiotherapy: Radiotherapy evolved shortly after the discovery of X-ray by Roentgen in 1895. This technology developed rapidly and as early as in the 1920s an effective therapy against laryngeal cancer was introduced. Ionizing radiation inhibits cell proliferation and can damage DNA for example. Normally, healthy cells have a repair system that will work against such damages. In tumor cells this system works less efficiently and the cell will die. It is important to carefully choose the appropriate radiation dose, time and number of treatments to kill the tumor cells with as little a risk as possible for subsequent complications.

Chemotherapy: The era of chemotherapy emerged in the 1940s with the development of nitrogen mustard. Nowadays, there are different cytostatic and cytotoxic agents used in chemotherapy. They can be divided into different classes such as:

- alkylating agents
- antitumor metal complexes (e.g. cisplatin, carboplatin)
- antimetabolites
- topoisomerase I and II inhibitors
- hormones and hormone antagonists

Chemotherapy is used for tumors that have metastasized already. It is important to destroy as many tumor cells as possible without damaging the healthy cells. Most chemotherapeutics act on proliferating cells. This means that excessive doses of chemotherapeutics also have an effect on healthy cells. [5,6,7]

2.2 Experimental antitumor compounds

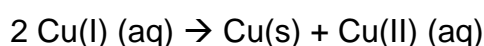
2.2.1 Copper

Copper is a long known metal. As early as 5000-4000 BC copper was used to manufacture tools and played a very important role in the history of mankind as a component of bronze.

Copper belongs to the coin metals, because it is easy to mine and to handle. Similar to silver, it has a high conductivity. It is, though, significantly cheaper than silver, therefore it is widely used in electric wiring and the like today.

In the earth's crust copper is found in 68×10^{-4} mass%. The natural abundance of copper isotopes is given as follows: ^{63}Cu 69.2 % and ^{65}Cu 30.8 %. The electron configuration of copper is $[\text{Ar}]3d^{10}4s^1$ and consequently the preferred oxidation states are Cu(I) and more importantly Cu(II).

Cu(I), cuprous, forms diamagnetic salts and disproportionates in aqueous solutions according to the following equation:



Cu_2O , Cu_2S , CuI and complexes thereof are well known and have a low solubility in water. In medicine, Fehling's solution is used to test for sugars in urine. For this purpose, CuSO_4 , tartrate and NaOH are added to reducing sugars (such as aldehydes). Cu(II) is reduced to Cu_2O , a red compound.

Cu(II) , cupric, is subjected to Jahn-Teller distortions as predicted for octahedral d^9 ions. In aqueous solution, the $[\text{Cu}(\text{H}_2\text{O})_6]^{+2}$ ion is formed. Copper(II) sulfate and nitrate are fungicides and used as solutions in water.

In biological systems copper plays an important role, too. It is a structural and catalytic cofactor that is involved in important biochemical processes. Copper exhibits redox activity due to the two oxidation states (Cu(I) , Cu(II)). In these two states it prefers different ligands. Cu(II) prefers "harder" ligands such as nitrogen or oxygen donors whereas Cu(I) prefers "softer" ones such as sulfur donors. [8,9]

2.2.2 Ruthenium

Ruthenium is like osmium a member of the platinum-metal group in the periodic table. Its electron configuration in the ground state is $[\text{Kr}]5s^14d^7$. The oxidation states vary from -II in $\text{Ru}(\text{CO})_4^{2-}$ to +VIII in RuO_4 , with +III as the most stable oxidation state. Ruthenium has 7 natural isotopes ($^{96,98,99,100,101,102,104}\text{Ru}$), and $^{99,101}\text{Ru}$ are commonly used for NMR-spectroscopic measurements due to their favorable magnetic properties. [9,10,11]

There is a number of interesting, distinct features for the development of ruthenium-based antitumor drugs, such as the ability to mimic iron, its octahedral coordination geometry, physiological oxidation states ($(+II)$, $+III$, $+IV$), advantageous ligand exchange rates and well-understood coordination chemistry. [12]

The first ruthenium-based anticancer drugs in clinical trials were NAMI-A and KP1019. [13] They are administered intravenously. Consequently, primary binding partners are proteins that occur in the blood stream such as transferrin and albumin (HAS).

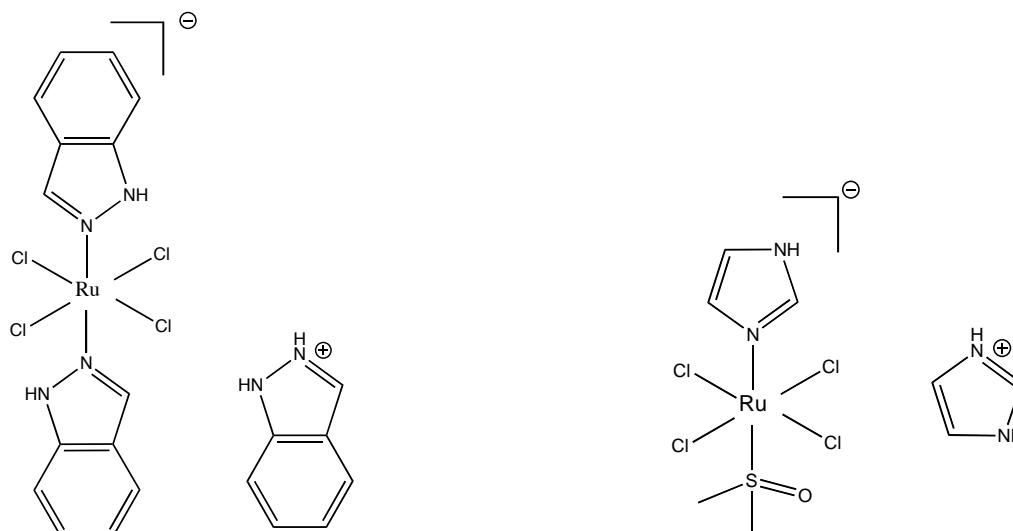


Fig. 2 KP1019, indazolium *trans*-[tetrachlorobis-(1*H*-indazole)ruthenate(III)] (left) and NAMI-A, imidazolium *trans*-[tetrachloro(dimethylsulfoxide)(1*H*-imidazole)ruthenate(III)] (right) [15]

Ru(II)/Ru(III) electron transfer does not lead to a change of the coordination number and interatomic bond distances, as opposed to Pt(IV) that is reduced to Pt(II). This could be one reason for the different mode of action and an explanation why KP1019 shows effects on cisplatin-resistant tumors. Most likely the activity of NAMI-A and KP1019 derives from a direct coordination of the metal to a biological target. This would mean that a reduction to Ru(II) is happening. Still, if the metal ion binds to the biological target and this specific interaction is responsible for the activity, these compounds can be described as functional compounds. [12,13,14,15]

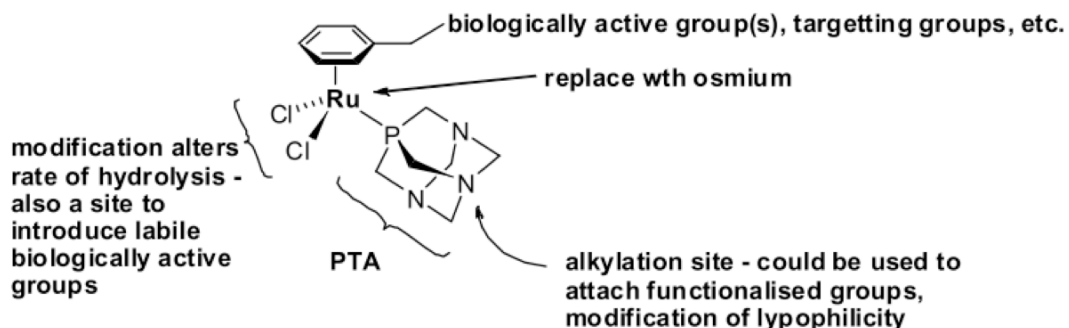


Fig. 3 „Generic RAPTA structure $\text{Ru}(\eta^6\text{-arene})\text{Cl}_2(\text{pta})$ with potential sites for modification indicated.“ [16]

RAPTA-C [$\text{Ru}(\eta^6\text{-cymene})\text{Cl}_2(\text{pta})$], has been subject to intense research. It has been showed that the chloride ligands can be hydrolyzed in aqueous environments. In blood plasma the chloride concentration is high enough that the ligands will stay coordinated to the complex, but in the cytoplasm they may be exchanged. This could be one possible activation pathway. [16] So far, a lot of different RAPTA-type compounds were produced. In comparison to other antitumor drugs such as cisplatin, RAPTA complexes are less cytotoxic, but have a high selectivity for some cancer cell lines, for example TS/A, whereas they are harmless for healthy cells. [17]

2.2.3 Osmium

Osmium is a noble metal. Like ruthenium it belongs to the platinum-metal group. It was discovered 1804 by S. Tennant. Its ground state electron configuration is $[\text{Xe}]4f^{14}6s^25d^5$ and the possible oxidation states range from -II to +VIII as in the case of ruthenium, but the preferred state is +IV. Again, there are 7 natural isotopes ($^{184,186,187,188,189,190,192}\text{Os}$) and two of them $^{187,189}\text{Os}$ are commonly employed in NMR-spectroscopic measurements. [18]

Osmium(II) arene complexes were reported to be cytotoxic in cancer cells. [19] The ligand exchange rates of Os(II) and Ru(II) are different, as the Os(II) and Os(III) complexes are kinetically more inert than their ruthenium analogues. [20] How its organometallic complexes behave in aqueous environments is not yet fully understood. [22] It was shown that osmium(II) arene complexes with an N,N-chelating ligand are hydrolyzed more slowly than those with an O,O-chelating ligand. The hydrolysis barrier for $[\text{Os}(\eta^6\text{-biphenyl})(\text{en})\text{Cl}]^+$ (N,N-chelating) is higher than for $[\text{Os}(\eta^6\text{-p-cym})(\text{acac})\text{Cl}]$ (O,O-chelating), for example, and in comparison to Ru(II) analogues of $[\text{Os}(\eta^6\text{-biphenyl})(\text{en})\text{Cl}]^+$ the osmium analogue hydrolyses 40 times slower at physiological pH than the corresponding osmium complex. Hence, not only the metals in the complexes are important for activity and hydrolysis, but the chelating ligand plays a major role as well. [20,21,22]

2.2.4 Indoloquinolines

Indolo-[3,2-c]quinolines are composed of an indole and a quinolin-2(1H)-one moiety.

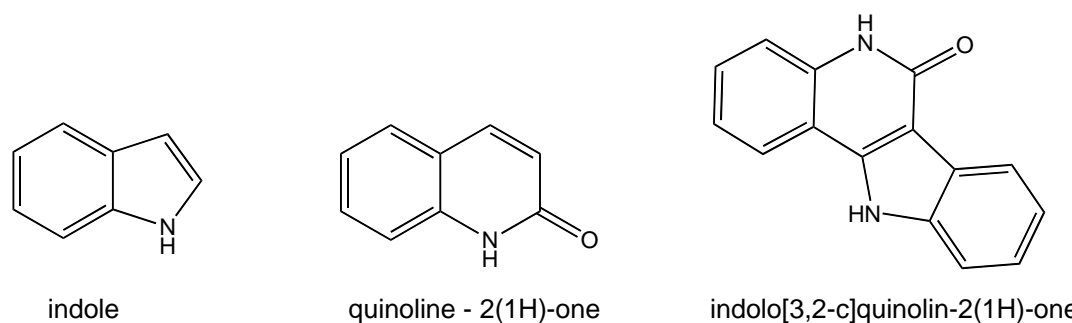


Fig. 4 Structure of indole, quinoline-2(1H)-one components and indolo[3,2-c]quinolin-2(1H)-one

The indole scaffold is a structural feature of some clinically used anticancer drugs e.g. vinblastine [23] and vincristine [24], and quinolin-2(1H)-one is contained in many biologically active compounds. [25] Isocryptolepine or cryptolepin, indoloquinoline derivatives that can be isolated from *Cryptolepis sanguinolenta*, are used in traditional medicine for malaria treatment or other diseases. [26]

Indolo-[3,2-c]quinolin-2(1H)-one showed an inhibitory activity (GI_{50} value of $19.0 \mu\text{M}$) in a human tumor cell line screen conducted by the US National Cancer Institute. [27] Different indoloquinoline derivatives have shown biological activity in cancer. [25,27,28]

To improve solubility of derivatives and to increase anti-proliferative properties, metal-complexes are formed. [25,35] The heteroaromatic system of the complex is planar and has a high potential to intercalate into DNA. [29]

2.2.5 Test compounds

As seen in **Fig. 5** and **Fig. 6** two different groups of metal compounds were investigated. Complexes of indolo[3,2-c]benzazepines, also named as Paullones, and related indolo[3,2-c]quinolines with different substitutions and copper(II) as the metal center were tested. The main difference is found in the six- or seven-membered ring of the ligands, implying that indoloquinolines have

a planar structure whereas Paullones are folded. Additionally, substituents in position 8 and 14 were varied. Due to bad solubility of the corresponding ligands, the ligands themselves could not be tested. This shows that complexation results in higher solubility.

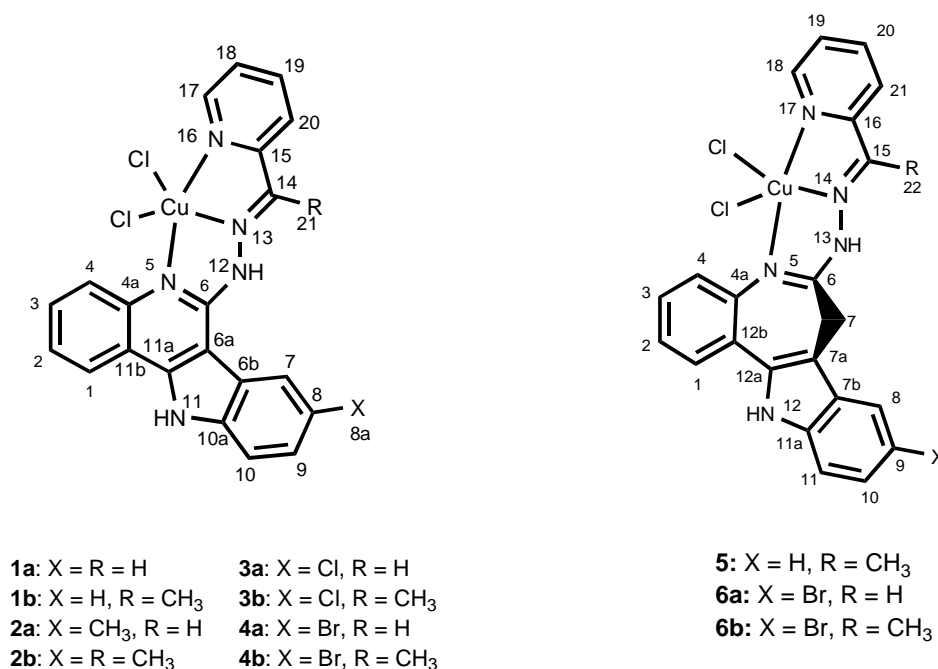


Fig. 5 Copper(II) compounds with modified indoloquinoline and Paullone ligands

The second group of tested compounds was ruthenium(II) (**7a**, **8a**, **9a**) and osmium(II) (**7b**, **8b**, **9b**) complexes with modified indoloquinoline ligands. These complexes are the first ones coordinated via position 2 of the indoloquinoline backbone. In the case of **9a,b** an underivatized lactam moiety is present. This was found to be necessary for efficient cdk inhibition in the case of the Paullones. [30]

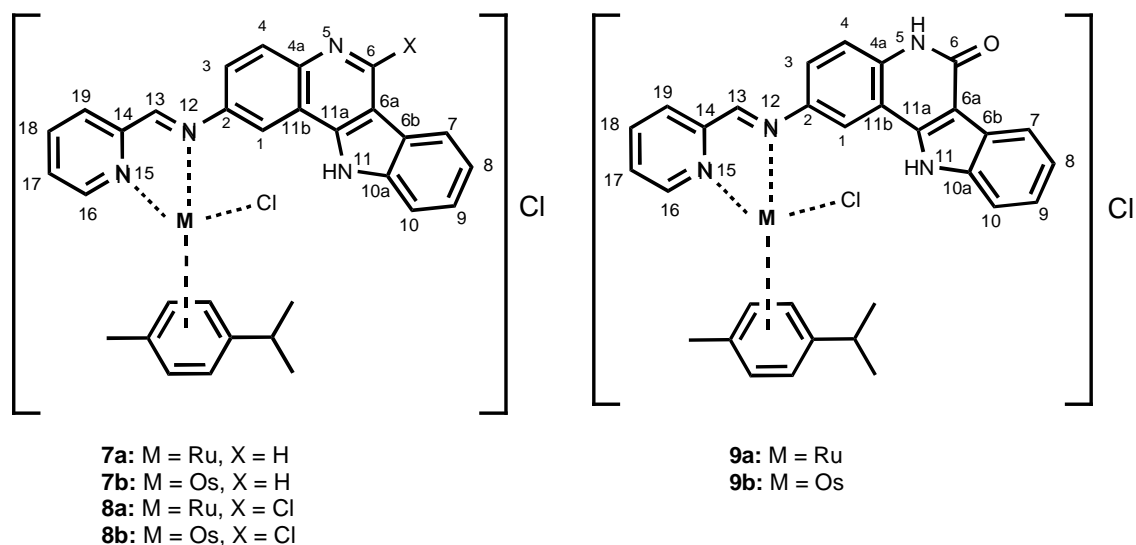


Fig. 6 Ruthenium(II) and osmium(II) compounds with various indoloquinoline ligands

2.3 Biological studies of antitumor compounds

2.3.1 Cytotoxicity Analysis

For testing the cytotoxic activity of new potential anticancer drugs the so-called colorimetric MTT assay is used (MTT stands for 3-(4,5-dimethyl-2-thiazolyl)-2,5-diphenyl-2H-tetrazolium bromide). In principle, the assay is based on the reducing properties of living cells. [31]

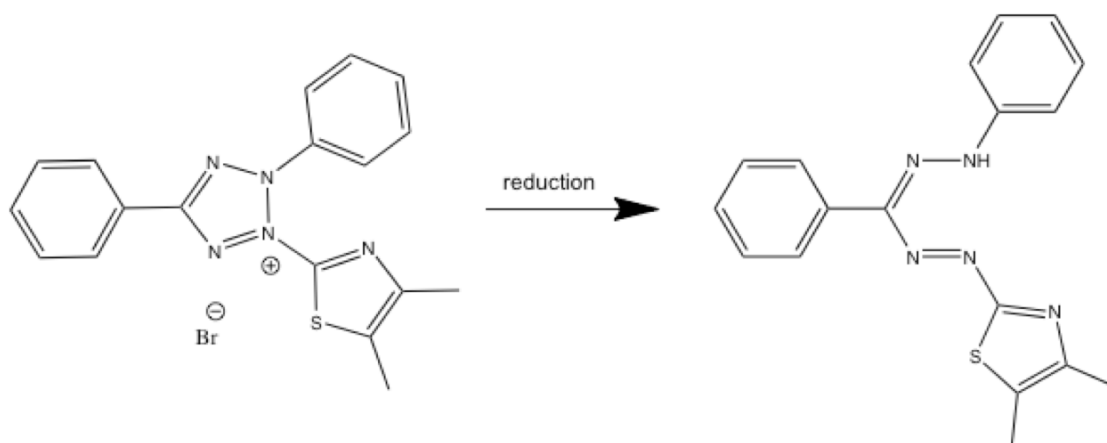


Fig. 7 3-(4,5-dimethyl-2-thiazolyl)-2,5-diphenyl-2H-tetrazolium bromide reduced to the formazan product

MTT is membrane impermeable and therefore the uptake happens via endocytosis. The transport of the formazan to the cell surface takes place through exocytosis. [32]

After treatment of the cells with the compound to be tested, the MTT reagent, a yellow, water-soluble tetrazolium dye, is added to the cells. In living cells the tetrazolium salt is reduced to a purple-colored formazan product. The formed formazan product is water insoluble and has to be solubilised in another solvent such as DMSO. The optical density (at 550 nm and at 690 nm reference wavelength) of the formazan product is measured on a spectrophotometer, and consequently the amount of viable cells can be determined, because the relationship between the formazan product and the number of living cells is linear. [33,34,35]

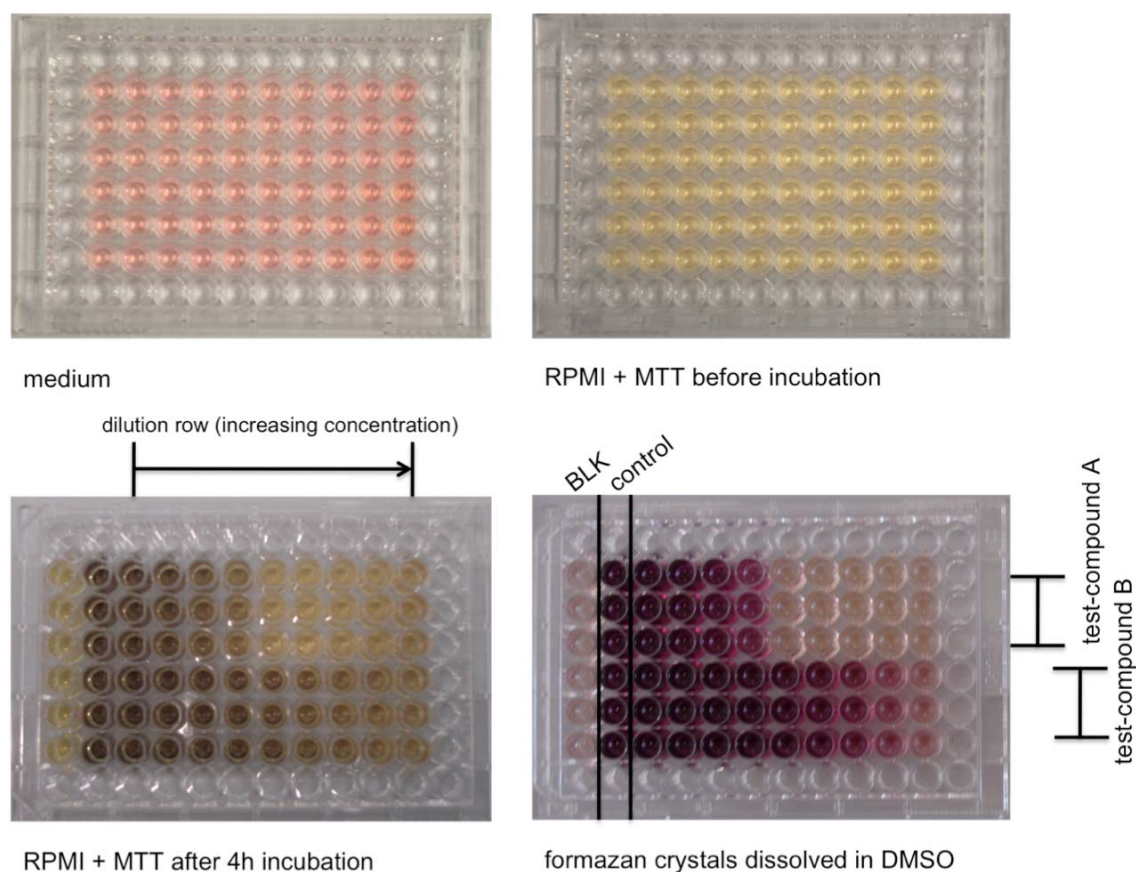


Fig. 8 MTT plates, description of the procedure. (top left) medium with treated cells, (top right) added RPMI/MTT solution, (bottom left) after 4 h incubation, formazan crystals are formed, (bottom right) dilution with DMSO, different concentration of the formazan can be seen.

The IC_{50} (50% inhibition concentration) is an index number used to quantify the anti-proliferative activity. The IC_{50} is defined as the concentration of the agent that results in a 50% lower cell number compared to the untreated control. [36] This value is calculated from the concentration-effect curve of the treated cells by interpolation.

2.3.2 Cell Cycle Analysis

The cell cycle (cf. **Fig. 9**) is the series of events that takes place in a cell that ultimately leads to its duplication and division. There are two major phases of the cell cycle: the interphase and the mitosis or M phase. The interphase is divided into three subphases called G₁, S and G₂ phase where G stands for gap. These gap phases give the cell more time to grow and monitor the internal and external environments. During the S phase, DNA replication occurs. In the M phase, also named mitosis, nuclear division and cytokinesis proceeds.

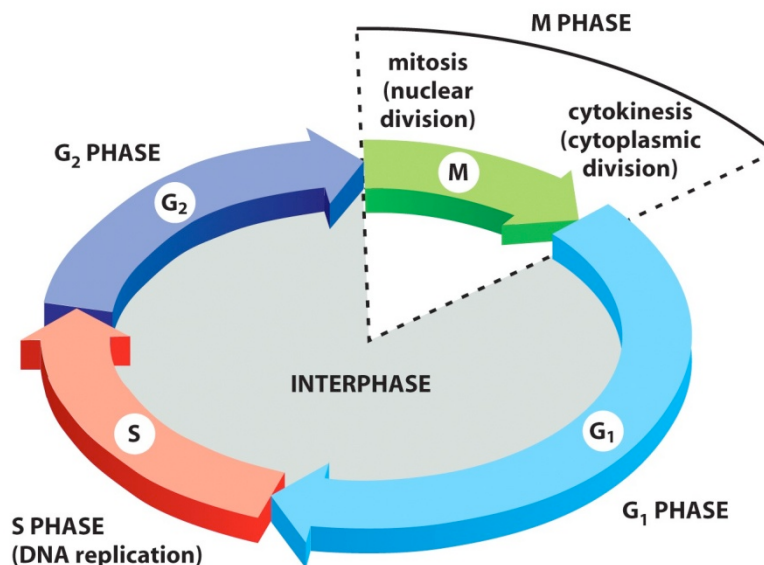


Fig. 9 The four phases of the cell cycle [37]

In the cell cycle there are checkpoints that are a part of the cell cycle control system. These checkpoints trigger mitosis, cytokinesis and DNA replication. If the environment is not favorable, DNA does not replicate or the chromosomes do not attach to the mitotic spindle, the cell is going into a cell cycle arrest.

For cell cycle analysis, flow cytometry is used to measure in which phase of the cell cycle the cells are. Thousands of cells can be measured within a few seconds or minutes using this method. For this purpose, the cells are stained with a fluorescent, DNA intercalating dye such as propidium iodide (cf. **Fig. 10**). [38]

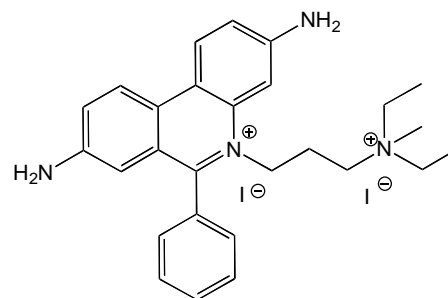


Fig. 10 Propidium Iodide

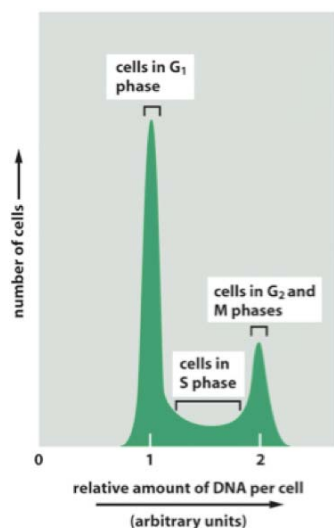


Fig. 11 Flow cytometric histogram of analysis of cellular DNA content

In the different phases of the cell cycle, different amounts of DNA are present in the cell. There is twice as much DNA, for example, in the G₂/M phase than in G₁. Most methods cannot discriminate between G₂ and M phase, though. In the S phase there is an intermediate amount of DNA. The amount of the DNA is proportional to the amount of fluorescence. The histogram shows two peaks of cells in G₁ and G₂/M, hence. In between these two peaks the cells in S phase are found (cf. **Fig. 11**). Changes in the cell cycle are observed by comparison to an untreated control. [37,39]

2.3.3 Intercalation Assay

This assay is also known as the methyl green assay. Methyl green [40] (nowadays also ethyl green is used) (cf. **Fig. 12**) binds to DNA and has an absorption maximum at 642 nm. [25] It was shown that methyl green is a major groove binder that binds to poly[d(A-T)]. [41] It is important to know that methyl green is just interacting with polymerized DNA, because depolymerized DNA (by e.g. heating) cannot protect methyl green in neutral pH. The methyl green-

DNA complex is stable at pH > 5. [42] Free methyl green shows no absorption because it forms a colorless carbinol. [43]

If a DNA-intercalating compound interacts or binds to the DNA-methyl green complex, it leads to a displacement and consequently to a release of methyl green.

As a result, the optical density in the sample decreases. Partial planarity or at least a hydrogen bond should exist for functional intercalations. [44]

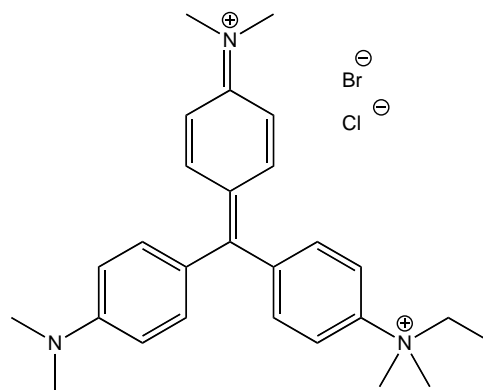


Fig. 12 4-((4-(Dimethylamino)phenyl)(4-(dimethyliminio)cyclohexa-2,5-dien-1-ylidene)methyl)-N-ethyl-N,N-dimethylanilinium-bromide-chloride [40]

The methyl green assay and his usefulness has been documented in numerous papers. A lot of different DNA-complexing substances were tested and their biochemical or biological activity e.g. to antibacterial properties as well as immunosuppressive activity, were correlated to methyl green displacement. [45]

2.3.4 Detection of Apoptosis

2.3.4.1 Western blotting

Western blotting or immunoblotting is a method that allows the transfer of proteins onto a nitrocellulose-membrane for further identification or quantification by detection with antibodies, for example.

The method can be described consisting of three main parts:

- Gel electrophoresis
- Transfer to membrane
- Detection

Sample preparation in the beginning is one of the most important steps. The proteins must not be fragmented or be destroyed by proteases.

Separation of proteins in the sample is accomplished by discontinuous SDS-PAGE (polyacrylamid-gel electrophoresis) where the anionic detergent SDS destroys the hydrophobic interactions of the protein and additionally charges the

protein negatively. As a result, the proteins are separated depending on their respective molecular masses. Discontinuously means that first the proteins are added into a stacking gel, then they are focused with low voltage and after entering the separation part of the gel, voltage is increased.

After that, transfer onto the membrane is done via Semi-dry blotting. Semi-dry blotting procedure resembles the wet blotting. The main differences are that less buffer is needed and the device works horizontally instead of vertically. The assembly of a sandwich in a semi-dry blot is shown in **Fig. 13**.



Fig. 13 Sandwich assembly of a semi-dry blot

After the transfer, the membrane is blocked with blocking proteins such as BSA or by using milk in order to prevent unspecific binding of the detection antibodies. At least two antibodies are used: a primary antibody against the protein and a secondary antibody against the primary. The second one is conjugated to an enzyme e.g. HRP or labeled with a fluorescence marker. [46] The following luminescence or fluorescence measurement can be done employing CCD-Imaging systems or the like.

2.3.4.2 PARP

PARP (poly(ADP-ribose)polymerase) is a 116 kDa Zn-finger nuclear protein that is involved in DNA repair response. It is activated by DNA strand breaks and uses β NAD⁺ to catalyze (ADP-ribose) polymers on nuclear proteins. PARP cleavage by caspase-3 or caspase-7 plays an important role early in apoptosis. At first PARP is accumulated in the early apoptotic cells and then it is cleaved. This happens between Asp²¹⁴ and Gly²¹⁵. Hence, the resulting fragments weigh 89 kDa (from the carboxyl-terminal catalytic domain) and 24 kDa (from amino-terminal DNA binding domain). This cleavage inactivates the poly(ADP-ribosylation) process and PARP is inactive towards DNA damage, consequently. [47,48,49]

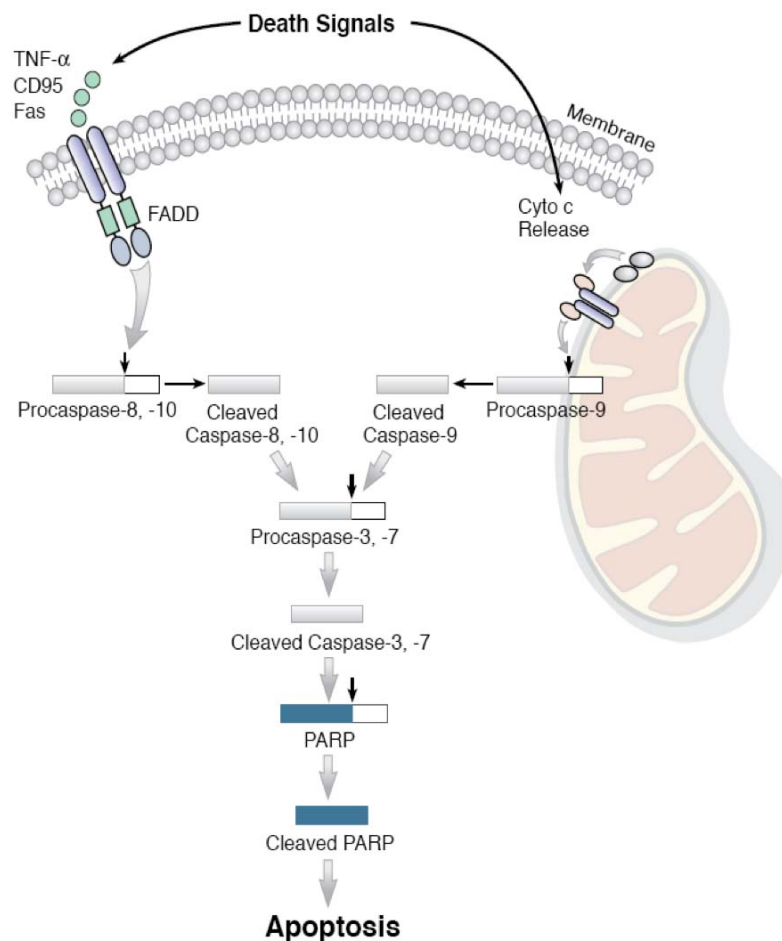


Fig. 14 Apoptosis cascade and cleavages of PARP [48]

3 Materials and Methods

3.1 Cell Lines

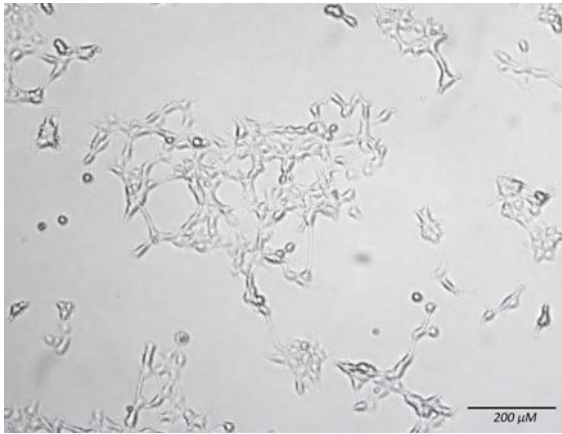


Fig. 16 CH1 cells



Fig. 15 SW480 cells

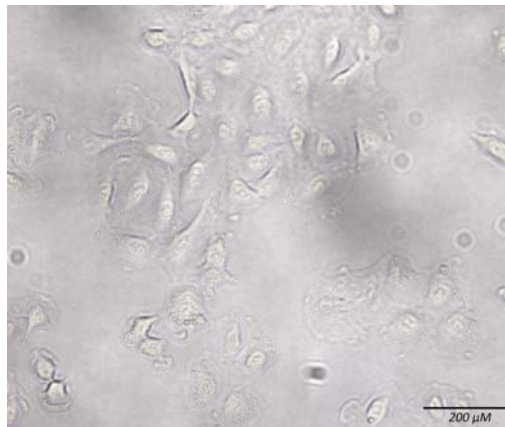


Fig. 17 A549 cells

Fig. 16 CH1 (ovarian carcinoma), kindly provided by Lloyd R. Kelland, CRC Centre for Cancer Therapeutics, Institute of Cancer Research, Sutton, U.K.

Fig. 15 SW480 (colon carcinoma) kindly provided by Brigitte Marian, Institute of Cancer Research Department of Medicine I, Medical University Vienna, Austria

Fig. 17 A549 (non-small cell lung cancer) kindly provided by Brigitte Marian, Institute of Cancer Research Department of Medicine I, Medical University Vienna, Austria

3.2 Media

3.2.1 Minimal Essential Medium (MEM)

Minimum Essential Medium Eagle (Sigma Aldrich, M2279) supplemented with:

- 10% heat-inactivated fetal bovine serum (FSB Fetal Bovine Serum, GIBCO 10270, invitrogen)
- 1 mM sodium pyruvate (Sodium Pyruvate 100 mM Solution, Sigma Aldrich, S8636)
- 1% non-essential amino acid (non-essential amino acid solution 100x – Sigma Aldrich, M7145)
- 4 mM L-glutamine (L-Glutamine 200 mM, Sigma Aldrich, G7513)

3.2.2 RPMI 1640 medium supplemented with:

RPMI 1640 Medium, HEPES Modification (Sigma Aldrich, R5886) supplemented with:

- 10% heat-inactivated fetal bovine serum (FSB Fetal Bovine Serum, GIBCO 10270, invitrogen)
- 4 mM L-glutamine (L-Glutamine 200 mM, Sigma Aldrich, G7513)

3.3 Buffer

3.3.1 PBS

Dulbecco's Phosphate Buffered Saline (Sigma Aldrich, D8537)

3.3.2 HSF Buffer (hypotonic fluorochrome solution)

- 0.1% (v/v) Triton X-100
- 0.1% (w/v) Sodium Citrate
- PBS (Dulbecco's Phosphate Buffered Saline (Sigma Aldrich, D8537))

3.3.3 RIPA Buffer (Radio Immuno Precipitation Assay buffer)

- 150 mM sodium chloride
- 1.0% Triton X-100

- 0.5% sodium deoxycholate
- 0.1% SDS (sodium dodecyl sulfate)
- 50 mM Tris, pH 8.0

3.3.4 Electrophoresis Buffer 10x

- 30.3 g Tris
- 144.13 g glycine
- 10 g SDS
- 1 l milli Q water

3.3.5 Transfer Buffer 10x

- 30.3 g Tris/HCl
- 144.13 g Glycine
- 1 l milli Q water
- pH 8.3

3.3.6 Transfer Buffer 1x

- 100 ml Transfer Buffer 10x
- 200 ml Methanol
- 700 ml milli Q water

3.3.7 Blocking Buffer

- milk 5%, TBST (Tween 0.1%) (Blotting Grade Blocker Non-Fat Dry Milk, Bio-Rad Laboratories, 170-6404)
- BSA 5%, TBST (Tween 0.1%) (Albumin, from bovine serum (Sigma Aldrich, A7906))

3.3.8 Stripping Buffer

- 15 g glycine
- 1 g SDS
- 10 ml Tween 20 (polyoxyethylene sorbitan monolaurate, Bio-Rad Laboratories, 170-6531)
- pH to 2.2
- diluted to 1 l with milli Q water

3.3.9 TBS 10x

- 24,2 g Tris
- 80 g NaCl
- adjusted to pH 7,6 with HCl
- diluted to 1 l with milli Q water

3.3.10 TBST 1x

- 100 ml 10xTBS
- 1 ml Tween-20
- diluted to 1 l with milli Q water

3.3.11 Laemmli 6x Buffer

- 12% SDS
- 30% 2-mercaptoethanol
- 60% glycerol
- 0.012% bromophenol blue
- 0.375 M Tris HCl
- pH 6.8

3.4 Diverse Reagents

- 0.25% Trypsin – EDTA Solution (Sigma Aldrich, T4049)
- Super Signal West Pico Chemiluminescent Substrate (Thermo Scientific, #34080)
- Deoxyribonucleic acid (DNA) Sodium Salt from Salmon Testes (Sigma Aldrich D-1626)
- Acrylamid/bis-Acrylamid, 30% Solution Electrophoresis Reagent (Sigma Aldrich)
- N,N,N',N'-Tetramethylethylenediamine (Sigma Aldrich, T9281)
- Sodium dodecyl sulfate (Sigma Aldrich, L4390)
- Thiazolyl Blue Tetrazolium Bromide, approx. 98% TLC (Sigma Aldrich, M2128)
- For MTT-Assay, 5 mg/ml in PBS

- Ammonium persulfate, for electrophoresis, = 98% (Sigma Aldrich, A3678)
- Propidium iodide (Fluka, 81845)
- Ethidium bromide (Serva, 21251)

3.5 Cell Culture Conditions

All cells were grown in 75 cm² culture flasks as adherent monolayer cultures in MEM (Minimum Essential Medium) without antibiotics at 37 °C under a moist atmosphere containing 5% CO₂ and 95% air.

3.6 Cytotoxicity Assay

Cytotoxicity of all compounds was determined by using the colorimetric MTT assay (3-/4,5-dimethyl-2-thiazolyl)-2,5-diphenal-2*H*-tetrazolium bromide). After harvesting by trypsinization cells were seeded into 96-well micro culture plates (100 µL/well and three replicates per concentration). For the copper complexes, different cell densities were used as follows: CH1 - 1.5 x 10³ cells/well, SW480 - 2.5 x 10³ cells/well and A549 - 4.0 x 10³ cells/well. For the ruthenium- and osmium-based complexes, CH1 cells were seeded in a density of 1.0 x 10³ cells/well; the other cell lines were used with the same densities as used for the copper compounds. These densities were chosen to ensure exponential growth of the untreated controls over the whole time of experiment. After 24 h the test compounds were dissolved in DMSO, mixed with medium to a maximum DMSO concentration of 1% v/v, serially diluted and added to the plates in volumes of 100 µL/well. For the highest concentration (80 µM) of Ru and Os compounds, medium was removed and 200 µl of medium with the final concentration of the test compound was added. Therefore the maximum DMSO concentration was 0.5% v/v. After continuous exposure for 96 h at 37 °C and under 5% CO₂, the medium was replaced by 100 µL/well RPMI 1640 medium and 20 µL/well MTT solution. After 4 h incubation (same conditions as before) the medium was removed and the formed formazan product was dissolved in DMSO (150 µL/well). With a 96-well micro plate reader (Tecan Spectra Classic) optical

densities at 550 nm (690 nm reference wavelength) were measured. The 50% inhibitory concentrations (IC_{50}) were calculated from the concentration-effect curves by interpolation. The tests were repeated at least three times in independent experiments. [35]

3.7 Cell Cycle Analysis

For this assay A549 cells were harvested by trypsinization and 3×10^5 cells in 2 ml/well were seeded into 6-well plates. After 24 h incubation at 37 °C and 5% CO_2 , the test compounds, dissolved in DMSO, were added directly to the plates, with a maximum concentration of 1% v/v DMSO. After continuous incubation for 24 h (under same conditions as before) the cells were washed with PBS and trypsinized. Trypsinization was stopped with MEM, the cells were centrifuged (1200 rpm, 3 min) and the supernatant was discarded. Then the cells were washed with PBS again and resuspended in 300 μ L PI/HSF-buffer with a concentration of 50 μ g PI/ml. After incubation over night/weekend in the fridge (4 °C) in the dark, 1×10^4 cells were measured by flow cytometry on a BD FACS Calibur instrument. [50,51]

3.8 DNA Intercalation Assay

dsDNA (from salmon testes) solution (10 mg/ml) was prepared in MEM one day before usage and shook at 37 °C until it was a highly viscous liquid. This stock solution was further diluted 1:100 in MEM. Medium was used, because earlier test (not reported here) had shown, that with the standard procedure (using milli Q water to dilute DNA and PBS for sample preparation) these compounds build a kind of jelly-looking fallout, so the sample could not be measured and very bad reproducibility was observed. Methyl green was prepared in milli Q water (1 mg/ml). The samples were prepared as shown in **Tab. 1**. To achieve the same concentration of DMSO, additional pure DMSO was added to gain an overall amount of 1% in every sample. First the samples were prepared without the drugs and incubated for 1 h at 37 °C in the dark to allow methyl green to intercalation into the DNA.

Tab. 1 Composition of samples for the methyl green assay compounds were diluted and 1% DMSO was added to every sample.

		DNA [μ l] (100 μ g/ml)	Methyl green [μ l] (1 mg/ml)	MEM [μ l]	Compound [μ l]	Final compound concentration [μ M]
1	Blank	0	40	1940	20	0
2	Control	1000	40	940	20	0
3	Pos. Control 1	1000	40	940	20	100
4	Pos. Control 2	1000	40	940	20	50
5	Sample 1	1000	40	940	20	50

Subsequently the compounds and DMSO were added and incubated for 2 hours in the dark at 37 °C. EtBr was used as positive control due to the knowledge that EtBr is a DNA intercalator. Additionally KP1779, a strongly intercalating indoloquinoline-complex with osmium as metal center, was used as a second positive control. During this time the test substances can interact with DNA to replace the methyl green. Aliquots of 300 μ l of the sample solution were filled into a 96-well plate (three replicates per sample), and the absorption was measured at 642 nm with a Bio-Tek (Synergy HT) reader.

3.9 Western Blot

For the Western blot experiments, 3×10^5 CH1 cells/well were seeded into 6-well plates. After 24 h the test-compounds were added in different concentrations. After different incubation times (12 h, 16 h, 18 h, 24 h) the medium was removed and the cells were washed with cold PBS. Afterwards the cells were lysed with RIPA buffer (with 1:100 protease-inhibitor cocktail P8340 Sigma added), scraped down with a rubber policeman and transferred into a cooled Eppendorf tube. The lysates were vortexed and gently shaken for 20-30 min, afterwards they were centrifuged at 14 000 rpm for 10 min at 4 °C. The supernatant was removed and added to fresh cooled Eppendorf tubes which were then stored at -80 °C.

For the gel electrophoresis, 5% SDS PAGE stacking gel and 9% SDS-PAGE separation gels (1 mm) were prepared. (SDS PAGE gels containing: 30% polyacrylamide, TEMED, 10% SDS, H₂O, 10% APS, Tris (1.5 M, pH 8.8 separating gel, 1 M, pH 6.8 stacking gel). Before lysates were loaded onto the gel, they were mixed with Laemmli 6x Loading Buffer and heated 5 min at 95 °C. The marker P 7711 (ColorPlus Prestained Protein Ladder, Broad Range (10-230 kDa), New England BioLabs) was used. With 80 V the proteins were focused in the stacking gel, and subsequently they were separated with higher voltage of 120-160 V.

With semi-dry blotting the proteins were transferred from the gel to the nitrocellulose-membrane. The run took 1 h 30 min with 75-80 mA/membrane. Blocking was done with 5% milk/TBST for at least 1 h. Afterwards the membrane was incubated with the primary polyclonal antibody PARP (#9542, Cell Signaling Technology) 1:1000 dilution, gentle shaking over night at 4 °C. After three washing steps (each 5 min) with TBST, the membrane was incubated with the secondary antibody (Anti-rabbit IgG, HRP-linked Antibody, #7074, Cell Signaling Technology) 1:1000 dilution, for 1 h. Then the membrane was washed three times with TBST (5 min each), chemiluminescent substrate was added and incubated for 5 min. Measurement was done by the CCD-imaging system, Fusion FX7.

After the measurement, the antibodies were removed by stripping. Mild stripping was done as described in [52], furthermore 5% BSA/TBST was used for blocking over a period of 1 h. Then primary antibody against β -actin (β -Actin (13E5) Rabbit mAb, Cell Signaling Technology; 1:2000 dilution) was added and the membrane incubated for at least 1 h. Again the membrane was washed with TBST three times (5 min each), and the secondary antibody (Anti-rabbit IgG, HRP-linked Antibody, #7074, Cell Signaling Technology; 1:1000 dilution) was added and incubated for 1 h. The washing process was repeated and chemiluminescent substrate was added and the membrane incubated for 5 min. Measurement was done by the CCD-imaging system, Fusion FX7.

4 Results and Discussion

4.1 Cytotoxicity Assay

The cytotoxicity of the compounds was determined using the colorimetric MTT assay in the described cell lines. Some compounds showed IC_{50} values in the range of 10^{-8} to 10^{-6} M (**Tab. 2**). The copper(II) complexes showed a higher sensitivity in all cell lines than the ruthenium(II) and osmium(II) complexes. The corresponding uncomplexed ligands could not be tested due to their insufficient solubility. A549, the most chemo-resistant cell line in the experiment, was the least sensitive one for all the tested compounds, whereas in CH1, a chemo-sensitive cell line, IC_{50} values of all compounds within the applicable range of concentrations were detected.

The following structure-activity relationships of the copper(II) complexes were observed: A substitution at position 8 with a methyl (**2a**), chloro (**3a**) or bromo (**4a**) group has nearly no impact on the cytotoxicity compared to compound **1a** that has no substituent in this position. Adding a methyl group at position 14 results in a dramatic enhancement of cytotoxicity, indicating that this position is crucial responsible for the activity of the compounds. In A549 and CH1 cells, IC_{50} values are about 10 times lower, and in SW480 cells a 50-fold increase of cytotoxicity was found, e.g. compound **1b** (**Fig. 18**). The IC_{50} values of **2b**, **3b** and **4b** are one order of magnitude lower than those of the analogues **2a**, **3a** and **4a**. This approves, the irrelevance of methyl, chloro and bromo substitutions at position 8 as well as the impact of the methyl substitution at position 14. [35]

Copper(II) complexes with Paullone ligands (**5**, **6a** and **6b**) were compared to their analogues of indoloquinoline ligands (**1b**, **4a** and **4b**). The main difference of these ligands is located in the seven membered azepine ring instead of the planar six membered ring found in indoloquinolines. [35]

Comparison between indoloquinoline and Paullone complexes of ruthenium(II) and osmium(II) has been reported in literature. [25] The comparison of **4b** with

6b and **1b** with **5** in SW480 cells showed the highest difference with a 6 and 9 times higher cytotoxicity of the indoloquinoline complexes (**Fig. 19**). In contrast, **4a** and **6a** have a comparable cytotoxicity in all three cell lines. There can be several reasons for the generally smaller differences as well as the generally higher cytotoxicity of the copper(II) complexes. One may be related to the different central metal (copper(II) instead of ruthenium(II) or osmium(II)) or the different side chain of the ligands and with it the consequences for coordination of the metal or a combination of both. [35]

For ruthenium(II) and osmium(II) complexes IC_{50} values in the micromolar range were found. A549 was the least sensitive cell line for all the tested compounds. For three of them (**8b**, **9a**, **9b**), it was not possible to determine IC_{50} values ($> 80 \mu\text{M}$) due to the insufficient solubility in medium. Furthermore no IC_{50} values in SW480 could be determined for **9a**. Some compounds showed a four-fold increase of cytotoxicity (**7a**) in SW480 and up to forty times (**8a**) lower IC_{50} values in CH1 than in A549.

Comparison of the ruthenium(II) with the osmium(II) complexes revealed the following relationships: In general CH1 is 9-40 times more sensitive than the cell line A549, and for all tested compounds IC_{50} values were reached with applicable concentrations. In A549 cells, ruthenium complexes (**7a**, **8a**) are more active than osmium complexes (**7b**, **8b**). In CH1 and SW480 cells, ruthenium complexes are at least twice up to four times more active than osmium complexes except for the pair **9a** and **9b**, of which the osmium complex is more active. A reason could be the structural difference at the lactam unit. The ruthenium compound **9a** is the least active one of all tested compounds. **7a** compared with **8a** (chloro substituent at position 6) showed twice as high activity in A549 and SW480 cells, whereas in CH1 cells **7a** is less active. **7b** and **8b** give a similar picture, except that in SW480 cells the IC_{50} values are nearly the same.

Tab. 2 50% inhibitory concentrations (means \pm standard deviations from at least three independent experiments), as obtained by the MTT assay using exposure times of 96 h.

compound	IC ₅₀ (μ M), 96 h		
	A549	SW480	CH1
1a	1.72 \pm 0.03	1.3 \pm 0.1	0.40 \pm 0.07
1b	0.18 \pm 0.04	0.024 \pm 0.001	0.030 \pm 0.005
2a	1.7 \pm 0.1	0.75 \pm 0.04	0.33 \pm 0.07
2b	0.14 \pm 0.01	0.024 \pm 0.002	0.026 \pm 0.006
3a	1.4 \pm 0.3	0.64 \pm 0.11	0.41 \pm 0.05
3b	0.23 \pm 0.01	0.049 \pm 0.003	0.065 \pm 0.012
4a	1.6 \pm 0.1	0.47 \pm 0.03	0.36 \pm 0.03
4b	0.20 \pm 0.03	0.032 \pm 0.004	0.052 \pm 0.008
5	0.67 \pm 0.15	0.21 \pm 0.04	0.064 \pm 0.015
6a	1.28 \pm 0.03	0.40 \pm 0.04	0.28 \pm 0.03
6b	0.43 \pm 0.03	0.18 \pm 0.02	0.080 \pm 0.005
7a	27 \pm 3	7.03 \pm 1.66	3.2 \pm 0.3
7b	53 \pm 9	28 \pm 6	9.9 \pm 2.1
8a	51 \pm 2	17 \pm 3	1.3 \pm 0.5
8b	> 80	25 \pm 2	3.1 \pm 0.8
9a	> 80	> 80	20 \pm 2
9b	> 80	48 \pm 5	7.9 \pm 0.9

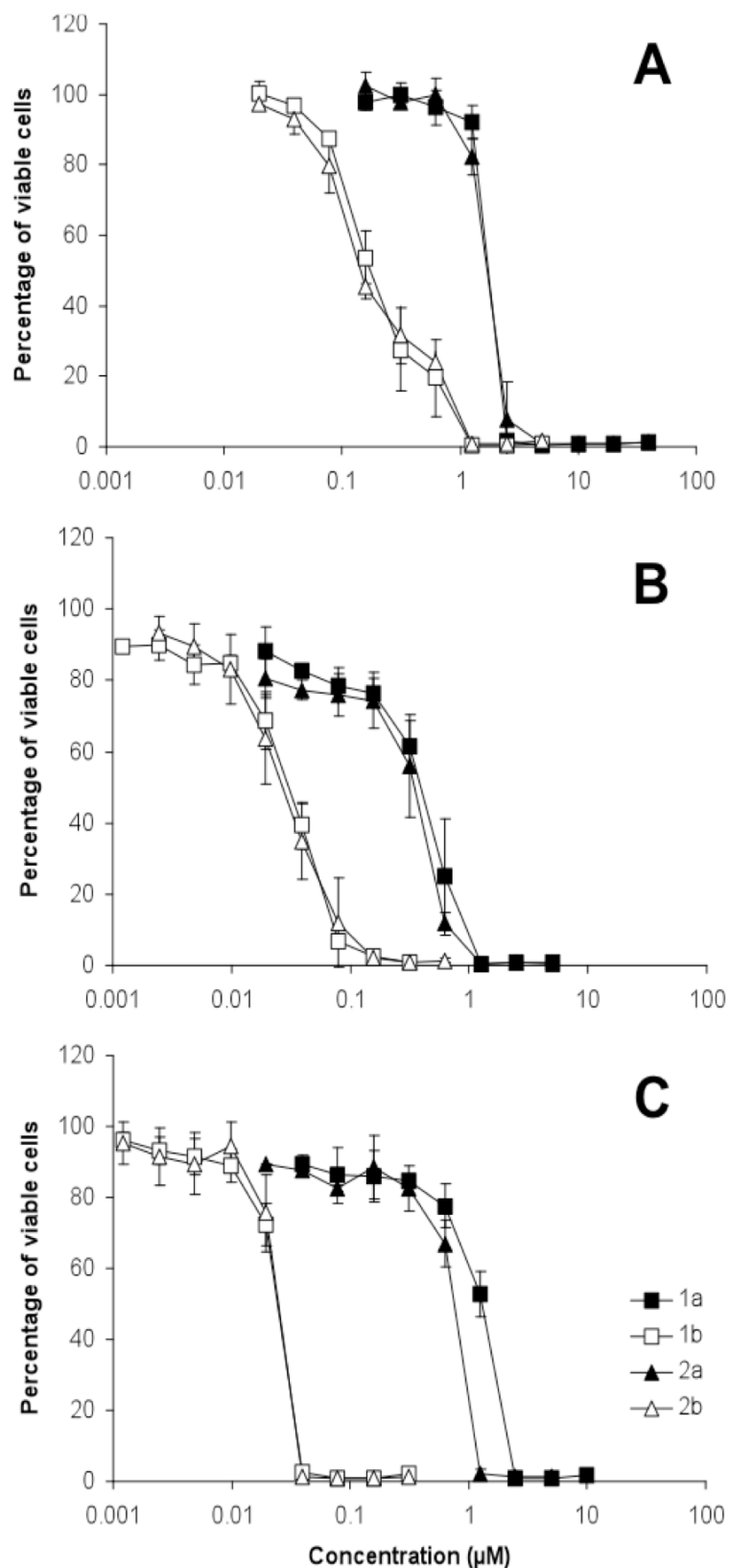


Fig. 18 Concentration-effect curves of copper-indoloquinoline complexes **1a**, **1b**, **2a** and **2b** in the human cancer cell lines A549 (A), CH1 (B), SW480 (C), indicating the different impact of methyl substitution depending on the position. [35]

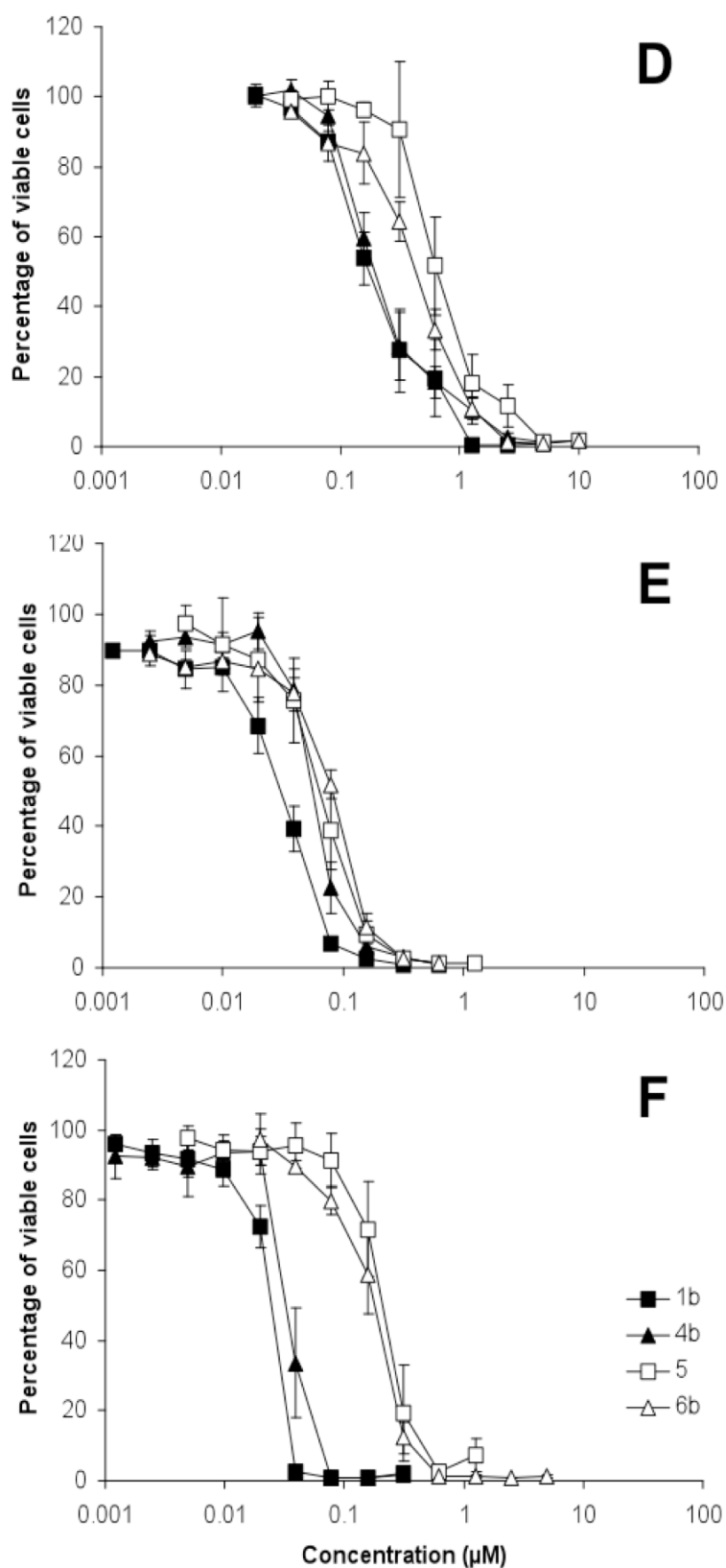


Fig. 19 Concentration-effect curves of copper-indoloquinoline complexes **1b** and **4b** in comparison with the corresponding Paullone complexes **5** and **6b** in the human cancer cell lines A549 (D), CH1 (E), SW480 (F), all determined by the MTT assay using continuous exposure for 96 h. [35]

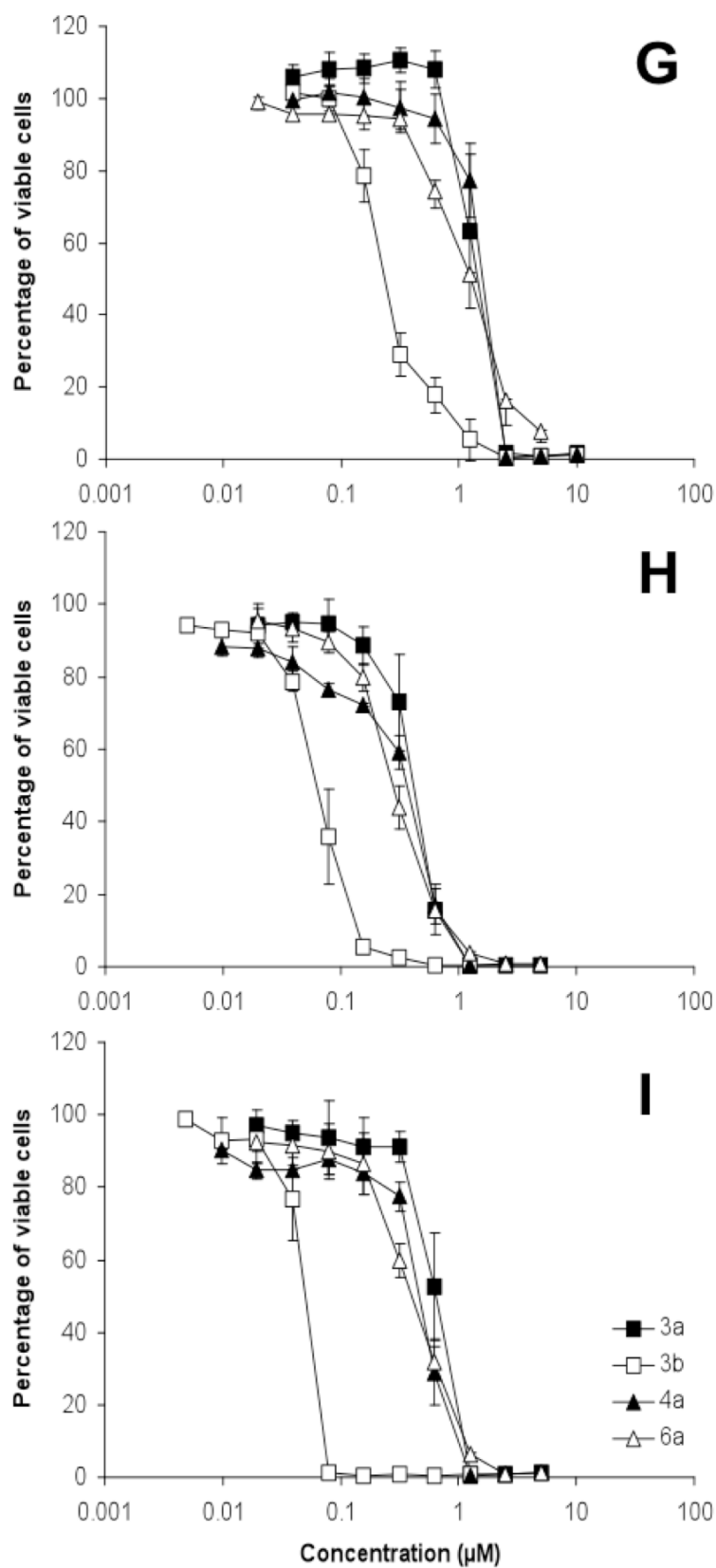


Fig. 20 Concentration-effect curves of copper-indoloquinoline complexes **3a**, **3b**, **4a** and copper-Paullone complex **6a** in the human cancer cell lines A549 (G), CH1 (H), SW480 (I), determined by the MTT assay using continuous exposure for 96 h. [35]

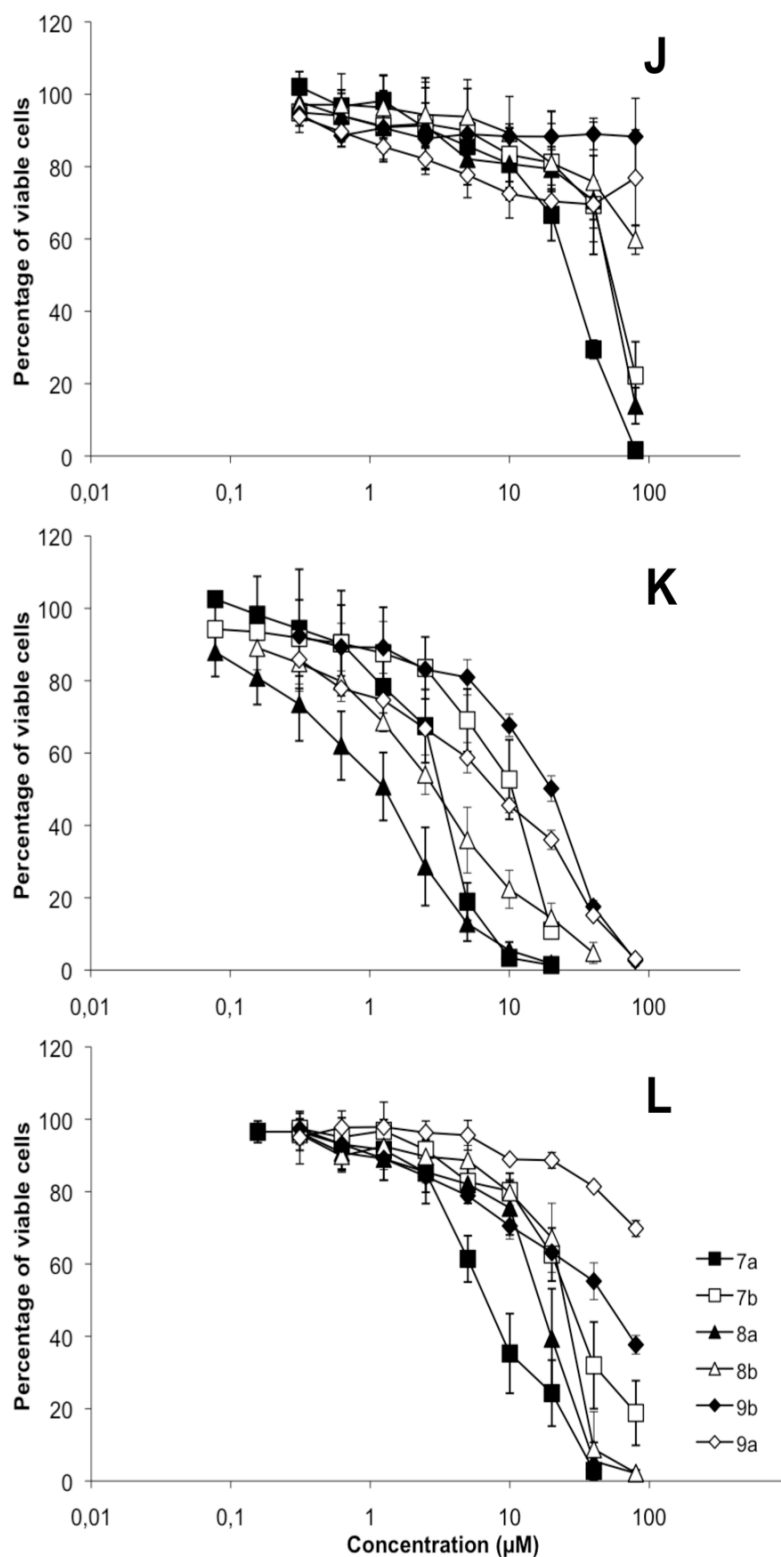


Fig. 21 Concentration-effect curves of ruthenium- and osmium- indoloquinoline complexes **7a**, **7b**, **8a**, **8b**, **9a** and **9b** in the human cancer cell lines A549 (J), CH1 (K), SW480 (L), determined by the MTT assay using continuous exposure for 96 h.

4.2 Cell Cycle Analysis

Filak et al. [29] stated that indoloquinolines show effect on the cell cycle. They observed that the complexes lead to an arrest in the G2/M phase and inhibition of cdk2/cyclin E was found in a cell free setting.

Based on this fact, the activity on the cell cycle of the copper complexes **1a**, **1b**, **2a**, and **2b** was tested. Incubation time (24 h) and concentrations were chosen in such a way that apoptosis was avoided.

As seen in **Fig. 22** and **Fig. 23**, none of the tested compounds showed a significant effect on the cell cycle. The sub G0 peak or the debris (results not shown) was nearly the same in all measured samples, with an average amount of 2%, indicating that the chosen concentrations of the compounds do not cause cell death to a noteworthy extent. Because of the lack of cell cycle effects we did not expect a relevant effect on cdk activity. In fact, these observations strongly argue against cdk as the critical target of these complexes. This was the reason why cdk inhibition was not studied.

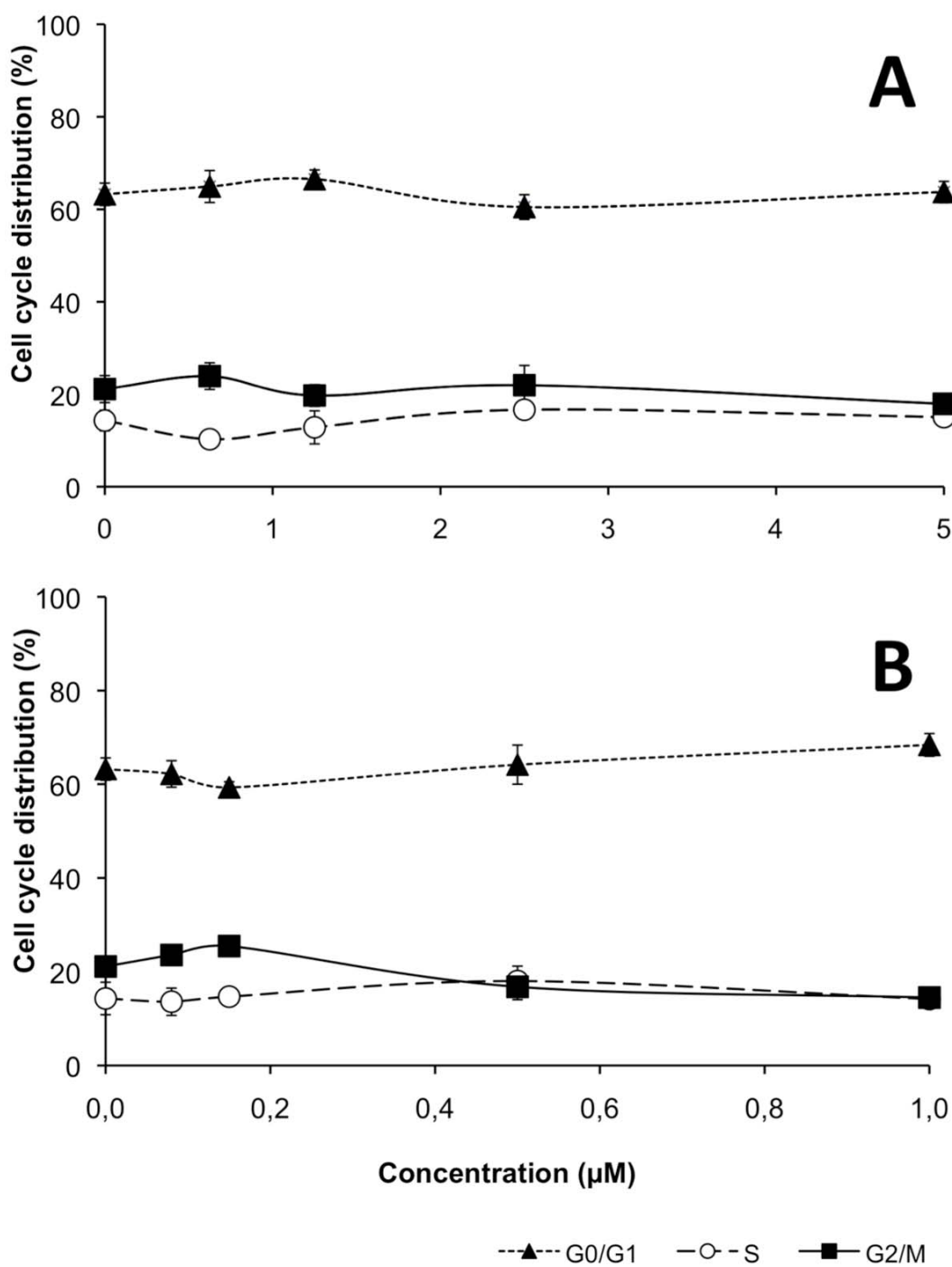


Fig. 22 Concentration-effect curves of complexes **1a** (A) and **1b** (B) in the human cancer cell line A549, determined by cell cycle analysis using continuous exposure for 24h

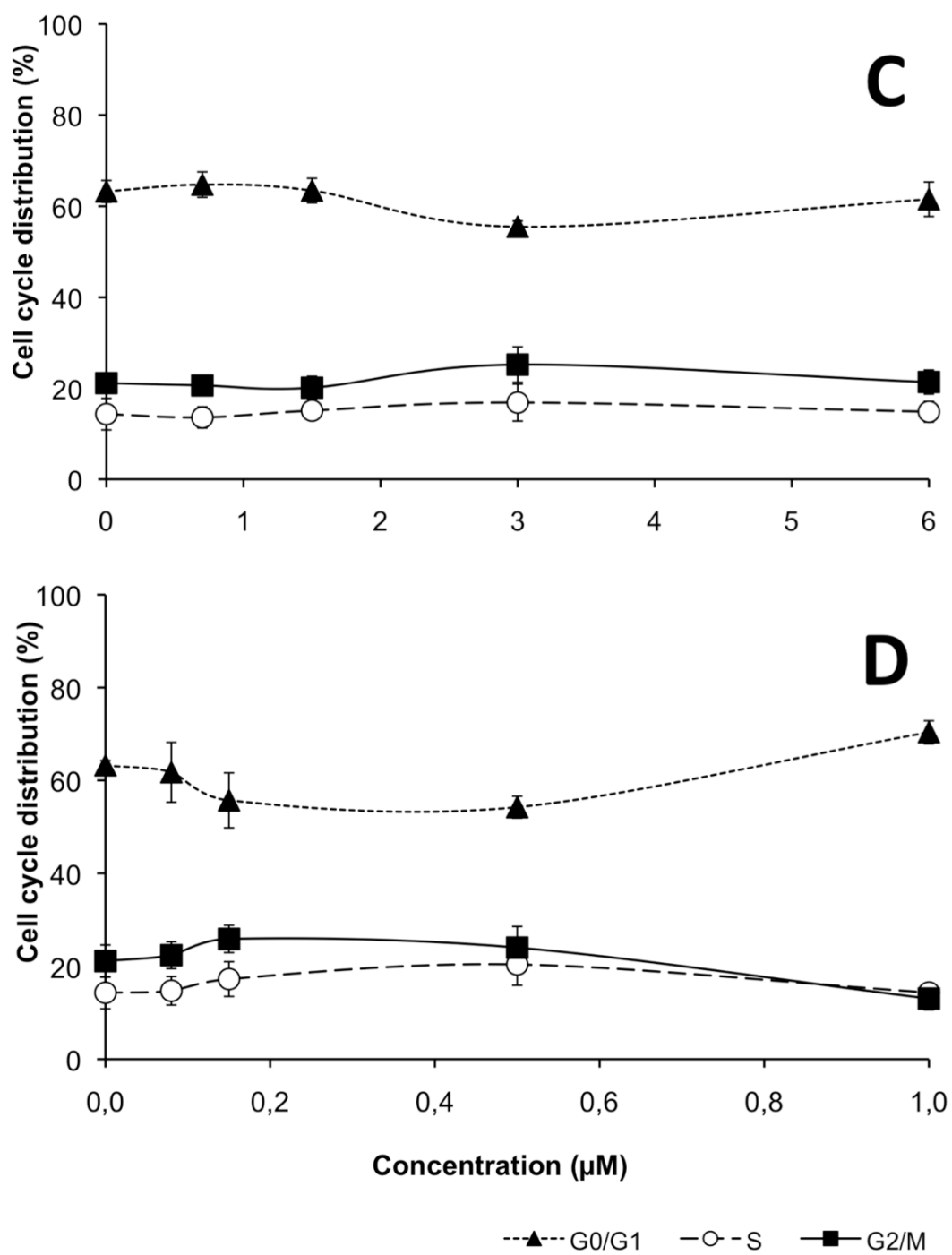


Fig. 23 Concentration-effect curves of complexes **2a** (C) and **2b** (D) in the human cancer cell line A549, determined by cell cycle analysis using continuous exposure for 24h

4.3 Intercalation

As reported in Filak et al. [22], indoloquinolines show a high potential to intercalate into dsDNA. Due to the reported results, intercalation ability of compounds **1a-2b** was expected. Ethidium bromide (EtBr) and $[(\eta^6\text{-p-Cymene})\text{-Os}^{\text{II}}(\text{L}^2)\text{Cl}]\text{Cl}, (\eta^6\text{-p-cymene})(\kappa\text{N}^1\text{-[11H-indolo[3,2-c]quinolin-6-ylidene]-}\kappa\text{N,N-dimethylethane-1,2-diamine})\text{chloridoosmium(II)chloride}$ (KP1779), a strongly DNA intercalating compound of similar structural form, were used as positive controls to prove that the change of the solvent from PBS to medium does not affect the performance of the method. As shown in **Fig. 23**, methyl green displacement of about 90% by EtBr as well as intercalation by KP1779 comparable to Filak et al. were found. These results confirm that the method is not affected. To exclude effects caused by the usage of DMSO as substance solvent, the same amount of DMSO was added to every sample. Hence, no errors should be produced by that.

For the copper compounds, no reliable and meaningful degree of intercalation was found. Even some rather mind negative values can be seen in some cases. These might suggest a slight enhancement of methyl green binding to DNA, but might as well be mere artifacts of unknown come.

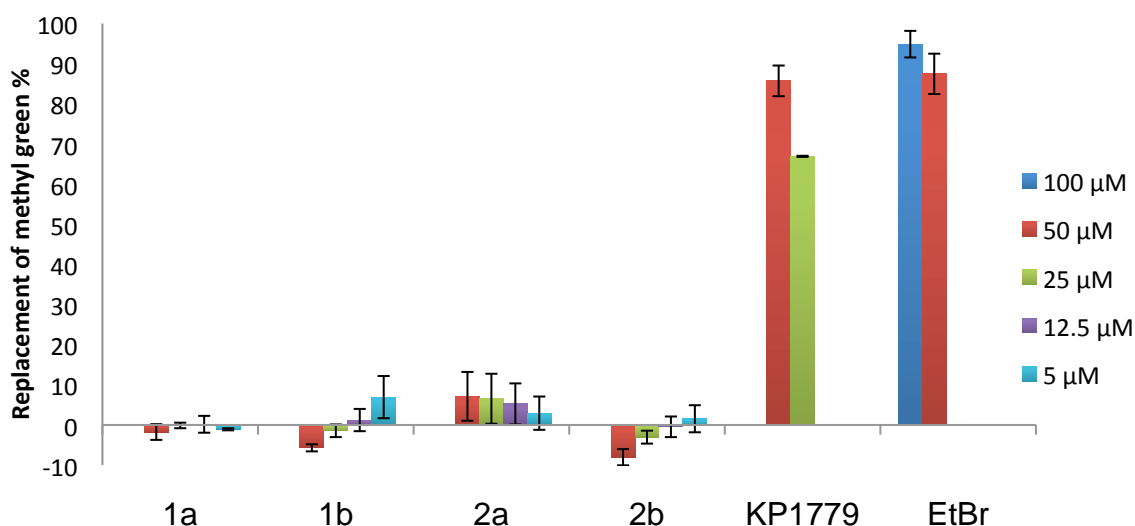


Fig. 24 Replacement of methyl green of **1a**, **1b**, **2a**, **2b**, KP1779 and EtBr at different concentrations

Although the structurally related compound KP1779 is showing intercalating properties, the copper(II) indoloquinolines are not active in the methyl green assay. The comparison of KP1779 and the tested copper compounds shows different coordination sites of the metals. In the case of copper(II) complexes, copper is coordinated via the quinoline nitrogen to the indoloquinoline moiety, whereas in KP1779 osmium(II) is coordinated only via the side chain of the ligand. As quinoline is the potential intercalation site, [53] it seems that the coordination of copper is hindrance enough that an intercalation is not possible any longer.

4.4 Western Blot

For Western blot analysis two copper(II) compounds **1a** and **1b** were examined. **1a** is the copper(II) complex with an indoloquinoline ligand lacking substituents in position 8 and 14, and **1b** is the analogue with a methyl substituent at position 14. MTT cytotoxicity test showed that this substitution results in strongly cytotoxicity (**Tab. 2**). These compounds were chosen to determine if apoptosis is induced via a pathway involving PARP/cleaved PARP. For Western blotting, treated CH1 cells were used (IC_{50} values of $0.40 \pm 0.07 \mu\text{M}$ for **1a** and $0.030 \pm 0.005 \mu\text{M}$ for **1b**).

In a first experiment, cells were treated with concentrations of 0.2-2 μM for **1a** and 0.05-1 μM for **1b** over 24 h. With increasing concentrations of the compounds the intensities of the PARP bands are decreasing, but surprisingly no cleaved PARP was observed **Fig. 25**. To control that comparable protein amounts were added onto the gel, β -actin was used as loading control. Actin is omnipresent in the cell and the β -form is also known as cytoplasmic actin [54], furthermore under apoptotic conditions, actin is degraded.[55] The β -actin control illustrates that less proteins were added in samples treated with the highest concentration, which seems to be too cytotoxic.

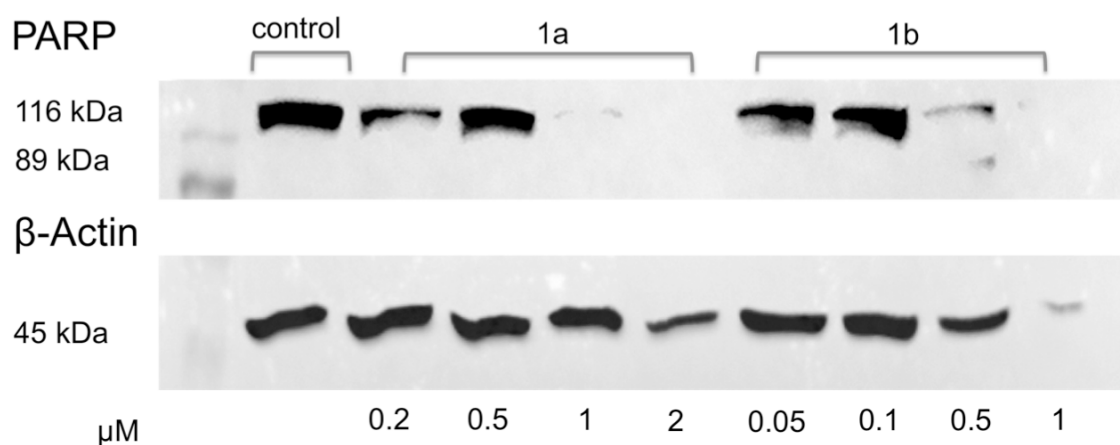


Fig. 25 Detection of PARP (116 kDa), and cleaved PARP (89 kDa) by Western blotting, after continuous exposure for 24 h with **1a** and **1b**. Control bands of β -actin at 45 kDa.

In the second experiment, the incubation time was reduced and the concentrations of the compounds were increased. After 18 h cleaved PARP was found in the case of **1a** treatment nearly in every concentration and in case

of **1b** at least in one (1 μM), but again the loaded protein concentrations were not equal. β -actin and PARP could not be detected in samples from cells treated with the highest concentration of **1b**, however reduced amounts of PARP were detected in the case of the two highest concentrations of **1a** and in 2 μM and 3 μM of **1b** (**Fig. 26**).

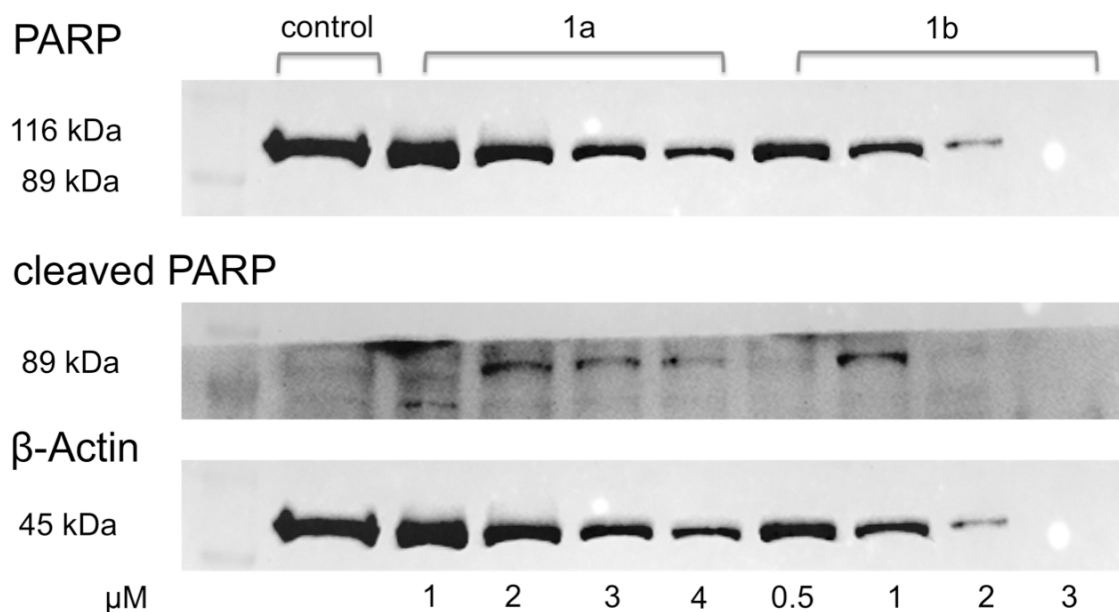


Fig. 26 Detection of PARP (116 kDa), and cleaved PARP (89 kDa) by Western Blotting, after continuous exposure for 18 h with **1a** and **1b**. Control bands of β -actin at 45 kDa.

In the next experiment the incubation time was reduced from 18 h to 12 h using the same concentrations of **1a** and **1b**. The results were not encouraging, nearly no cleaved PARP was found, which could be an evidence that apoptosis has not started after 12 h (**Fig. 27**).

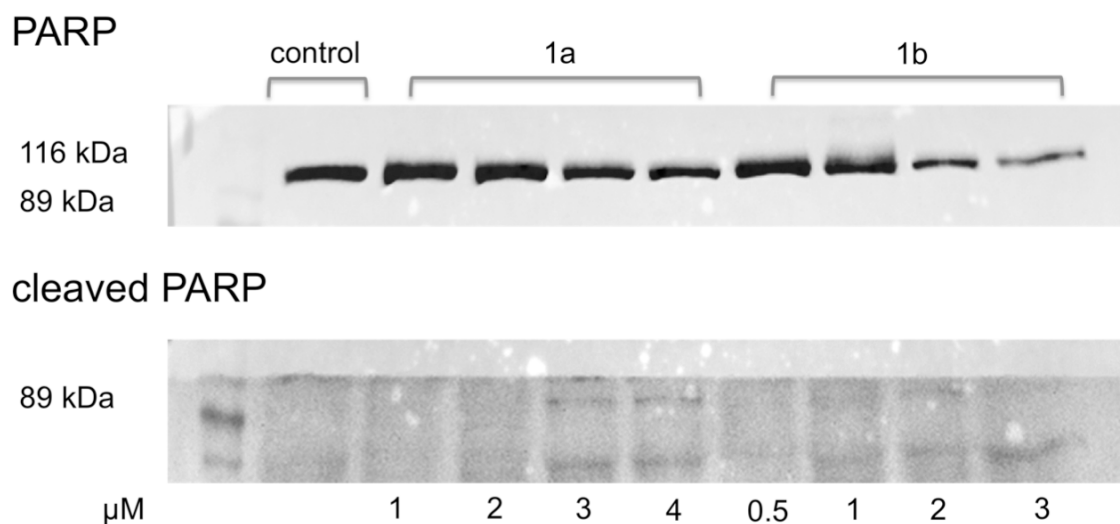


Fig. 27 Detection of PARP (116 kDa), and cleaved PARP (89 kDa) by Western blotting, after continuous exposure for 12 h with **1a** and **1b**.

As a consequence the incubation time was increased to 16 h with highest concentration of 4 μM for **1a** and 2 μM for **1b**. **Fig. 28** shows that cleavage of PARP occurred and β -actin bands indicate that the protein concentration was the same for all concentrations.

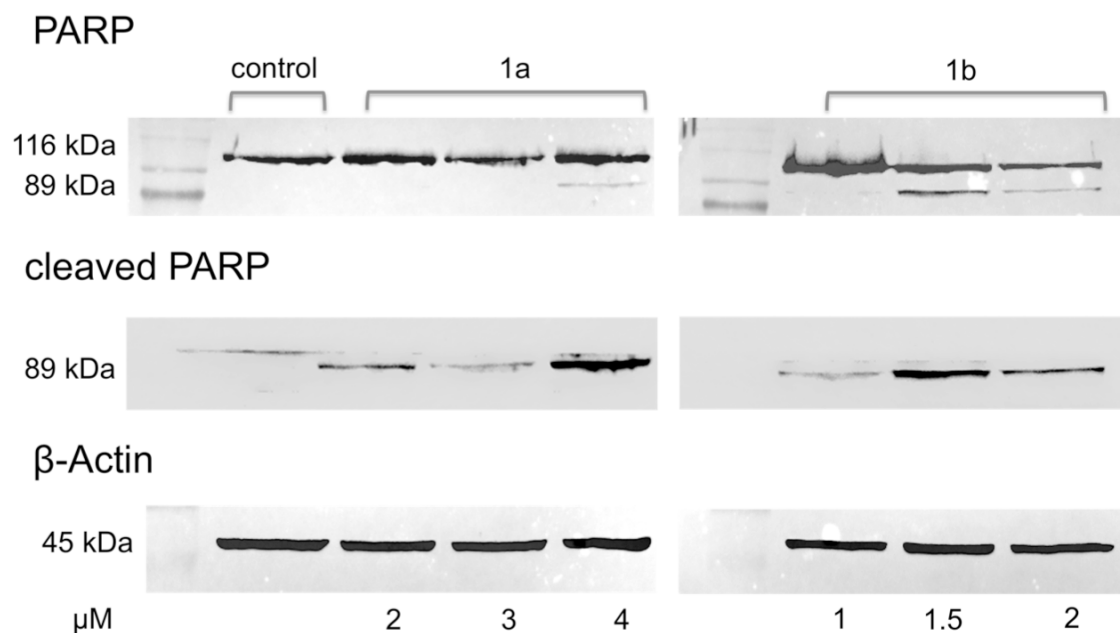


Fig. 28 Detection of PARP (116 kDa), and cleaved PARP (89 kDa) by Western blotting, after continuous exposure for 16 h with **1a** and **1b**. Control bands of β -actin at 45 kDa.

As a final conclusion of the Western blot analysis, the compounds **1a** and **1b** induce apoptosis via a pathway involving PARP/cleaved PARP. The incubation time and the concentrations are critical factors for induction of apoptosis. Different protein concentrations are caused by too long incubation or high concentrations. The optimal conditions for these compounds were found after 16 h incubation with the described concentrations.

5 Conclusions

Copper(II), ruthenium(II) and osmium(II) complexes with modified indoloquinoline ligands have been tested for their antitumor efficiency in vitro, by use of the following techniques: cytotoxicity tests, cell cycle analysis, intercalation experiments and Western blot studies.

All copper(II) compounds exhibited high cytotoxic effects in all tested cell lines, furthermore IC_{50} values down to micromolar and nanomolar range have been found. In contrast to Filak et al. [25], the expected cytotoxic activity of the ruthenium(II) and osmium(II) complexes was not observed most likely as a consequence of the altered substitution pattern of the ligands.

Due to the encouraging results of the copper(II) compounds, cell cycle analysis and intercalation experiments with compounds **1a**, **1b**, **2a** and **2b** were performed. Previous studies [25] demonstrated that indoloquinolines show an effect on the cell cycle, leading to a G2/M arrest, and a high extend of intercalation (80% replacement of methyl green) was detected. As a consequence, similar results for the copper complexes were expected. However, no effects on the cell cycle and no intercalating properties were found. These data indicate that perhaps cdks are not the crucial target and maybe other DNA interactions with these new compounds are playing an important role.

In addition, Western blot studies of the apoptosis marker PARP/cleaved PARP were performed. Incubation time of 16 h and concentrations of 2-4 μ M of **1a** and 1-2 μ M of **1b** were chosen in order to provide an optimal setting for apoptosis and PARP cleavage. Both compounds showed cleaved PARP bands from which follows that **1a** and **1b** are inducing apoptosis.

Finally, these results are leading to the conclusion that metal complexes with indoloquinoline ligands have a high potential for antitumor activity. Further studies are necessary to verify the main target of these compounds, in addition the cellular uptake of the complexes as well as drug-DNA interactions are points of interest.

6 References

1 History of Cancer

<http://www.cancer.org/Cancer/CancerBasics/TheHistoryofCancer/index> (2011-06-16)

2 WHO, Cancer Fact Sheet N°297 / February 2011

<http://www.who.int/mediacentre/factsheets/fs297/en/index.html> (2011-06-16)

3 GLOBOCAN 2008 (IARC) Section of Cancer Information

<http://globocan.iarc.fr/factsheets/populations/factsheet.asp?uno=900> (2011-06-16)

4 D. Hanahan, R. A. Weinberg, "Hallmarks of Cancer: The Next Generation", *Cell*, vol. 144, pp. 646-674, 2011

5 R.E. Lenhard et al, "Clinical Oncology" *The American Cancer Society's*, American Cancer Society, 2001

6 A.E. Chang et al, "Oncology An Evidence-Based Approach", Springer Science+Business Media, 2006

7 Österreichische Krebshilfe Wien

<http://www.krebshilfe-wien.at/Therapien.20.0.html> (2011-06-18)

8 Wollrab, "Organische Chemie Eine Einführung für Lehramts- und Nebenfachstudenten", Springer, 3. Auflage, 2009

9 C.E. Housecroft, A.G. Sharpe, "Inorganic chemistry" Pearson Prentice Hall, 2nd Edition, 2005

10 K.J.D. Mackenzie et al., "Multinuclear Solid-State NMR of Inorganic Materials" Pergamon Materials Series, Pergamon, 2002

- 11 S. Murahashi, "Ruthenium in Organic Synthesis", WILEY-VCH Verlag GmbH & Co. KGaA, 2004
- 12 M.A. Jakupec, M. Galanski, V.B. Arion, C.G. Hartinger B. K. Keppler, "Antitumour metal compounds: more than theme and variations", *Dalton Transactions*, pp. 183-194, 2008
- 13 C.G. Hartinger, S. Zorbas-Seifried, M.A. Jakupec, B. Kynast, H. Zorbas, B.K. Keppler, "From bench to bedside – preclinical and early clinical development of the anticancer agent indazolium trans-[tetrachlorobis(1H-indazole)ruthenate(III)] (KP1019 or FFC14A)", *Journal of Inorganic Biochemistry*, vol. 100, pp. 891–904, 2006
- 14 T. Gianferrara, I. Bratsos, E. Alessio, "A categorization of metal anticancer compounds based on their mode of action", *Dalton Transactions*, pp. 7588–7598, 2009
- 15 G. Hartinger, M.A. Jakupec, S. Zorbas-Seifried, et al., "KP1019, A New Redox-Active Anticancer Agent – Preclinical Development and Results of a Clinical Phase I Study in Tumor Patients", *CHEMISTRY & BIODIVERSITY*, vol. 5, pp. 2140-2155, 2008
- 16 P.J. Dyson, "Systematic Design of a Targeted Organometallic Antitumour Drug in Pre-clinical Development", *Chimia*, vol. 61, pp. 698-703, 2007
- 17 W.H. Ang, P.J. Dyson, "Classical and Non-Classical Ruthenium-Based Anticancer Drugs: Towards Targeted Chemotherapy", *European Journal of Inorganic Chemistry*, pp. 4003-4018, 2006
- 18 A. F Holleman, E. Wiberg, „Lehrbuch der Anorganischen Chemie“, de Gruyter, 101st Edition, 1995
- 19 W.F. Schmid R. O. John, G. Mühlgassner, et al., "Metal-Based Paullones as Putative CDK Inhibitors for Antitumor Chemotherapy", *Journal of Medicinal Chemistry*, vol. 50, pp. 6343-6355, 2007

- 20 A.F.A. Peacock, M.Melchart, R.J. Deeth et al., "Osmium(II) and Ruthenium(II) Arene Maltolato Complexes: Rapid Hydrolysis and Nucleobase Binding", *Chemistry A European Journal*, vol. 13, pp. 2601-2613, 2007
- 21 A.F.A. Peacock, A. Habtemariam, R. Fernández et al., "Tuning the Reactivity of Osmium(II) and Ruthenium(II) Arene Complexes under Physiological Conditions", *Journal of the American Chemical Society*, vol. 128, pp. 1739-1748, 2006
- 22 A.F.A. Peacock, S. Parsons, P.J. Sadler, "Tuning the Hydrolytic Aqueous Chemistry of Osmium Arene Complexes with N,O-Chelating Ligands to Achieve Cancer Cell Cytotoxicity", *Journal of the American Chemical Society*, vol. 129, pp. 3348-3357, 2007
- 23 Rowinsky EK, Donehower RC, Perry MC(ed) The chemotherapy source book, vol. , Williams & Wilkins, Baltimore, 1998
- 24 Donehower RC, Rowienstky EK, De Vita VT, Hellman S, Rosenberg SA (eds), Cancer: principles and practice oncology, Lippincott, Philadelphia, 1993
- 25 L. Filak, G. Mühlgassner, M.A. Jakupec, P. Heffeter, W. Berger, V.B. Arion, B.K. Keppler, "Organometallic indolo[3,2-c]quinolines versus indolo[3,2-d]benzazepines: synthesis, structural and spectroscopic characterization, and biological efficacy", *Journal of Biological Inorganic Chemistry*, vol. 15, No.6, pp. 903-918, 2010
- 26 Onyeibor, O.; Croft, S. L.; Dodson, H. I.; Feiz-Haddad, M.; Kendrick, H.; Millington, N. J.; Parapini, S.; Phillips, R. M.; Seville, S.; Shnyder, S. D.; Taramelli, D.; Wright, C. W.," Synthesis of Some Cryptolepine Analogues, Assessment of Their Antimalarial and Cytotoxic Activities, and Consideration of Their Antimalarial Mode of Action", *Journal of Medicinal Chemistry*, vol. 48, pp. 2701-2709, 2005

- 27 Y.L. Chen, C.H. Chung, I.L. Chen, P.H. Chen, H.Y. Jeng, "Synthesis and Cytotoxic Activity Evaluation of Indolo-, Pyrrolo-, and Benzofuro-Quinolin-2(1H)-Ones and 6-Anilinoindoloquinoline Derivatives", *Bioorganic & Medicinal Chemistry*, vol. 10, pp. 2705–2712, 2002
- 28 Y.L. Chen, H.M. Hung, C.M. Lu, K.C. Li, C.C. Tzeng, "Synthesis and anticancer evaluation of certain indolo[2,3-b]quinoline derivatives", *Bioorganic & Medicinal Chemistry*, vol. 12, pp. 6539-6546, 2004
- 29 L.K. Filak, G. Mühlgassner, F. Bacher, A. Roller, M. Galanski, M.A. Jakupec, B.K. Keppler, V.B. Arion, "Ruthenium- and Osmium-Arene Complexes of 2-Substituted Indolo[3,2-c]quinolines: Synthesis, Structure, Spectroscopic Properties, and Antiproliferative Activity", *Organometallics*, vol. 30, pp. 273-283, 2011
- 30 C. Schultz, A. Link, M. Leost, et al., „ Paullones, a Series of Cyclin-Dependent Kinase Inhibitors: Synthesis, Evaluation of CDK1/Cyclin B Inhibition, and in Vitro Antitumor Activity“, *Journal of Medicinal Chemistry*, vol. 42, pp. 2909-2919, 1999
- 31 T. Mosmann, "Rapid Colorimetric Assay for Cellular Growth and Survival: Application to Proliferation and Cytotoxicity Assays", *Journal of Immunological Methods*, vol. 65, pp. 55-63, 1983
- 32 Y. Liu, D. A. Peterson, H. Kimura, D. Schubert, "Mechanism of Cellular 3-(4,5-Dimethylthiazol-2-yl) -2,5- Diphenyltetrazolium Bromide (MTT) Reduction", *Journal of Neurochemistry*, vol. 69, No. 2, pp. 581-593, 1997
- 33 D. Gelier, N. Thomasset," Use of MTT colorimetric assay to measure cell activation", *Journal of Immunological Methods*, vol. 94, pp. 57-63, 1986
- 34 S. P. Langdon, "Cancer Cell Culture Methods and Protocols", *Methods in Molecular Medicine*, Humana Press, 2004

- 35 M. Primik, S. Göschl, M. A. Jakupec, A. Roller, B. K. Keppler, V. B. Arion, "Structure-Activity Relationships of Highly Cytotoxic Copper(II) Complexes with Modified Indolo[3,2-c]quinoline Ligands", *Inorganic Chemistry*, vol. 49, No. 23, pp. 11084-95, 2010
- 36 R.D. Blumenthal, "Chemosensitivity Volume 1 In Vitro Assays", *Methods in Molecular Medicine*, Humana Press, 2005
- 37 Alberts et al, "Molecular Biology of the Cell", Taylor & Francis Group, 5th Edition, 2008
- 38 A. Krishan, "Rapid Flow Cytofluorometric Analysis of Mammalian Cell Cycle by Propidium Iodide Staining", *The Journal of Cell Biology*, vol. 66, No.1, pp. 188-193, 1975
- 39 H.B. Lieberman, "Cell Cycle Check point Control Protocols", *Methods in Molecular Biology*, vol. 241, Humana Press, 2004
- 40 Methyl green, Sigma Aldrich
http://www.sigmaaldrich.com/catalog/ProductDetail.do?lang=de&N4=M8884|SIAL&N5=SEARCH_CONCAT_PNO|BRAND_KEY&F=SPEC (31.10.2011)
- 41 S.K. Kim, B. Nordén, "Methyl green A DNA major-groove binding drug", *Federation of European Biochemical Societies*, vol. 315, no.1, pp. 61-64, 1993
- 42 N. B. Kurnick, M. Foster, "Reaction with desoxyribonucleic acid, stoichiometry, and behavior of the reaction product" *The Journal of General Physiology*, pp. 147-159, 1950
- 43 N.S. Burres, A. Frigo, R.R. Rasmussen, J.B. McAlpine, "A colorimetric microassay for the detection of agents that interact with DNA", *Journal of Natural Products*, vol. 55, no. 11, pp. 1582-1587, 1992
- 44 R. Dornetshuber, P. Heffeter, R. Lemmens-Gruber et al., "Oxidative stress and DNA interactions are not involved in Enniatin- and Beauvericin-mediated apoptosis induction" *Molecular Nutrition & Food Research*, vol. 53, pp. 1112-1122, 2009

- 45 A.K. Krey, F.E. Hahn, "Studies on the Methyl Green - DNA complex and its dissociation drugs", *Biochemistry*, vol. 14, no. 23, pp. 5061-5067, 1975
- 46 W. Luttmann et al, "Der Experimentator Immunologie", Spektrum Akademischer Verlag, 3rd Edition, 2009
- 47 A. H.Boulares, A. G. Yakovlev, V. Ivanova, B. A. Stoica, G. Wang, S. Iyer, M. Smulson, "Role of Poly(ADP-ribose) Polymerase (PARP) Cleavage in Apoptosis CASPASE 3-RESISTANT PARP MUTANT INCREASES RATES OF APOPTOSIS IN TRANSFECTED CELLS", *The Journal of Biological Chemistry*, vol. 274, No.33, pp. 22932-22940, 1999
- 48 PARP Antibody #9542, Cell Signaling Technology, rev. 07/22/10
- 49 C. Soldani, A. I. Scovassi, "Poly(ADP-ribose) polymerase-1 cleavage during apoptosis: An update", *Apoptosis*, vol. 7, pp. 321-328, 2002
- 50 J. Fried, A.G. Perez, B.D. Clarkson, "Rapid Hypotonic Method for flow cytofluorometry of monolayer cell cultures some pitfalls in staining and data analysis", *The Journal of Histochemistry and Cytochemistry*, vol. 26, No.11, pp. 921-933, 1978
- 51 I. Nicoletti, G. Migliorati, M.C. Pagliacci, F. Grignani, C. Riccardi, "A rapid and simple method for measuring thymocyte apoptosis by propidium iodide staining and flow cytometry", *Journal of Immunological Methods*, vol. 139, pp. 271-279, 1991
- 52 Stripping for reprobing western blots, abcam,
<http://www.abcam.com/ps/pdf/protocols/Stripping%20for%20reprobing.pdf>
(2011-06-21)
- 53 V.E. Marquez, J.W. Cranston, R.W. Ruddon, L.B. Kier, J.H. Burckhalter, "Mechanism of action of amodiaquine. Synthesis of its indoloquinoline analog", *Journal of Medicinal Chemistry*, vol. 15, No. 1, pp. 36-39, 1972
- 54 β -Actin (13E5) Rabbit mAb Antibody, #4970, Cell Signaling Technology, rev. 11/17/10

55 C. Kayalar, T. Örd, et al., "Cleavage of actin by interleukin 1 β -converting enzyme to reverse DNase I inhibition", *Proceedings of the National Academy of Sciences*, vol. 93, pp. 2234-2238, 1996

7 Appendix

M. Primik, S. Göschl, M. A. Jakupec, A. Roller, B. K. Keppler, V. B. Arion, "Structure-Activity Relationships of Highly Cytotoxic Copper(II) Complexes with Modified Indolo[3,2-c]quinoline Ligands", *Inorganic Chemistry*, vol. 49, No. 23, pp. 11084-95, 2010

11084 *Inorg. Chem.* 2010, 49, 11084–11095
DOI: 10.1021/ic101633z

Inorganic Chemistry
Article

Structure–Activity Relationships of Highly Cytotoxic Copper(II) Complexes with Modified Indolo[3,2-*c*]quinoline Ligands

Michael F. Primik, Simone Göschl, Michael A. Jakupec, Alexander Roller, Bernhard K. Keppler, and Vladimir B. Arion*

Institute of Inorganic Chemistry, University of Vienna, Währinger Str. 42, A-1090 Vienna, Austria

Received August 11, 2010

A number of indolo[3,2-*c*]quinolines were synthesized and modified at the lactam unit to provide a peripheral binding site able to accommodate metal ions. Potentially tridentate ligands HL^{1a} – HL^{4a} and HL^{1b} – HL^{4b} were reacted with copper(II) chloride in isopropanol/methanol to give novel five-coordinate copper(II) complexes $[\text{Cu}(\text{HL}^{1a-4a})\text{Cl}_2]$ and $[\text{Cu}(\text{HL}^{1b-4b})\text{Cl}_2]$. In addition, a new complex $[\text{Cu}(\text{HL}^{5b})\text{Cl}_2]$ and two previously reported compounds $[\text{Cu}(\text{HL}^{6a})\text{Cl}_2]$ and $[\text{Cu}(\text{HL}^{6b})\text{Cl}_2]$ with modified paullone ligands HL^{5b} , HL^{6a} , and HL^{6b} , which can be regarded as close analogues of indoloquinolines HL^{1b} , HL^{4a} , and HL^{4b} , in which the pyridine ring was formally substituted by a seven-membered azepine ring, were synthesized for comparison. The new ligands and copper(II) complexes were characterized by ^1H and ^{13}C NMR, IR and electronic absorption spectroscopy, ESI mass spectrometry, magnetic susceptibility measurements in solution at 298 K ($[\text{Cu}(\text{HL}^{1a})\text{Cl}_2]$ and $[\text{Cu}(\text{HL}^{4b})\text{Cl}_2]$), and X-ray crystallography ($[\text{Cu}(\text{HL}^{3b})\text{Cl}_2] \cdot 3\text{DMF}$, $[\text{Cu}(\text{HL}^{4b})\text{Cl}_2] \cdot 2.4\text{DMF}$, HL^{5b} and $[\text{Cu}(\text{HL}^{5b})\text{Cl}_2] \cdot 0.5\text{CH}_3\text{OH}$). All complexes were tested for cytotoxicity in the human cancer cell lines CH1 (ovarian carcinoma), A549 (non-small cell lung cancer), and SW480 (colon carcinoma). The compounds are highly cytotoxic, with IC_{50} values ranging from nanomolar to very low micromolar concentrations. Substitution of the seven-membered azepine ring in paullones by a pyridine ring resulted in a six- to nine-fold increase of cytotoxicity in SW480 cells. Electron-releasing or electron-withdrawing substituents in position 8 of the indoloquinoline backbone do not exert any effect on cytotoxicity of copper(II) complexes, whereas copper(II) compounds with Schiff bases obtained from 2-acetylpyridine and indoloquinoline hydrazines are 10 to 50 times more cytotoxic than those with ligands prepared from 2-formylpyridine and indoloquinoline hydrazines.

Introduction

In recent years, metal complexes which are able to interfere with cellular structures have attracted great interest as potential anticancer drugs. Complexes with biologically active ligands are particularly attractive, as they combine qualities of classic non-targeted coordination compounds and organic ligands

with selectivity for cellular targets (e.g., enzymes)^{1–10}. Indolo[3,2-*d*]benzazepines, also named paullones, have been reported as potent inhibitors of intracellular proteins, for example, cyclin-dependent kinases (CDKs), glycogen synthase kinase-3 β and mitochondrial malate dehydrogenase.^{11–13} Since the original paullones do not possess suitable binding sites for metal ions, novel derivatives able to coordinate to gallium(III), ruthenium(II), osmium(II), and copper(II) have been designed and synthesized.^{14–18} All complexes exhibit remarkable cytotoxicity in vitro, whereby the complexes with copper(II), the only physiologically relevant metal ion used, showed IC_{50}

*To whom correspondence should be addressed. Phone: +431427752615. Fax: +431427752680. E-mail: vladimir.arion@univie.ac.at.

(1) Ang, W. H.; Dyson, P. J. *Eur. J. Inorg. Chem.* 2006, 20, 4003–4018.
(2) Hefeter, P.; Jungwirth, U.; Jakupec, M.; Hartinger, C.; Galanski, M.; Elbling, L.; Micksche, M.; Keppler, B.; Berger, W. *Drug Resist. Updates* 2008, 11, 1–16.

(3) Frezza, M.; Hindo, S. S.; Tomco, D.; Allard, M. M.; Cui, Q. C.; Heeg, M. J.; Chen, D.; Dou, Q. P.; Verani, C. N. *Inorg. Chem.* 2009, 48, 5928–5937.
(4) Bregman, H.; Carroll, P. J.; Meggers, E. *J. Am. Chem. Soc.* 2006, 128, 877–884.

(5) Zagermann, J.; Kuchta, M. C.; Merz, K.; Metzler-Nolte, N. *J. Organomet. Chem.* 2009, 694, 862–867.

(6) Atilla-Gökumen, G. E.; Williams, D. S.; Bregman, H.; Pagano, N.; Meggers, E. *ChemBioChem* 2006, 7, 1443–1450.

(7) Maloň, M.; Trávníček, Z.; Maryško, M.; Zbořil, R.; Mašláň, M.; Marek, J.; Doležal, K.; Rolčík, J.; Krýstov, V.; Strnad, M. *Inorg. Chim. Acta* 2001, 323, 119–129.

(8) Chen, C.-Y.; Chen, Q.-Z.; Wang, X.-F.; Liu, M.-S.; Chen, Y.-F. *Transition Met. Chem.* 2009, 34, 757–763.

(9) Tan, J.; Wang, B.; Zhu, L. *J. Biol. Inorg. Chem.* 2009, 14, 727–739.

(10) Meggers, E. *Chem. Commun.* 2009, 9, 1001–1010.

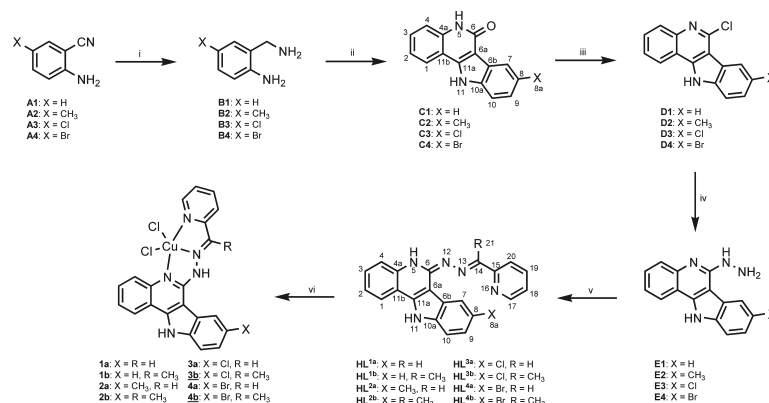
(11) Huwe, A.; Mazitschek, R.; Giannīs, A. *Angew. Chem., Int. Ed.* 2003, 42, 2122–2138.

(12) Kunick, C. *Arch. Pharm. (Weinheim, Ger.)* 1992, 325, 297–299.

(13) Knockaert, M.; Wieking, K.; Schmitt, S.; Leost, M.; Grant, K. M.; Mottram, J. C.; Kunick, C.; Meijer, L. *J. Biol. Chem.* 2002, 277, 25493–25501.

(14) Schmid, W. F.; Zorbas-Seifried, S.; John, R. O.; Arion, V. B.; Jakupec, M. A.; Roller, A.; Galanski, M.; Chiorescu, I.; Zorbas, H.; Keppler, B. K. *Inorg. Chem.* 2007, 46, 3645–3656.

(15) Schmid, W. F.; John, R. O.; Mühlgassner, G.; Hefeter, P.; Jakupec, M. A.; Galanski, M.; Berger, W.; Arion, V. B.; Keppler, B. K. *J. Med. Chem.* 2007, 50, 6343–6355.

Scheme 1. Synthesis of **1a–4b^d** and Numbering Schemes for Original and Modified Indoloquinolines^b

^a Reagents and conditions: (i) borane, 1.0 M in THF, THF, Ar, rt, 48 h (**B1**, 61%), 24 h (**B3**, 96%), 72 h (**B4**, 83%); (ii) glacial AcOH, reflux, 4 h [(**C1**, 80%), (**C2**, 56%), (**C3**, 60%), (**C4**, 64%)]]; (iii) POCl₃, reflux, 24 h/NaOH, extraction with ethyl acetate [(**D1**, 97%), (**D2**, 72%), (**D3**, 86%), (**D4**, 90%)]; (iv) N₂H₄·H₂O, reflux, 24 h [(**E1**, 95%), (**E2**, 86%), (**E3**, 92%), (**E4**, 86%)]; (v) 2-formylpyridine, ethanol, reflux, 24 h [(**HL¹⁹**, 89%), (**HL²⁰**, 82%), (**HL²¹**, 90%), (**HL²²**, 78%)] or 2-acetylpyridine, ethanol, reflux, 24 h [(**HL¹⁹**, 89%), (**HL²⁰**, 83%), (**HL²¹**, 94%), (**HL²²**, 84%)]; (vi) CuCl₂·2H₂O, isopropanol, reflux, 30 min [(**1a**, 82%), (**1b**, 90%), (**2a**, 86%), (**2b**, 94%), (**3a**, 83%), (**3b**, 86%), (**4a**, 85%), (**4b**, 91%)]. ^b Underlined compounds have been characterized by X-ray crystallography.

values in the low micromolar and high nanomolar concentration range.¹⁸ Furthermore, the effect of metal coordination on solubility in aqueous media and on the impact on cell cycle progression have been reported as well.^{14–18}

As an extension to this previous work, we were interested in studying the effect of substitution of the folded seven-membered azepine ring in indolo[3,2-*d*]benzazepines by a flat six-membered pyridine ring, prompting us to prepare the corresponding indolo[3,2-*c*]quinolines. Quite recently, the first ruthenium(II) and osmium(II) complexes with indolo[3,2-*c*]quinolines have been reported.¹⁹ The modified indolo[3,2-*c*]quinoline ligands as well as their ruthenium(II) and osmium(II) complexes were all more cytotoxic than the corresponding modified paullone ligands and their complexes.¹⁹ Furthermore, the indoloquinolines and their complexes readily intercalate into DNA as evidenced by 90% replacement of methyl green in a competitive replacement assay.¹⁹ These results are in accord with the previous suggestion of other authors that DNA is a possible intracellular target of indoloquinolines.²⁰

The pharmacological relevance of indoloquinolines is also demonstrated by the fact that isocryptolepine, a derivative of indolo[3,2-*c*]quinoline, and the closely related cryptolepine, a derivative of indolo[3,2-*b*]quinoline, could be isolated from the roots of *Cryptolepis sanguinolenta*, an African

plant used in traditional medicine to fight malaria.^{21–23} Whereas cryptolepine was extensively studied for its medicinal applicability, isocryptolepine and further indolo[3,2-*c*]quinolines were only explored by researchers to a limited extent, although their antiproliferative activity in vitro has been confirmed.^{24–29}

Herein we report on the synthesis of the first copper(II) complexes with tridentate modified indolo[3,2-*c*]quinoline ligands (Scheme 1), related to the quite recently published copper(II) complexes with indolo[3,2-*d*]benzazepine-based ligands.¹⁸ To directly compare the two classes of heterocycles, one novel copper(II) complex with a *N*-(7,12-dihydroindolo[3,2-*d*][1]benzazepin-6-ylidene)-*N'*-(1-pyridin-2-yl-ethylidene)azine ligand and two complexes reported previously have been synthesized (Chart 1), and their cytotoxicity was compared to those of indoloquinolines. Effects of the substitution of the seven-membered azepine ring by the six-membered

(21) Pousset, J.-L.; Martin, M.-T.; Jossang, A.; Bodo, B. *Phytochemistry* **1995**, *39*, 735–736.

(22) Lavrado, J.; Paulo, A.; Gut, J.; Rosenthal, P. J.; Moreira, R. *Bioorg. Med. Chem. Lett.* **2008**, *18*, 1378–1381.

(23) Onyebor, O.; Croft, S. L.; Dodson, H. I.; Feiz-Haddad, M.; Kendrick, H.; Millington, N. J.; Parapini, S.; Phillips, R. M.; Seville, S.; Shnyder, S. D.; Taramelli, D.; Wright, C. W. *J. Med. Chem.* **2005**, *48*, 2701–2709.

(24) Beauchard, A.; Jaunet, A.; Murillo, L.; Baldeyrou, B.; Lansiaux, A.; Cherouvrier, J.-R.; Domon, L.; Picot, L.; Bailly, C.; Besson, T.; Thiéry, V. *Eur. J. Med. Chem.* **2009**, *44*, 3858–3865.

(25) Hostyn, S.; Maes, B. U. W.; Pieters, L.; Lemiere, G. L. F.; Matyus, P.; Hajos, G.; Domisse, R. A. *Tetrahedron* **2005**, *61*, 1571–1577.

(26) Lu, C.-M.; Chen, Y.-L.; Chen, H.-L.; Chen, C.-A.; Lu, P.-J.; Yang, C.-N.; Tzeng, C.-C. *Bioorg. Med. Chem.* **2010**, *18*, 1948–1957.

(27) Aragon, P.-J.; Yapi, A.-D.; Pinguet, F.; Chezal, J.-M.; Teulade, J.-C.; Blache, Y. *Chem. Pharm. Bull.* **2007**, *55*, 1349–1355.

(28) Go, M.-L.; Ngiam, T.-L.; Tan, A. L.-C.; Kuaha, K.; Wilairat, P. *Eur. J. Pharm. Sci.* **1998**, *6*, 19–26.

(29) Grelfier, P.; Ramiarmanana, L.; Millerioux, V.; Deharo, E.; Schrével, J. *Phytother. Res.* **1996**, *10*, 317–321.

(16) Dobrov, A.; Arion, V. B.; Kandler, N.; Ginzinger, W.; Jakupec, M. A.; Rufinska, A.; Graf von Keyserlingk, N.; Galanski, M.; Kowol, C.; Keppler, B. K. *Inorg. Chem.* **2006**, *45*, 1945–1950.

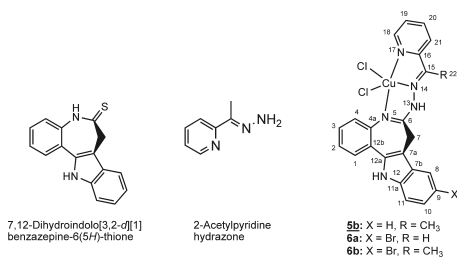
(17) Schmid, W. F.; John, R. O.; Arion, V. B.; Jakupec, M. A.; Keppler, B. K. *Organometallics* **2007**, *26*, 6643–6652.

(18) Primik, M. F.; Mühlgassner, G.; Jakupec, M. A.; Zava, O.; Dyson, P. J.; Arion, V. B.; Keppler, B. K. *Inorg. Chem.* **2010**, *49*, 302–311.

(19) Filak, L. K.; Mühlgassner, G.; Jakupec, M. A.; Heffeter, P.; Berger, W.; Arion, V. B.; Keppler, B. K. *J. Biol. Inorg. Chem.* **2010**, *15*, 903–918.

(20) Chen, Y.-L.; Chung, C.-H.; Chen, I.-L.; Chen, P.-H.; Jeng, H.-J. *Bioorg. Med. Chem.* **2002**, *10*, 2705–2712.

11086 Inorganic Chemistry, Vol. 49, No. 23, 2010

Chart 1. Starting Materials for the Synthesis of Complex **5b** and Numbering Scheme for Complexes **5b**, **6a**, and **6b** with Paullone-Based Tridentate Ligands^a

^aThe underlined compound has been characterized by X-ray crystallography. Compounds **6a** and **6b** were prepared as described recently.¹⁸

pyridine ring and other structure–activity relationships are discussed.

Experimental Section

Starting Materials. 2-Aminobenzonitrile (**A1**), 2-amino-5-methylbenzonitrile (**A2**), borane tetrahydrofuran complex solution, 2-aminobenzylamine (**B1**), isatin, glacial acetic acid, phosphorus oxychloride, hydrazine hydrate, 2-formylpyridine, 2-acetylpyridine, copper(II) chloride dihydrate and dimethylformamide were all purchased from Sigma-Aldrich and used without further purification. 2-Amino-5-chlorobenzonitrile (**A3**) and isopropanol (analytical reagent grade) were purchased from Acros Organics. Tetrahydrofuran (THF, analytical reagent grade) was purchased from Fisher Scientific and dried using standard protocols. Ethanol (96%) and diethyl ether were purchased from Brenntag and Donauchem, correspondingly. 2-Amino-5-bromobenzonitrile (**A4**) was synthesized according to Roche et al.³⁰ The substituted benzylamines (**B2–B4**), were obtained by reduction of compounds **A2–A4** with borane in dry THF, according to the procedure reported by Giordani et al.³¹ The syntheses of compounds **C1**,³² **DI**,²⁰ **E1**,³³ **HL**,³⁴ and **HL**^{1b} were performed following the literature procedures. 7,12-Dihydroindolo[3,2-d][1]benzazepine-6(5H)-thione (Chart 1) was prepared following a published protocol.³⁵ 2-Acetylpyridine hydrazone was obtained by reacting 2-acetylpyridine with excess hydrazine hydrate as the reagent and solvent at room temperature for 24 h.

General Procedure for the Synthesis of Substituted Benzylamines (B2**, **B3**).** To a solution of substituted benzonitrile in dry THF at 0 °C under an argon atmosphere was slowly added borane (1.0 M in THF). The reaction mixture was stirred for 10 min at 0 °C and further 48 h (**B2**), or 24 h (**B3**) at room temperature. The reaction mixture was cooled to 0 °C and quenched by addition of ethanol (96%). The resulting solution was saturated with gaseous HCl. The precipitated dihydrochloride was filtered off and then treated with an aqueous solution of ammonia.

(30) Roche, D.; Prasad, K.; Repic, O.; Blacklock, T. J. *Tetrahedron Lett.* **2000**, *41*, 2083–2085.

(31) Giordani, A.; Mandelli, S.; Verpillio, I.; Zanzola, S.; Tarchino, F.; Caselli, G.; Piepoli, T.; Mazzari, S.; Makovec, F.; Rovati, L. C. *PCT Int. Appl. WO 2008014822*, 2008, 57 pp.

(32) Bergman, J.; Engqvist, R.; Ståhlhandske, C.; Wallberg, H. *Tetrahedron* **2003**, *59*, 1033–1048.

(33) Mulwad, V. V.; Lohar, M. V. *Indian J. Chem. B* **2003**, *8*, 1937–1942.

(34) Filak, L. K.; Mühlhassner, G.; Roller, A.; Jakupec, M. A.; Galanski, M.; Keppler, B. K.; Arion, V. B. *Organometallics*, submitted.

(35) Schultz, C.; Link, A.; Leost, M.; Zaharevitz, D. W.; Gussio, R.; Sausville, E. A.; Meijer, L.; Kunick, C. J. *J. Med. Chem.* **1999**, *42*, 2909–2919.

The resulting suspension was extracted with ethyl acetate (3 × 20 mL). The combined organic layers were dried over sodium sulfate. Ethyl acetate was completely removed under reduced pressure and the product further dried in vacuo.

2-Amino-5-methylbenzylamine (B2**).** 2-Amino-5-methylbenzonitrile (0.95 g, 7.2 mmol), freshly dried THF (20 mL), borane (1.0 M in THF, 9 mL), 48 h. Yield: 0.59 g, 61%. C₈H₁₂N₂, *M_r* = 136.91 g/mol. ¹H NMR (CDCl₃, δ_H): 6.91 (d, 1H, ³J(H_{C3}) = 7.9 Hz, C4), 6.90 (s, 1H, C6), 6.63 (d, 1H, ³J(H_{C4}) = 7.3 Hz, C3), 4.36 (bs, 2H, N(C2)), 3.88 (s, 2H, C7), 2.25 (s, 3H, C8), 1.41 (bs, 2H, N(C7)). ¹³C{¹H} NMR (CDCl₃, δ_C): 143.63 (C2), 129.70 (C6), 128.59 (C4), 127.21 (C1), 126.40 (C6), 115.99 (C3), 44.93 (C7), 20.39 (C8).

2-Amino-5-chlorobenzylamine (B3**).** 2-Amino-5-chlorobenzonitrile (3.01 g, 19.76 mmol), freshly dried THF (50 mL), borane (1.0 M in THF, 24 mL), 24 h. Yield: 2.93 g, 96%. C₇H₈ClN₂, *M_r* = 156.61 g/mol. ¹H NMR (DMSO-*d*₆, δ_H): 7.08 (s, 1H, ⁴J(H_{C4}) = 2.4 Hz, C6), 6.93 (d, 1H, ³J(H_{C3}) = 8.5 Hz, ³J(H_{C6}) = 2.4 Hz, C4), 6.61 (d, 1H, ³J(H_{C4}) = 8.0 Hz, C3), 5.21 (s, 2H, N(C2)), 3.58 (s, 2H, C7), 1.80 (s, 2H, N(C7)). ¹³C{¹H} NMR (DMSO-*d*₆, δ_C): 145.94 (C2), 129.09 (C1), 127.67 (C6), 126.87 (C4), 119.57 (C5), 116.17 (C3), 42.97 (C7).

General Procedure for the Synthesis of 8-Substituted 5,11-Dihydroindolo[3,2-*c*]quinolin-6-ones. A mixture of isatin and the respective benzylamine in glacial acetic acid was refluxed for 4 h under argon atmosphere. After cooling to room temperature the light-brown precipitate was filtered off, washed with acetic acid (2 × 5 mL), water, and diethyl ether and dried in vacuo.

8-Methyl-5,11-dihydroindolo[3,2-*c*]quinolin-6-one (C2**).** Isatin (0.58 g, 3.94 mmol), 2-amino-5-methylbenzylamine (0.56 g, 4.04 mmol), glacial acetic acid (10 mL). Yield: 0.54 g, 56%. Anal. Calcd for C₁₆H₁₂N₂O (*M_r* = 248.28 g/mol) (%): C, 77.40; H, 4.87; N, 11.28. Found: C, 77.19; H, 4.78; N, 11.12. ¹H NMR (DMSO-*d*₆, δ_H): 12.41 (s, 1H, N11), 11.38 (s, 1H, N5), 8.16 (d, 1H, ³J(H_{C2}) = 7.9 Hz, C1), 8.01 (s, 1H, C7), 7.51–7.47 (m, 2H, C3, C10), 7.44 (d, 1H, ³J(H_{C3}) = 7.6 Hz, C2), 7.26 (dd, 1H, ³J(H_{C1}) = 7.6 Hz, ³J(H_{C3}) = 7.6 Hz, C2), 7.18 (d, 1H, ³J(H_{C10}) = 8.2 Hz, C9), 2.47 (s, 3H, C8a). ¹³C{¹H} NMR (DMSO-*d*₆, δ_C): 160.35 (C6), 141.15 (C11a), 138.34 (C4a), 136.42 (C10a), 130.28 (C8), 129.48 (C3), 125.86 (C9), 125.09 (6b), 122.49 (C1), 121.89 (C2), 121.01 (C7), 116.44 (C4), 112.51 (C11b), 111.77 (C10), 106.57 (C6a), 21.70 (C8a).

8-Chloro-5,11-dihydroindolo[3,2-*c*]quinolin-6-one (C3**).** Isatin (0.66 g, 4.50 mmol), 2-amino-5-chlorobenzylamine (0.80 g, 5.11 mmol), glacial acetic acid (10 mL). Yield: 0.72 g, 60%. Anal. Calcd for C₁₅H₉ClN₂O (*M_r* = 268.70 g/mol) (%): C, 67.05; H, 3.38; N, 10.43. Found: C, 66.67; H, 3.14; N, 10.29. ¹H NMR (DMSO-*d*₆, δ_H): 12.74 (s, 1H, N11), 11.51 (s, 1H, N5), 8.18 (d, 1H, ³J(H_{C2}) = 7.9 Hz, C1), 8.14 (s, 1H, C7), 7.63 (d, 1H, ³J(H_{C9}) = 8.5 Hz, C10), 7.53 (dd, 1H, ³J(H_{C2}) = 7.6 Hz, ³J(H_{C4}) = 7.6 Hz, C3), 7.46 (d, 1H, ³J(H_{C3}) = 7.6 Hz, C4), 7.37 (d, 1H, ³J(H_{C10}) = 8.5 Hz, C9), 7.31 (dd, 1H, ³J(H_{C1}) = 7.6 Hz, ³J(H_{C3}) = 7.6 Hz, C2). ¹³C{¹H} NMR (DMSO-*d*₆, δ_C): 160.05 (C6), 142.32 (C11a), 138.65 (C4a), 136.69 (C10a), 130.13 (C3), 126.00 (C6b), 125.99 (C8), 124.36 (C9), 122.75 (C1), 122.16 (C2), 120.15 (C7), 116.65 (C4), 113.78 (C10), 112.17 (C11b), 106.40 (C6a).

8-Bromo-5,11-dihydroindolo[3,2-*c*]quinolin-6-one (C4**).** Isatin (0.37 g, 2.51 mmol), 2-amino-5-bromobenzylamine (0.56 g, 2.76 mmol), glacial acetic acid (3.5 mL). Yield: 0.50 g, 64%. Anal. Calcd for C₁₅H₉BrN₂O (*M_r* = 313.15 g/mol) (%): C, 57.53; H, 2.90; N, 8.95. Found: C, 57.22; H, 2.71; N, 8.62. ¹H NMR (DMSO-*d*₆, δ_H): 12.75 (s, 1H, N11), 11.52 (s, 1H, N5), 8.29 (s, 1H, C7), 8.18 (d, 1H, ³J(H_{C2}) = 7.9 Hz, C1), 7.59 (d, 1H, ³J(H_{C9}) = 8.5 Hz, C10), 7.54 (dd, 1H, ³J(H_{C2}) = 7.6 Hz, ³J(H_{C4}) = 7.6 Hz, C3), 7.50 (d, 1H, ³J(H_{C10}) = 8.5 Hz, C9), 7.48 (d, 1H, ³J(H_{C3}) = 7.6 Hz, C4), 7.31 (dd, 1H, ³J(H_{C1}) = 7.9 Hz, ³J(H_{C3}) = 7.6 Hz, C2). ¹³C{¹H} NMR (DMSO-*d*₆, δ_C): 160.04 (C6), 142.14 (C11a), 138.66 (C4a), 136.96 (C10a), 130.14 (C3), 126.92 (C9), 126.62 (C6b), 123.17 (C7), 122.76 (C1), 122.17

Article

(C2), 116.65 (C4), 114.23 (C10), 113.89 (C8), 112.14 (C11b), 106.27 (C6a).

General Procedure for the Synthesis of 8-Substituted 6-Chloro-11*H*-indolo[3,2-*c*]quinolines. To 8-substituted 5,11-dihydroindolo[3,2-*c*]quinolin-6-one was added POCl₃ as a reagent and solvent under argon atmosphere. The reaction mixture was refluxed for 24 h. After cooling to room temperature the reaction mixture was poured onto ice (200 mL) and slowly neutralized with solid sodium hydroxide until a pH of 6–7 was reached. The resulting aqueous suspension was extracted with ethyl acetate (5 × 200 mL). The combined organic layers were washed with 5% NaHCO₃ aqueous solution (2 × 250 mL) and dried over Na₂SO₄. Ethyl acetate was evaporated under reduced pressure to yield the product as a beige solid, which was dried in vacuo.

6-Chloro-8-methyl-11*H*-indolo[3,2-*c*]quinoline (D2). C2 (0.51 g, 2.05 mmol), POCl₃ (20 mL). Yield: 0.40 g, 72%. Anal. Calcd for C₁₆H₁₁ClN₂·0.25C₄H₈O₂ (*M_r* = 288.75 g/mol) (%): C, 70.71; H, 4.54; N, 9.70. Found: C, 70.85; H, 4.35; N, 9.85. ¹H NMR (DMSO-*d*₆, δ_H): 12.99 (s, 1H, N11), 8.52 (d, 1H, ³*J*(H_{C2}) = 8.2 Hz, C1), 8.23 (s, 1H, C7), 8.03 (d, 1H, ³*J*(H_{C3}) = 8.2 Hz, C4), 7.77 (dd, 1H, ³*J*(H_{C2}) = 8.2 Hz, ³*J*(H_{C4}) = 8.4 Hz, C3), 7.71 (dd, 1H, ³*J*(H_{C1}) = 8.1 Hz, ³*J*(H_{C3}) = 8.1 Hz, C2), 7.65 (d, 1H, ³*J*(H_{C5}) = 8.4 Hz, C10), 7.38 (d, 1H, ³*J*(H_{C10}) = 8.4 Hz, C9), 2.54 (s, 3H, C8a). ¹³C{¹H} NMR (DMSO-*d*₆, δ_C): 144.92 (C6), 144.76 (C4a), 142.46 (C11a), 137.54 (C10a), 130.70 (C6b), 129.56 (C3), 128.83 (C4), 127.96 (C9), 126.70 (C2), 122.64 (C1), 121.47 (C8), 121.41 (C7), 117.03 (C11b), 112.32 (C10), 111.62 (C6a), 21.81 (C8a). ESI-MS in methanol (positive): 267 [(D2)H]⁺, 289 [(D2)Na]⁺, 555 [(D2)₂Na]⁺.

6,8-Dichloro-11*H*-indolo[3,2-*c*]quinoline (D3). C3 (0.72 g, 2.66 mmol), POCl₃ (20 mL). Yield: 0.66 g, 86%. Anal. Calcd for C₁₅H₈Cl₂N₂ (*M_r* = 287.14 g/mol) (%): C, 62.74; H, 2.81; N, 9.76. Found: C, 62.40; H, 2.86; N, 9.51. ¹H NMR (DMSO-*d*₆, δ_H): 13.26 (s, 1H, N11), 8.51 (d, 1H, ³*J*(H_{C2}) = 7.9 Hz, C1), 8.34 (s, 1H, C7), 8.04 (d, 1H, ³*J*(H_{C3}) = 8.2 Hz, C4), 7.80 (dd, 1H, ³*J*(H_{C3}) = 7.6 Hz, ³*J*(H_{C4}) = 7.9 Hz, C3), 7.77 (d, 1H, ³*J*(H_{C9}) = 8.5 Hz, C10), 7.73 (dd, 1H, ³*J*(H_{C1}) = 7.9 Hz, ³*J*(H_{C3}) = 7.6 Hz, C2), 7.56 (d, 1H, ³*J*(H_{C10}) = 8.5 Hz, C9). ¹³C{¹H} NMR (DMSO-*d*₆, δ_C): 145.03 (C4a), 144.71 (C6), 143.19 (C11a), 137.75 (C10a), 130.10 (C3), 128.91 (C4), 127.03 (C2), 126.47 (C9), 126.14 (C8), 122.76 (C1), 122.42 (C6b), 120.76 (C7), 116.89 (C11b), 114.28 (C10), 111.14 (C6a). ESI-MS in methanol (positive): 287 [(D3)H]⁺, 309 [(D3)Na]⁺.

8-Bromo-6-chloro-11*H*-indolo[3,2-*c*]quinoline (D4). C4 (0.48 g, 1.55 mmol), POCl₃ (20 mL). Yield: 0.05 g, 90%. C₁₅H₈BrClN₂, *M_r* = 331.59 g/mol. ¹H NMR (DMSO-*d*₆, δ_H): 13.28 (s, 1H, N11), 8.52 (d, 1H, ³*J*(H_{C2}) = 8.2 Hz, C1), 8.50 (s, 1H, C7), 8.05 (d, 1H, ³*J*(H_{C3}) = 8.2 Hz, C4), 7.82 (dd, 1H, ³*J*(H_{C3}) = 8.2 Hz, ³*J*(H_{C4}) = 8.2 Hz, C3), 7.76 (dd, 1H, ³*J*(H_{C1}) = 7.9 Hz, ³*J*(H_{C3}) = 8.1 Hz, C2), 7.73 (d, 1H, ³*J*(H_{C9}) = 8.7 Hz, C10), 7.68 (d, 1H, ³*J*(H_{C10}) = 8.7 Hz, C9). ¹³C{¹H} NMR (DMSO-*d*₆, δ_C): 145.04 (C4a), 144.70 (C6), 143.03 (C11a), 138.04 (C10a), 130.13 (C9), 129.07 (C3), 128.92 (C4), 127.07 (C2), 123.72 (C7), 123.03 (C6b), 122.79 (C1), 116.87 (C11b), 114.72 (C10), 113.98 (C8), 111.01 (C6a). ESI-MS in methanol (positive): 331 [(D4)H]⁺, 353 [(D4)Na]⁺.

General Procedure for the Synthesis of 8-Substituted 5,11-Dihydroindolo[3,2-*c*]quinolin-6-ylhydrazines. To 8-substituted 6-chloro-11*H*-indolo[3,2-*c*]quinoline hydrazine hydrate as reagent and solvent was added and the reaction mixture heated at 115 °C for 24 h under argon atmosphere. After cooling to room temperature, the resulting beige precipitate was filtered off, washed with water (2 × 10 mL), ethyl acetate and dried in vacuo.

8-Methyl-5,11-dihydroindolo[3,2-*c*]quinolin-6-ylhydrazine (E2). D2 (0.37 g, 1.4 mmol), hydrazine hydrate (10 mL). Yield: 0.31 g, 86%. Anal. Calcd for C₁₆H₁₄N₄·0.1H₂O (*M_r* = 264.11 g/mol): C, 72.76; H, 5.42; N, 21.21. Found: C, 73.13; H, 5.17; N, 20.91. ¹H NMR (DMSO-*d*₆, δ_H): 12.35 (s, 1H, N11), 8.25 (d, 1H, ³*J*(H_{C2}) = 7.3 Hz, C1), 8.19 (s, 1H, C7), 7.94 (s, 1H, N12),

Inorganic Chemistry, Vol. 49, No. 23, 2010 11087

7.74 (d, 1H, ³*J*(H_{C3}) = 7.0 Hz, C4), 7.56–7.50 (m, 2H, C3, C10), 7.36–7.28 (m, 1H, C2), 7.22 (d, 1H, ³*J*(H_{C10}) = 8.2 Hz, C9), 4.68 (s, 2H, N13), 2.50 (s, 3H, C8a). ESI-MS in methanol (positive): 263 [(E2)H]⁺.

8-Chloro-5,11-dihydroindolo[3,2-*c*]quinolin-6-ylhydrazine (E3). D3 (0.64 g, 2.2 mmol), hydrazine hydrate (10 mL). Yield: 0.58 g, 92%. Anal. Calcd for C₁₅H₁₁ClN₄·0.1C₄H₈O₂ (*M_r* = 291.54 g/mol): C, 63.44; H, 4.08; N, 19.22. Found: C, 63.69; H, 3.74; N, 19.15. ¹H NMR (DMSO-*d*₆, δ_H): 12.66 (s, 1H, N11), 8.49 (bs, 1H, N12), 8.26 (d, 1H, ³*J*(H_{C2}) = 6.3 Hz, C1), 8.20 (s, 1H, C7), 7.75 (d, 1H, ³*J*(H_{C3}) = 6.3 Hz, C4), 7.63 (d, 1H, ³*J*(H_{C9}) = 8.2 Hz, C10), 7.60–7.54 (m, 1H, C3), 7.39 (d, 1H, ³*J*(H_{C10}) = 7.9 Hz, C9), 7.37–7.31 (m, 1H, C2), 4.69 (s, 2H, N13). ESI-MS in methanol (positive): 283 [(E3)H]⁺.

8-Bromo-5,11-dihydroindolo[3,2-*c*]quinolin-6-ylhydrazine (E4). D4 (1.0 g, 3.0 mmol), hydrazine hydrate (25 mL). Yield: 0.90 g, 86%. C₁₅H₁₁BrN₄, *M_r* = 327.18 g/mol. ¹H NMR (DMSO-*d*₆, δ_H): 12.57 (bs, 1H, N11), 8.60 (bs, 1H), 8.36–8.16 (m, 2H), 7.79–7.70 (m, 1H), 7.64–7.45 (m, 3H), 7.41–7.24 (m, 1H), 4.58 (bs, 2H, N13). ESI-MS in methanol (positive): 327 [(E4)H]⁺.

General Procedure for the Synthesis of Ligands (HL^{2a–4b}). To a suspension of 8-substituted 5,11-dihydroindolo[3,2-*c*]quinolin-6-ylhydrazine in ethanol (96%, 10 mL) was added 2-formylpyridine or 2-acetylpyridine at 50 °C and the reaction mixture heated at reflux for 24 h, and then cooled to room temperature. The brightly yellow precipitate formed was filtered off and dried in vacuo.

N-(8-Methyl-5,11-dihydroindolo[3,2-*c*]quinolin-6-ylidene)-N'-(1-pyridin-2-yl-methylidene)azine (HL^{2a}). E2 (0.10 g, 0.38 mmol), 2-formylpyridine (40.1 μL, 0.42 mmol). Yield: 0.12 g, 86%. Anal. Calcd for C₂₃H₁₇N₅ (*M_r* = 351.40 g/mol) (%): C, 75.19; H, 4.88; N, 19.93. Found: C, 74.97; H, 4.80; N, 19.60. ¹H NMR (DMSO-*d*₆, δ_H): 12.44 (s, 1H, N11), 10.88 (s, 1H, N5), 8.62 (d, 1H, ³*J*(H_{C18}) = 4.9 Hz, C17), 8.58 (d, 1H, ³*J*(H_{C19}) = 7.9 Hz, C20), 8.52 (s, 1H, C14), 8.25 (s, 1H, C7), 8.13 (d, 1H, ³*J*(H_{C2}) = 7.9 Hz, C1), 7.92–7.87 (m, 2H, C4, C19), 7.51 (d, 1H, ³*J*(H_{C9}) = 8.4 Hz, C10), 7.49 (dd, 1H, ³*J*(H_{C2}) = 7.7 Hz, ³*J*(H_{C4}) = 7.7 Hz, C3), 7.36 (dd, 1H, ³*J*(H_{C17}) = 7.4 Hz, ³*J*(H_{C19}) = 7.4 Hz, C18), 7.26 (dd, 1H, ³*J*(H_{C1}) = 7.6 Hz, ³*J*(H_{C3}) = 7.6 Hz, C2), 7.20 (d, 1H, ³*J*(H_{C10}) = 8.4 Hz, C9), 2.50 (s, 3H, C8a). ¹³C{¹H} NMR (DMSO-*d*₆, δ_C): 155.52 (C15), 152.37 (C6), 150.85 (C14), 149.76 (C17), 139.05 (C11a), 137.92 (C4a), 136.97 (C10a), 136.57 (C19), 130.14 (C8), 129.53 (C3), 125.99 (C9), 124.33 (C6b), 123.71 (C18), 122.78 (C7), 122.32 (C1), 122.06 (C2), 121.42 (C20), 117.13 (C4), 113.67 (C11b), 111.69 (C10), 104.79 (C6a), 21.86 (C8a). The chemical shift of methyl group protons 8a was determined by a HSQC experiment, as the δ-value coincides with that of DMSO-*d*₆ solvent residual signal (see Supporting Information, Figure S1). ESI-MS in methanol (positive): 352 [(HL^{2a})H]⁺, 374 [(HL^{2a})Na]⁺. UV–vis (isopropanol), λ_{max} (ε, M⁻¹ cm⁻¹): 230 (36900), 266 (27100), 330 (13750), 357 (13300), 410 (18500), 425 (18700).

N-(8-Methyl-5,11-dihydroindolo[3,2-*c*]quinolin-6-ylidene)-N'-(1-pyridin-2-yl-ethylidene)azine (HL^{2b}). E2 (0.16 g, 0.59 mmol), 2-acetylpyridine (73 μL, 0.65 mmol). Yield: 0.18 g, 83%. Anal. Calcd for C₂₃H₁₉N₅·H₂O (*M_r* = 383.45 g/mol) (%): C, 72.04; H, 5.52; N, 18.26. Found: C, 71.82; H, 5.31; N, 17.98. ¹H NMR (DMSO-*d*₆, δ_H): 12.37 (s, 1H, N11), 10.66 (s, 1H, N5), 8.71 (d, 1H, ³*J*(H_{C19}) = 8.0 Hz, C20), 8.61 (d, 1H, ³*J*(H_{C18}) = 4.9 Hz, C17), 8.21 (s, 1H, C7), 8.10 (d, 1H, ³*J*(H_{C2}) = 8.0 Hz, C1), 7.86 (d, 1H, ³*J*(H_{C3}) = 7.6 Hz, C4), 7.83 (dd, 1H, ³*J*(H_{C18}) = 7.4 Hz, ³*J*(H_{C20}) = 7.4 Hz, C19), 7.50 (d, 1H, ³*J*(H_{C9}) = 8.2 Hz, C10), 7.45 (dd, 1H, ³*J*(H_{C2}) = 7.6 Hz, ³*J*(H_{C4}) = 7.6 Hz, C3), 7.35 (dd, 1H, ³*J*(H_{C19}) = 7.4 Hz, ³*J*(H_{C17}) = 7.4 Hz, C18), 7.25 (dd, 1H, ³*J*(H_{C1}) = 7.4 Hz, ³*J*(H_{C3}) = 7.6 Hz, C2), 7.20 (d, 1H, ³*J*(H_{C10}) = 8.2 Hz, C9), 2.70 (s, 3H, C21), 2.49 (s, 3H, C8a). ¹³C{¹H} NMR (DMSO-*d*₆, δ_C): 157.28 (C15), 156.43 (C14), 150.67 (C6), 148.86 (C17), 138.72 (C11a), 137.99 (C4a), 136.98 (C10a), 136.24 (C19), 130.00 (C8), 129.40 (C3), 125.85 (C9), 124.46 (C6b), 123.45 (C18), 122.73 (C7), 122.24 (C1), 121.87

11088 Inorganic Chemistry, Vol. 49, No. 23, 2010

(C2), 121.54 (C20), 117.20 (C4), 113.70 (C11b), 111.68 (C10), 105.59 (C6a), 22.03 (C8a), 13.55 (C21). The chemical shift of methyl group protons 8a was determined by a HSQC experiment, as the δ -value coincides with that of DMSO- d_6 solvent residual signal (see Supporting Information, Figure S2). ESI-MS in methanol (positive): 366 [(HL^{2b})H]⁺. UV-vis (isopropanol), λ_{max} (ϵ , M⁻¹ cm⁻¹): 230 (39700), 267 (31100), 328 (16800), 354 (16550), 408 (19300).

N-(8-Chloro-5,11-dihydroindolo[3,2-c]quinolin-6-ylidene)-N'-(1-pyridin-2-yl-methylidene)azine (HL^{3a}). E3 (0.24 g, 0.84 mmol), 2-formylpyridine (88 μ L, 0.92 mmol). Yield: 0.28 g, 90%. Anal. Calcd for C₂₁H₁₄ClN₅ (M_r = 371.82 g/mol) (%): C, 67.83; H, 3.80; N, 18.84. Found: C, 67.53; H, 3.64; N, 18.44. ¹H NMR (DMSO- d_6 , δ_{H}): 12.75 (s, 1H, N11), 10.94 (s, 1H, N5), 8.63 (d, 1H, ³J(H_{C18}) = 4.9 Hz, C17), 8.58 (d, 1H, ³J(H_{C19}) = 7.9 Hz, C20), 8.52 (s, 1H, C14), 8.39 (s, 1H, C7), 8.14 (d, 1H, ³J(H_{C2}) = 7.9 Hz, C1), 7.90 (d, 1H, ³J(H_{C2}) = 8.2 Hz, C4), 7.89 (dd, 1H, ³J(H_{C18}) = 7.7 Hz, ³J(H_{C20}) = 7.7 Hz, C19), 7.64 (d, 1H, ³J(H_{C9}) = 8.7 Hz, C10), 7.53 (dd, 1H, ³J(H_{C2}) = 7.9 Hz, ³J(H_{C4}) = 7.7 Hz, C3), 7.43–7.35 (m, 2H, C9, C18), 7.28 (dd, 1H, ³J(H_{C1}) = 7.6 Hz, ³J(H_{C3}) = 7.6 Hz, C2). ¹³C{¹H} NMR (DMSO- d_6 , δ_{C}): 155.35 (C15), 151.96 (C6), 151.49 (C14), 149.79 (C17), 140.19 (C11a), 138.30 (C4a), 137.20 (C10a), 136.60 (C19), 130.15 (C3), 125.82 (C8), 125.19 (C6b), 124.41 (C9), 123.87 (C18), 122.59 (C1), 122.24 (C2), 121.86 (C7), 121.52 (C20), 117.29 (C4), 113.66 (C10), 113.29 (C11b), 104.60 (C6a). ESI-MS in methanol (positive): 372 [(HL^{3a})H]⁺. UV-vis (isopropanol), λ_{max} (ϵ , M⁻¹ cm⁻¹): 233 (43350), 267 (32400), 304 (16400), 321 (13700), 363 (17400), 408 (19600).

N-(8-Chloro-5,11-dihydroindolo[3,2-c]quinolin-6-ylidene)-N'-(1-pyridin-2-yl-ethylidene)azine (HL^{3b}). E3 (0.24 g, 0.85 mmol), 2-acetylpyridine (106 μ L, 0.95 mmol). Yield: 0.31 g, 94%. Anal. Calcd for C₂₂H₁₆ClN₅·H₂O (M_r = 403.86 g/mol) (%): C, 65.43; H, 4.49; N, 17.34. Found: C, 65.46; H, 4.38; N, 17.07. ¹H NMR (DMSO- d_6 , δ_{H}): 12.69 (s, 1H, N11), 10.73 (s, 1H, N5), 8.71 (d, 1H, ³J(H_{C19}) = 7.9 Hz, C20), 8.62 (d, 1H, ³J(H_{C18}) = 4.9 Hz, C17), 8.36 (s, 1H, C7), 8.11 (d, 1H, ³J(H_{C2}) = 7.3 Hz, C1), 7.88 (d, 1H, ³J(H_{C3}) = 7.9 Hz, C4), 7.89 (dd, 1H, ³J(H_{C18}) = 7.6 Hz, ³J(H_{C20}) = 7.6 Hz, C19), 7.63 (d, 1H, ³J(H_{C9}) = 8.5 Hz, C10), 7.50 (dd, 1H, ³J(H_{C2}) = 7.6 Hz, ³J(H_{C4}) = 7.9 Hz, C3), 7.41–7.34 (m, 2H, C9, C18), 7.25 (dd, 1H, ³J(H_{C1}) = 7.6 Hz, ³J(H_{C3}) = 7.6 Hz, C2), 2.68 (s, 3H, C21). ¹³C{¹H} NMR (DMSO- d_6 , δ_{C}): 157.12 (C6), 156.93 (C15), 150.24 (C14), 148.88 (C17), 139.89 (C11a), 138.37 (C4a), 137.20 (C10a), 136.28 (C19), 130.02 (C3), 125.73 (C8), 125.31 (C6b), 124.25 (C9), 123.60 (C18), 122.51 (C1), 122.05 (C2), 121.81 (C7), 121.62 (C20), 117.36 (C4), 113.64 (C10), 113.32 (C11b), 105.42 (C6a), 13.51 (C21). ESI-MS in methanol (positive): 386 [(HL^{3b})H]⁺. UV-vis (isopropanol), λ_{max} (ϵ , M⁻¹ cm⁻¹): 231 (44200), 265 (34650), 309 (15900), 321 (15200), 360 (18650), 406 (19450).

N-(8-Bromo-5,11-dihydroindolo[3,2-c]quinolin-6-ylidene)-N'-(1-pyridin-2-yl-methylidene)azine (HL^{4a}). E4 (0.26 g, 0.77 mmol), 2-formylpyridine (82 μ L, 0.85 mmol). Yield: 0.25 g, 78%. Anal. Calcd for C₂₁H₁₄BrN₅·0.25H₂O (M_r = 420.78 g/mol) (%): C, 59.94; H, 3.47; N, 16.64. Found: C, 59.98; H, 3.32; N, 16.44. ¹H NMR (DMSO- d_6 , δ_{H}): 12.77 (s, 1H, N11), 10.94 (s, 1H, N5), 8.64 (d, 1H, ³J(H_{C18}) = 4.7 Hz, C17), 8.58 (d, 1H, ³J(H_{C19}) = 7.7 Hz, C20), 8.54 (s, 1H, C7), 8.51 (s, 1H, C14), 8.14 (d, 1H, ³J(H_{C2}) = 7.4 Hz, C1), 7.94–7.85 (m, 2H, C4, C19), 7.59 (d, 1H, ³J(H_{C9}) = 8.5 Hz, C10), 7.53 (dd, 1H, ³J(H_{C2}) = 7.7 Hz, ³J(H_{C4}) = 7.7 Hz, C3), 7.50 (d, 1H, ³J(H_{C10}) = 8.5 Hz, C9), 7.37 (dd, 1H, ³J(H_{C17}) = 6.9 Hz, ³J(H_{C19}) = 7.1 Hz, C18), 7.28 (dd, 1H, ³J(H_{C1}) = 7.3 Hz, ³J(H_{C3}) = 7.3 Hz, C2). ¹³C{¹H} NMR (DMSO- d_6 , δ_{C}): 155.31 (C15), 151.95 (C6), 151.47 (C14), 149.80 (C17), 140.02 (C11a), 138.29 (C4a), 137.48 (C10a), 136.63 (C19), 130.15 (C3), 126.99 (C9), 125.77 (C6b), 124.87 (C7), 123.87 (C18), 122.60 (C1), 122.27 (C2), 121.53 (C20), 117.29 (C4), 114.09 (C10), 113.75 (C8), 113.24 (C11b), 104.43 (C6a). ESI-MS in methanol (positive): 416 [(HL^{4a})H]⁺, 438 [(HL^{4a})Na]⁺. UV-vis (isopropanol), λ_{max}

(ϵ , M⁻¹ cm⁻¹): 233 (38700), 267 (29000), 303 (13350), 321 (12100), 361 (15150), 410 (18500).

N-(8-Bromo-5,11-dihydroindolo[3,2-c]quinolin-6-ylidene)-N'-(1-pyridin-2-yl-ethylidene)azine (HL^{4b}). E4 (0.22 g, 0.52 mmol), 2-acetylpyridine (85 μ L, 0.76 mmol). Yield: 0.19 g, 84%. Anal. Calcd for C₂₂H₁₆BrN₅·H₂O (M_r = 448.32 g/mol) (%): C, 58.94; H, 4.05; N, 15.62. Found: C, 58.81; H, 4.05; N, 15.38. ¹H NMR (DMSO- d_6 , δ_{H}): 12.70 (s, 1H, N11), 10.74 (s, 1H, N5), 8.72 (d, 1H, ³J(H_{C19}) = 8.0 Hz, C20), 8.63 (d, 1H, ³J(H_{C18}) = 4.7 Hz, C17), 8.52 (s, 1H, C7), 8.12 (d, 1H, ³J(H_{C2}) = 8.0 Hz, C1), 7.89 (d, 1H, ³J(H_{C3}) = 8.0 Hz, C4), 7.85 (dd, 1H, ³J(H_{C18}) = 7.7 Hz, ³J(H_{C20}) = 7.7 Hz, C19), 7.59 (d, 1H, ³J(H_{C9}) = 8.5 Hz, C10), 7.54–7.49 (m, 2H, C3, C9), 7.37 (dd, 1H, ³J(H_{C17}) = 7.3 Hz, ³J(H_{C19}) = 7.3 Hz, C18), 7.26 (dd, 1H, ³J(H_{C1}) = 7.5 Hz, ³J(H_{C3}) = 7.5 Hz, C2), 2.68 (s, 3H, C21). ¹³C{¹H} NMR (DMSO- d_6 , δ_{C}): 157.13 (C14), 157.00 (C15), 150.24 (C6), 148.89 (C17), 139.72 (C11a), 138.38 (C4a), 137.47 (C10a), 136.29 (C19), 130.05 (C3), 126.82 (C9), 125.94 (C6b), 124.91 (C7), 123.62 (C18), 122.54 (C1), 122.07 (C2), 121.64 (C20), 117.38 (C4), 114.10 (C10), 113.70 (C8), 113.29 (C11b), 105.30 (C6a), 13.48 (C21). ESI-MS in methanol (positive): 430 [(HL^{4b})H]⁺, 452 [(HL^{4b})Na]⁺. UV-vis (isopropanol), λ_{max} (ϵ , M⁻¹ cm⁻¹): 231 (40400), 265 (32500), 310 (14500), 322 (13950), 360 (17450), 407 (18000).

Synthesis of Indolotriazolopyridine L¹, HL^{2a} (19 mg, 0.05 mmol) was dissolved in hot ethanol (96%, 15 mL). The solution was filtered, concentrated to two-thirds of the initial volume and left to stand at –20 °C for 96 h. The yellow precipitate formed was filtered off and dried in vacuo. Yield: 15 mg, 80%. C₂₂H₁₅N₅, M_r = 349.39 g/mol. ¹H NMR (DMSO- d_6 , δ_{H}): 12.67 (s, 1H, N11), 8.85 (d, 1H, ³J(H_{C18}) = 4.7 Hz, C17), 8.49 (d, 1H, ³J(H_{C2}) = 7.9 Hz, C1), 8.20–8.14 (m, 2H, C8, C19), 8.03 (d, 1H, ³J(H_{C19}) = 7.7 Hz, C20), 7.71 (dd, 1H, ³J(H_{C17}) = 7.9 Hz, ³J(H_{C19}) = 7.9 Hz, C18), 7.65 (dd, 1H, ³J(H_{C1}) = 7.7 Hz, ³J(H_{C3}) = 7.7 Hz, C2), 7.62 (d, 1H, ³J(H_{C9}) = 8.4 Hz, C10), 7.53 (d, 1H, ³J(H_{C3}) = 8.4 Hz, C4), 7.46 (dd, 1H, ³J(H_{C2}) = 7.9 Hz, ³J(H_{C4}) = 7.9 Hz, C3), 7.31 (d, 1H, ³J(H_{C10}) = 8.4 Hz, C9), 2.57 (s, 3H, C8a). ¹³C{¹H} NMR (DMSO- d_6 , δ_{C}): 150.29 (C17), 149.59 (C15), 148.03 (C14), 147.61 (C6), 138.49 (C19), 137.09 (C10a), 134.55 (C11a), 130.64 (C8), 130.56 (C4a), 128.27 (C3), 126.88 (C9), 126.77 (C2), 126.44 (C20), 125.74 (C18), 123.69 (C1), 122.82 (C6b), 121.22 (C7), 118.92 (C4), 117.07 (C11b), 112.36 (C10), 101.57 (C6a), 21.73 (C8a).

General Procedure for the Synthesis of Complexes 1a–4b. To a solution of the corresponding ligand in isopropanol, a solution of CuCl₂·2H₂O in methanol (1 mL) was added at 60 °C. The reaction mixture, which turned dark-red, was heated at reflux for further 15 min. The reaction mixture was cooled to room temperature and the dark-red solid filtered off, washed with isopropanol, and dried in vacuo.

N-(11H-Indolo[3,2-c]quinolin-6-ylidene)-N'-(1-pyridin-2-yl-methylidene)azine-dichlorido-copper(II) (1a). HL^{1a} (0.10 g, 0.30 mmol), CuCl₂·2H₂O (0.06 g, 0.35 mmol), isopropanol (70 mL). Yield: 0.115 g, 82%. Anal. Calcd for C₃₁H₁₅Cl₂CuN₅·0.5·CH₃OH (M_r = 487.85 g/mol) (%): C, 52.93; H, 3.51; N, 14.36. Found: C, 52.98; H, 3.25; N, 14.33. ESI-MS in methanol (positive): 399 [CuL^{1a}]⁺, 435 [Cu(HL^{1a})Cl]⁺, 736 [CuL^{1a}(HL^{1a})]⁺. ATR-IR, selected bands, cm⁻¹: 3090, 1581, 1527, 1224, 912, 741. UV-vis (1% v/v DMSO/H₂O), λ_{max} (ϵ , M⁻¹ cm⁻¹): 238 (38100), 249 (34600), 257 (33400), 298 (18900), 319 (17500), 333 (15100), 461 (15000).

N-(11H-Indolo[3,2-c]quinolin-6-ylidene)-N'-(1-pyridin-2-yl-ethylidene)azine-dichlorido-copper(II) (1b). HL^{1b} (0.10 g, 0.28 mmol), CuCl₂·2H₂O (0.06 g, 0.35 mmol), isopropanol (70 mL). Yield: 0.125 g, 90%. Anal. Calcd for C₃₂H₁₇Cl₂CuN₅ (M_r = 485.86 g/mol) (%): C, 54.39; H, 3.53; N, 14.41. Found: C, 54.16; H, 3.42; N, 14.17. ESI-MS in methanol (positive): 413 [CuL^{1b}]⁺, 449 [Cu(HL^{1b})Cl]⁺. ATR-IR, selected bands, cm⁻¹: 3029, 1584, 1533, 1205, 750. UV-vis (1% v/v DMSO/H₂O), λ_{max} (ϵ , M⁻¹ cm⁻¹): 237 (41450), 256 (33850), 299 (19850), 318 (19300), 333 (16900), 453 (17200).

Article

N-(8-Methyl-11*H*-indolo[3,2-*c*]quinolin-6-ylidene)-*N'*-(1-pyridin-2-yl-methylidene)azine-dichlorido-copper(II) (**2a**). **HL**^{2a} (0.02 g, 0.06 mmol), CuCl₂·2H₂O (0.01 g, 0.07 mmol), isopropanol (20 mL). Yield: 0.026 g, 86%. Anal. Calcd for C₂₂H₁₇Cl₂CuN₅·0.5H₂O (*M*_r = 494.86 g/mol) (%): C, 53.40; H, 3.67; N, 14.15. Found: C, 53.79; H, 3.53; N, 13.90. ESI-MS in methanol (positive): 413 [CuL^{2a}]⁺, 449 [Cu(HL^{2a})Cl]⁺. ATR-IR, selected bands, cm⁻¹: 3214, 1585, 1536, 1230, 756. UV-vis (1% v/v DMSO/H₂O), λ_{max} (ε, M⁻¹ cm⁻¹): 237 (39000), 253 (35300), 302 (18300), 323 (17900), 336 (16100), 462 (15250).

N-(8-Methyl-11*H*-indolo[3,2-*c*]quinolin-6-ylidene)-*N'*-(1-pyridin-2-yl-ethylidene)azine-dichlorido-copper(II) (**2b**). **HL**^{2b} (0.06 g, 0.15 mmol), CuCl₂·2H₂O (0.03 g, 0.18 mmol), isopropanol (70 mL). Yield: 0.052 g, 94%. Anal. Calcd for C₂₃H₁₉Cl₂CuN₅·0.5H₂O (*M*_r = 508.89 g/mol) (%): C, 54.28; H, 3.96; N, 13.76. Found: C, 54.23; H, 3.75; N, 13.43. ESI-MS in methanol (positive): 427 [CuL^{2b}]⁺, 463 [Cu(HL^{2b})Cl]⁺. ATR-IR, selected bands, cm⁻¹: 3141, 1585, 1523, 1188, 768. UV-vis (1% v/v DMSO/H₂O), λ_{max} (ε, M⁻¹ cm⁻¹): 237 (42000), 255 (35500), 300 (19700), 320 (19600), 334 (17500), 454 (16300).

N-(8-Chloro-11*H*-indolo[3,2-*c*]quinolin-6-ylidene)-*N'*-(1-pyridin-2-yl-methylidene)azine-dichlorido-copper(II) (**3a**). **HL**^{3a} (0.07 g, 0.19 mmol), CuCl₂·2H₂O (0.04 g, 0.22 mmol), isopropanol (70 mL). Yield: 0.077 g, 83%. Anal. Calcd for C₂₁H₁₄Cl₃CuN₅·0.2C₃H₈O (*M*_r = 518.29 g/mol) (%): C, 50.05; H, 3.03; N, 13.51. Found: C, 49.71; H, 2.76; N, 13.16. ESI-MS in methanol (positive): 372 [(HL^{3a})H]⁺, 433 [CuL^{3a}]⁺, 469 [Cu(HL^{3a})Cl]⁺, 804 [CuL^{3a}(HL^{3a})]⁺. ATR-IR, selected bands, cm⁻¹: 3271, 3203, 3045, 1583, 1230, 755. UV-vis (1% v/v DMSO/H₂O), λ_{max} (ε, M⁻¹ cm⁻¹): 232 (52300), 260 (31200), 299 (17150), 320 (15200), 336 (13900), 465 (9700).

N-(8-Chloro-11*H*-indolo[3,2-*c*]quinolin-6-ylidene)-*N'*-(1-pyridin-2-yl-ethylidene)azine-dichlorido-copper(II) (**3b**). **HL**^{3b} (0.07 g, 0.18 mmol), CuCl₂·2H₂O (0.04 g, 0.21 mmol), isopropanol (70 mL). Yield: 0.078 g, 86%. Anal. Calcd for C₂₂H₁₆Cl₃CuN₅·0.2C₃H₈O (*M*_r = 532.32 g/mol) (%): C, 50.99; H, 3.33; N, 13.16. Found: C, 50.65; H, 3.08; N, 12.93. ESI-MS in methanol (positive): 447 [CuL^{3b}]⁺, 483 [Cu(HL^{3b})Cl]⁺, 832 [CuL^{3b}(HL^{3b})]⁺. ATR-IR, selected bands, cm⁻¹: 3144, 2659, 1579, 1527, 1210, 933, 763. UV-vis (1% v/v DMSO/H₂O), λ_{max} (ε, M⁻¹ cm⁻¹): 235 (54800), 260 (33000), 303 (20000), 318 (19400), 333 (17700), 453 (15800). Single crystals of the composition **3b**·3DMF, suitable for an X-ray diffraction study, were obtained by slow diffusion of diethyl ether into a solution of the complex in DMF.

N-(8-Bromo-11*H*-indolo[3,2-*c*]quinolin-6-ylidene)-*N'*-(1-pyridin-2-yl-methylidene)azine-dichlorido-copper(II) (**4a**). **HL**^{4a} (0.09 g, 0.22 mmol), CuCl₂·2H₂O (0.04 g, 0.26 mmol), isopropanol (80 mL). Yield: 0.078 g, 85%. Anal. Calcd for C₂₁H₁₄BrCl₂CuN₅·0.25H₂O (*M*_r = 555.23 g/mol) (%): C, 45.42; H, 2.63; N, 12.61. Found: C, 45.66; H, 2.52; N, 12.21. ESI-MS in methanol (positive): 477 [CuL^{4a}]⁺, 513 [Cu(HL^{4a})Cl]⁺, 892 [CuL^{4a}(HL^{4a})]⁺. ATR-IR, selected bands, cm⁻¹: 3129, 1580, 1528, 1368, 1220, 761. UV-vis (1% v/v DMSO/H₂O), λ_{max} (ε, M⁻¹ cm⁻¹): 238 (47300), 303 (17500), 320 (16800), 336 (15600), 461 (14100).

N-(8-Bromo-11*H*-indolo[3,2-*c*]quinolin-6-ylidene)-*N'*-(1-pyridin-2-yl-ethylidene)azine-dichlorido-copper(II) (**4b**). **HL**^{4b} (0.09 g, 0.21 mmol), CuCl₂·2H₂O (0.05 g, 0.28 mmol), isopropanol (80 mL). Yield: 0.082 g, 91%. Anal. Calcd for C₂₂H₁₆BrCl₂CuN₅ (*M*_r = 564.75 g/mol) (%): C, 46.79; H, 2.86; N, 12.40. Found: C, 46.96; H, 2.81; N, 12.11. ESI-MS in methanol (positive): 491 [CuL^{4b}]⁺, 527 [Cu(HL^{4b})Cl]⁺. ATR-IR, selected bands, cm⁻¹: 3140, 2831, 1575, 1526, 1212, 757. UV-vis (1% v/v DMSO/H₂O), λ_{max} (ε, M⁻¹ cm⁻¹): 237 (47700), 304 (17650), 319 (16850), 333 (15600), 456 (13800). Single crystals of X-ray diffraction quality of the composition **4b**·2.4DMF were obtained by slow diffusion of diethyl ether into a solution of the complex in DMF.

Inorganic Chemistry, Vol. 49, No. 23, 2010 11089

N-(7,12-Dihydroindolo[3,2-*d*]1[benzazepin-6-ylidene)-*N'*-(1-pyridin-2-yl-ethylidene)azine-dichlorido-copper(II) (**5b**). A mixture of 7,12-dihydroindolo[3,2-*d*]1[benzazepin-6(5*H*)-thione (0.31 g, 1.2 mmol) and 2-acetylpyridine hydrazone (0.20 g, 1.5 mmol) in dry ethanol (25 mL) was refluxed for 96 h. The yellow precipitate formed was filtered off, washed with ethanol, and dried in vacuo. The ¹H NMR spectrum confirmed the formation of the ligand and the presence of minor amounts of side products. The mother liquor allowed to stand at -20 °C for 2 days generated X-ray diffraction quality single crystals of **HL**^{5b}. To a refluxed solution of the crude ligand (0.11 g) in methanol (14 mL) was added copper(II) chloride dihydrate (0.052 g) in methanol (1 mL). The resulting brown solution was filtered hot and allowed to stand at room temperature for 48 h. The crystals formed were filtered off, washed with cold methanol, and dried in vacuo. Yield: 0.07 g. Anal. Calcd for C₂₃H₁₉Cl₂CuN₅·0.5CH₃OH (*M*_r = 515.90 g/mol) (%): C, 54.71; H, 4.10; N, 13.57. Found: C, 54.46; H, 3.90; N, 13.33. ESI-MS in methanol (positive): 427 [CuL^{5b}]⁺. UV-vis (1% v/v DMSO/H₂O), λ_{max} (ε, M⁻¹ cm⁻¹): 239 (31400), 299 (20400), 422 (8800). Single crystals of the composition **5b**·0.5CH₃OH suitable for an X-ray diffraction study were picked directly from the reaction vessel.

Physical Measurements. ¹H and ¹³C, NOE difference and two-dimensional ¹H-¹H COSY, ¹H-¹H TOCSY, ¹H-¹³C HSQC and ¹H-¹³C HMBC NMR spectra were recorded on a Bruker Avance III spectrometer (Ultraschield Magnet) in DMSO-*d*₆ or CDCl₃ at 25 °C using standard pulse programs at 500.10 (¹H) and 125.76 (¹³C) MHz. ¹H and ¹³C chemical shifts are quoted relative to the residual solvent signals. Elemental analyses were carried out at the Microanalytical Service of the Faculty of Chemistry of the University of Vienna. Electrospray ionization mass spectrometry was carried out using a Bruker Esquire 3000 instrument (Bruker Daltonic, Bremen, Germany) on samples dissolved in methanol. UV-vis spectra were recorded on a Perkin-Elmer Lambda 650 spectrophotometer, using samples dissolved in isopropanol for **HL**^{1a-4b} and 1% (v/v) DMSO-water mixture for **1a-5b**. The aqueous solution behavior of complexes **1a**, **1b**, **4a**, **4b**, and **5b** was monitored on a Perkin-Elmer 12 UV-vis spectrophotometer in a 1% (v/v) DMSO/water mixture at room temperature over 24 h. IR spectra were measured with a Bruker Vertex 70 Fourier transform IR spectrometer by means of the attenuated total reflection (ATR) technique. Magnetic susceptibility measurements were conducted in solution on a Bruker Avance III spectrometer (Ultraschield Magnet) in DMSO-*d*₆ at 298 K using the Evans method.⁴¹⁻⁴³ The μ_{eff} calculated for a 0.018 M Cu(acac)₂ solution in DMSO-*d*₆ was 1.75 μ_B.

Crystallographic Structure Determination. X-ray diffraction measurements were performed on a Bruker X8 APEXII CCD diffractometer. Single crystals were positioned at 35 mm from the detector, and 1241, 2557, 1226, and 2619 frames were measured, each for 60, 80, 90, and 20 s over 1° scan width for **3b**·3DMF, **4b**·2.4DMF, **HL**^{5b}, and **5b**·0.5CH₃OH, correspondingly. The data were processed using the SAINT software.³⁶ Crystal data, data collection parameters, and structure refinement details are given in Table 1. The structures were solved by direct methods and refined by full-matrix least-squares techniques. Non-H atoms

(36) SAINT-Plus, version 7.06a, and APEX2; Bruker-Nonius AXS Inc.; Madison, WI, 2004.

(37) Sheldrick, G. M. *SHELXS-97, Program for Crystal Structure Solution*; University of Göttingen: Göttingen, Germany, 1997.

(38) Sheldrick, G. M. *SHELXL-97, Program for Crystal Structure Refinement*; University of Göttingen: Göttingen, Germany, 1997.

(39) Johnson, G. K. Report ORNL-5138; OAK Ridge National Laboratory: Oak Ridge, TN, 1976.

(40) Kunick, C. *Liebigs Ann. Chem.* **1993**, 1141-1143.

(41) Evans, D. F. *J. Chem. Soc.* **1959**, 2003-2005.

(42) Sur, S. K. *Magn. Res.* **1989**, 82, 169-173.

(43) Ginzinger, W.; Arion, V. B.; Giester, G.; Galanski, M.; Keppler, B. K. *Cent. Eur. J. Chem.* **2008**, 6, 340-346.

Table 1. Crystal Data and Details of Data Collection for **3b**·3DMF, **4b**·2.4DMF, **HL**^{5b}, and **5b**·0.5CH₃OH

	3b ·3DMF	4b ·2.4DMF	HL ^{5b}	5b ·0.5CH ₃ OH
empirical formula	C ₃₁ H ₃₇ Cl ₃ CuN ₈ O ₃	C _{29.2} H _{32.8} BrCl ₂ CuN _{7.4} O _{2.4}	C ₂₃ H ₁₉ N ₅	C _{23.5} H ₃₁ Cl ₂ CuN ₅ O _{0.5}
Fw	739.58	740.18	365.43	515.89
space group	<i>P</i> 2 ₁ / <i>c</i>	<i>P</i> 2 ₁ / <i>c</i>	<i>P</i> 2 ₁ / <i>c</i>	<i>P</i> 2 ₁ / <i>c</i>
<i>a</i> [Å]	17.5197(16)	17.439(2)	10.6889(7)	12.6541(4)
<i>b</i> [Å]	14.2545(12)	14.3150(17)	13.6296(11)	13.9929(5)
<i>c</i> [Å]	14.4463(11)	14.5007(18)	12.8100(9)	13.3138(4)
α [deg]				
β [deg]	113.551(4)	113.292(5)	107.747(4)	107.041(2)
γ [deg]				
<i>V</i> [Å ³]	3307.2(5)	3324.9(7)	1777.4(2)	2253.94(13)
<i>Z</i>	4	4	4	4
λ [Å]	0.71073	0.71073	0.71073	0.71073
ρ _{calcd} [g cm ⁻³]	1.485	1.479	1.366	1.520
crystal size [mm ³]	0.25 × 0.25 × 0.01	0.40 × 0.15 × 0.01	0.14 × 0.09 × 0.02	0.20 × 0.12 × 0.07
<i>T</i> [K]	100(2)	100(2)	100(2)	100(2)
μ [mm ⁻¹]	0.949	2.059	0.084	1.230
<i>R</i> ₁ ^a	0.0758	0.0865	0.0572	0.0327
<i>wR</i> ₂ ^b	0.2069	0.2404	0.1308	0.0990
GOF ^c	1.017	1.092	0.931	1.024

^a $R_1 = \sum ||F_o| - |F_c|| / \sum |F_o|$, ^b $wR_2 = (\sum w(F_o^2 - F_c^2)^2 / \sum w(F_o^2)^2)^{1/2}$, ^c $GOF = (\sum [w(F_o^2 - F_c^2)] / (n - p))^{1/2}$, where *n* is the number of reflections and *p* is the total number of parameters refined.

were refined with anisotropic displacement parameters with exception of those of co-crystallized solvent molecules in **3b**·3DMF, **4b**·2.4DMF, and **5b**·0.5CH₃OH. H atoms were inserted in calculated positions and refined with a riding model. The disorder of solvent molecules in **3b**·3DMF was resolved with constrained isotropic displacement parameters and restrained bond distances using SADI instructions of SHELX97. The following software programs were used: structure solution, SHELXS-97;³⁷ refinement, SHELXL-97;³⁸ molecular diagrams, ORTEP,³⁹ computer, Pentium IV.

Cell Lines and Cell Culture Conditions. For cytotoxicity determination, three different human cancer cell lines were used: A549 (non-small cell lung cancer) and SW480 (colon carcinoma) (both kindly provided by Brigitte Marian, Institute of Cancer Research, Department of Medicine I, Medical University Vienna, Austria) as well as CH1 (ovarian carcinoma) (kindly provided by Lloyd R. Kelland, CRC Centre for Cancer Therapeutics, Institute of Cancer Research, Sutton, U.K.). Cells were grown as adherent monolayer cultures in 75 cm² culture flasks (Iwaki/Asahi Technoglass) in Minimal Essential Medium supplemented with 10% heat-inactivated fetal bovine serum, 1 mM sodium pyruvate, 1% non essential amino acids (100×) and 2 mM L-glutamine but without antibiotics at 37 °C under a moist atmosphere containing 5% CO₂ and 95% air. All cell culture media and reagents were purchased from Sigma-Aldrich Austria.

Cytotoxicity Assay. Cytotoxicity was determined by the colorimetric MTT assay (MTT = 3-(4,5-dimethyl-2-thiazolyl)-2,5-diphenyl-2H-tetrazolium bromide). For this assay, cells were harvested by trypsinization and seeded into 96-well plates in volumes of 100 μL/well. Depending on the cell line, different cell densities were used to ensure exponential growth of the untreated controls during the experiment: 1.5 × 10³ cells/well (CH1), 2.5 × 10³ cells/well (SW480), 4.0 × 10³ cells/well (A549). In the first 24 h the cells were allowed to settle and resume exponential growth. Then the test compounds were dissolved in DMSO, mixed with medium to a maximum DMSO concentration of 0.5% v/v, serially diluted and added to the plates in volumes of 100 μL/well. After continuous exposure for 96 h (in the incubator at 37 °C and under 5% CO₂), the medium was replaced by 100 μL/well RPMI 1640 medium (supplemented with 10% heat-inactivated fetal bovine serum and 2 mM L-glutamine) and 20 μL/well MTT solution (MTT reagent in phosphate-buffered saline, 5 mg/mL), and plates were incubated for further 4 h. Then the medium/MTT mixture was removed

and the formed formazan product was dissolved in DMSO (150 μL/well). Optical densities at 550 nm (and at a reference wavelength of 690 nm) were measured with a microplate reader (Tecan Spectra Classic). The quantity of vital cells was expressed as a percentage of untreated controls, and 50% inhibitory concentrations (IC₅₀) were calculated from the concentration-effect curves by interpolation. Every test was repeated in at least three independent experiments, each consisting of three replicates per concentration level.

Results and Discussion

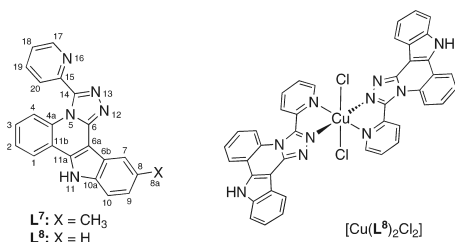
Syntheses of Ligands and Copper(II) Complexes. The syntheses of modified indoloquinoline ligands and their copper(II) complexes were performed as shown in Scheme 1. Efforts by us were focused on the synthesis of potentially tridentate ligands, taking into account our recent experience with bi- and tridentate paullone ligands and their copper(II) complexes. The copper(II) complexes with bidentate paullones were found to dissociate easily in an aqueous DMSO solution, while those of tridentate paullones remained intact over 20 h.¹⁸

The 8-substituted 5,11-dihydroindolo[3,2-*c*]quinolin-6-ones (**C1**–**C4**) were synthesized from isatin and the corresponding benzylamines **B1**–**B4** via the mechanism described by Bergman et al.³² in moderate to good yields (56–80%). It should be noted that the use of dihydrochlorides of **B2**–**B4** as starting materials leads in each case to the formation of an unidentified side product, which can not be separated from the desired indoloquinoline. Reaction of **C1**–**C4** with POCl₃ provided the 8-substituted 6-chloro-11*H*-indolo[3,2-*c*]quinolines (**D1**³⁵–**D4**) in good to excellent yields (72–97%). Treatment of these compounds with hydrazine hydrate yielded the hydrazine derivatives **E1**–**E4** in very good yields (86–92%).

The potentially tridentate Schiff bases **HL**^{1a}–**HL**^{4b} were obtained by condensation reaction of the hydrazines (**E1**–**E4**) with 2-formylpyridine (**HL**^{1a}, **HL**^{2a}, **HL**^{3a}, and **HL**^{4a}) and 2-acetylpyridine (**HL**^{1b}, **HL**^{2b}, **HL**^{3b}, **HL**^{4b}), respectively, in good to excellent yields.

Attempts to recrystallize **HL**^{2a} from ethanol (96%) in the presence of air oxygen resulted in formation of

Article

Chart 2. Structures of the Ligand **L**⁷ and Copper(II) Complex [Cu(**L**⁸)₂Cl₂] with a Relevant Atom Numbering Scheme

indolotriazoloquinoline **L**⁷ (Chart 2). A similar transformation was discovered for **HL**^{1a} coordinated to copper(II). Crystallization of [Cu(**HL**^{1a})Cl₂] (**1a**) from DMSO at room temperature over 3 weeks afforded a new complex of the composition [Cu(**L**⁸)₂Cl₂] (Chart 2). The structure of this compound was established by X-ray diffraction (Supporting Information, Figure S4), although the collected data set was generally rather poor.

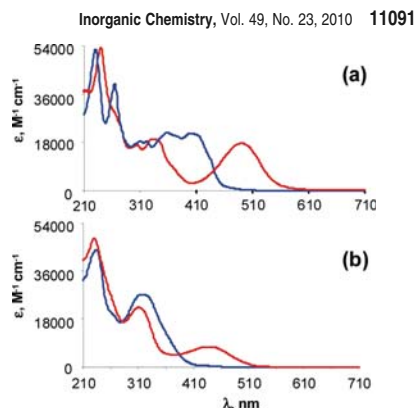
Cyclization to a triazole ring with formation of chelating ligands **L**⁷ and **L**⁸ presumably occurs via nucleophilic attack by a secondary amino group =N²H at the imino carbon atom C¹⁴ of the neighboring Schiff base forming C=N bond in **HL**^{2a} and **HL**^{1a}, respectively, accompanied by 2 electron oxidation coupled with a loss of two protons. It should be also noted that the synthesis of some indolotriazolobenzazepines, which, however, are not suitable for chelating metal ions, is well-documented in the literature.⁴⁰ In contrast, we did not observe cyclization with triazole ring formation in the case of **HL**^{6a} (Chart 2), indicating its lower reactivity compared to related indoloquinolines.

Complexes **1a–4b** were obtained in good to excellent yields (82–94%), as shown in Scheme 1, by reacting the corresponding ligands **HL**^{1a–4b} in hot isopropanol with copper(II) chloride dihydrate in methanol. The new complex **5b** and previously reported complexes **6a** and **6b** were prepared analogously starting from **HL**^{5b}, **HL**^{6a}, and **HL**^{6b}, and copper(II) chloride dihydrate in methanol.¹⁸ The modified paullone **HL**^{5b} resulted from reaction of 7,12-dihydroindolo[3,2-*d*][1]benzazepine-6(*5H*)-thione with 2-acetylpyridine hydrazone in dry boiling ethanol. The synthesis of **HL**^{6a} and **HL**^{6b} was realized in two steps. First, 9-bromo-7,12-dihydroindolo[3,2-*d*][1]benzazepine-6(*5H*)-thione was reacted with hydrazine hydrate in dry ethanol, yielding 9-bromo-7,12-dihydroindolo[3,2-*d*][1]benzazepin-6-ylhydrazine. This species was further condensed with 2-formylpyridine or 2-acetylpyridine, affording **HL**^{6a} and **HL**^{6b}, correspondingly.

Characterization of Ligands and Copper(II) Complexes.

Analytical data of the ligands and complexes are in agreement with their formulations. The ¹H and ¹³C NMR spectral data of the ligands along with their assignments are given in the Experimental Section. All ligands adopt a configuration with an exocyclic C⁶=N¹² double bond, which could be confirmed by the presence of a proton at N³ in the ¹H NMR spectra and the chemical shifts of C⁶ in the ¹³C NMR spectra.

Formation of copper(II) complexes was confirmed by ESI mass spectrometry and magnetic susceptibility

**Figure 1.** UV-vis spectra of (a) **HL**^{4b} (blue) and **4b** (red), compared with (b) **HL**^{6b} (blue) and **6b** in methanol.

measurements in solution. The spectra of complexes in methanol showed peaks with *m/z* 399 (**1a**), 413 (**1b**), 413 (**2a**), 427 (**2b**), 433 (**3a**), 447 (**3b**), 477 (**4a**), 491 (**4b**) and 427 (**5**), which were attributed to [CuL]⁺. In addition peaks with *m/z* 435 (**1a**), 449 (**1b**), 449 (**2a**), 463 (**2b**), 469 (**3a**), 483 (**3b**), 513 (**4a**), and 527 (**4b**) were assigned to [Cu(HL)C]⁺. In some cases, peaks with high *m/z* values of 736 (**1a**), 804 (**3a**), 832 (**3b**), and 892 (**4a**) were attributed to the formation of [CuL(HL)]⁺ ions in the mass spectrometer.

Magnetic susceptibility measurements were carried out in DMSO-*d*₆ at 298 K exemplarily for complexes **1a** and **4b** using the Evans method.^{41,42} The calculated effective magnetic moments of 1.76 and 1.75 μ_B, respectively, are in accord with the d⁹ electronic configuration of copper(II) with *S* = 1/2.

UV-vis spectra of complexes **4b**, **6b** and their corresponding ligands **HL**^{4b} and **HL**^{6b} in methanol are shown in Figure 1. The spectrum of the heteroaromatic indoloquinoline-based ligand **HL**^{4b} differs strongly from that of the paullone ligand **HL**^{6b}, in which the extended π system is disrupted by methylene group carbon atom C⁷, and as a result the ligand as a whole is non-planar. The light absorption by **HL**^{4b} is extended to the visible region, with strong bands between 360 and 430 nm.

Coordination of ligands **HL**^{4b} and **HL**^{6b} to copper(II) via the pyridine nitrogen atom, the hydrazine nitrogen and the pyridine ring nitrogen atom or azepine nitrogen atom, correspondingly, alters significantly the conjugated π systems in both ligands, resulting in significantly different electronic absorption spectra. The orange solution of **4b** and the yellow solution of **6b** show significant absorption in the visible region, namely, a broad charge-transfer band with a maximum at 490 and 420 nm, respectively.

Crystal Structures. The molecular structures of copper(II) complexes **3b** and **4b** are shown in Figure 2. Selected bond distances (Å) and bond angles (deg) are given in the legend to the figure. Both complexes (**3b** and **4b**) crystallized in the monoclinic space group *P2₁/c* with 3 and 2.4 molecules of dimethylformamide, correspondingly, in

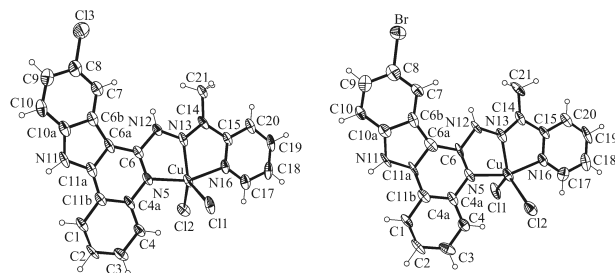


Figure 2. ORTEP plot of the molecules of **3b** (left) and **4b** (right) with thermal ellipsoids drawn at the 50% probability level. Selected bond distances (Å) and bond angles (deg) in **3b**: Cu–Cl1 2.4304(18), Cu–Cl2 2.3045(19), Cu–N5 2.027(5), Cu–N13 1.974(6), Cu–N16 2.023(5) Å, N5–Cu–N16 157.7(2), N13–Cu–Cl2 133.86(16)°; in **4b**: Cu–Cl1 2.439(3), Cu–Cl2 2.309(3), Cu–N5 2.021(8), Cu–N13 1.988(9), Cu–N16 2.019(8) Å, N5–Cu–N16 158.5(4), N13–Cu–Cl2 134.2(2)°.

the asymmetric unit. The molecules **3b** partake in intermolecular hydrogen bonding interactions of the type N11–H...Cl1ⁱ [N11...Cl1ⁱ 3.180 Å], where *i* denotes a symmetry code $-x, y + 0.5, -z + 0.5$ for generating equivalent atom positions. In addition, a hydrogen bond between the molecule of **3b** and one of the neighboring dimethylformamide molecules N12–H...O1ⁱ [N12...O1ⁱ 2.760 Å] is evident in the crystal structure (Supporting Information, Figure S3). The pattern of hydrogen bonding interactions in the crystal structure of **4b**·2.4DMF is similar.

HL^{3b} and **HL^{4b}** act as neutral tridentate ligands in **3b** and **4b**, respectively, coordinating to copper(II) via the quinoline nitrogen atom N5 [Cu–N5 = 2.027(5) (**3b**) and 2.021(8) Å (**4b**)], the hydrazine group nitrogen atom N13 [Cu–N13 = 1.974(6) (**3b**) and 1.988(9) Å (**4b**)], and the pyridine ring nitrogen atom N16 [Cu–N16 = 2.023(5) (**3b**) and 2.019(8) Å (**4b**)]. In contrast to paullone ligands, which have a folded conformation both in the metal-free and in the coordinated forms, the indoloquinolines **HL^{3b}** and **HL^{4b}** in **3b** and **4b** are essentially planar. The copper(II) center is five-coordinate, the remaining two coordinating sites being occupied by two chlorido ligands. The τ descriptor for **3b** and **4b**, expressed as the difference between the angles N5–Cu–N16 and N13–Cu–Cl2 [157.7(2) and 133.86(16)° (**3b**), and 158.5(4) and 134.2(2)° (**4b**)] divided by 60°, gives the same value for both complexes (0.40), which is between that for a trigonal bipyramid (1) and that for a square pyramid (0), and close to 0.52 found in [Ga(L^{6b})Cl₂].⁴³ Furthermore, the interatomic bond distance Cu–Cl2 is significantly longer in complexes **3b** [Cu–Cl2 = 2.3045(19) Å] and **4b** [Cu–Cl2 = 2.309(3) Å] with indoloquinoline ligands than in complexes **5b** [Cu–Cl2 = 2.2461(5) Å] and [Cu(HL^{6a})Cl₂]¹⁸ [Cu–Cl2 = 2.2411(8) Å] with paullone ligands.

The results of X-ray diffraction studies of the ligand **HL^{5b}** and complex **5b**·0.5CH₃OH are shown in Figure 3, and selected bond lengths and bond angles are given in the caption. Both the ligand and the complex crystallized in the monoclinic space group *P*2₁/*c*.

Formation of a centrosymmetric dimer is due to a bifurcated hydrogen bonding interaction between N12 as a proton donor and atoms N17ⁱ and N14ⁱ as proton acceptors [N12–H 0.880, H...N17ⁱ 2.079, N12...N17ⁱ 2.881 Å, N12–H...N17ⁱ 151.1°; H...N14ⁱ 2.633,

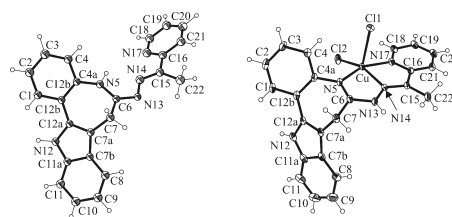


Figure 3. ORTEP plots of metal-free ligand molecule **HL^{5b}** and its copper(II) complex in **5**·0.5CH₃OH. Selected bond distances (Å) and bond angles (deg) in **HL^{5b}**: C4a–N5 1.417(3), N5–C6 1.359(3), C6–N13 1.329(3), N13–N14 1.382(3), N14–C15 1.297(3); in **5b**: Cu–Cl1 2.4681(5), Cu–Cl2 2.2461(5), Cu–N5 2.0220(15), Cu–N14 1.9787(15), Cu–N17 2.0466(15), N5–Cu–N14 78.94(6), N14–Cu–N17 78.18(6), N5–Cu–N17 156.85(6), N14–Cu–Cl2 153.96(5), N14–Cu–Cl1 98.79(4).

N12...N14ⁱ 3.356 Å, N12–H...N14ⁱ 151.1°]; *i* denotes a symmetry code $-x + 1, -y, -z + 2$ for generating equivalent atom positions (Supporting Information, Figure S5). In addition, a hydrogen bond between N5 and N12ⁱ [N5–H 0.880, H...N12ⁱ 2.528, N5...N12ⁱ 3.335 Å, N5–H...N12ⁱ 152.78°] is evident in the crystal structure of **HL^{5b}**.

The distribution of electron density over the fragment N5–C6–N13 [N5–C6 1.359(3), C6–N13 1.329(3) Å] indicates the presence of an exocyclic amidine double bond. As expected, the conformation of the metal-free ligand **HL^{5b}** is very similar to that of the 9-bromo-derivative.⁴⁴ The indolobenzazepine backbone in both **HL^{5b}** and **5b** mainly consists of sp²-hybridized carbon and nitrogen atoms. The only exception is the methylene group carbon atom in the seven-membered azepine ring, which is sp³-hybridized. This atom disrupts the conjugation of the π system, and as a result the ligand as a whole is non-planar.

Intermolecular hydrogen bonding interaction between molecules of **5b**, namely, N12–H...Cl2ⁱ [N12–H 0.880, H...Cl2ⁱ 2.612, N12...Cl2ⁱ 3.338 Å, N12–H...Cl2ⁱ 140.56°], are responsible for their association in a dimer (*i* denotes the symmetry code $-x + 1, -y + 2, -z + 1$) (Supporting Information, Figure S6). An interdimeric hydrogen bond N13–H...Cl1ⁱⁱ (*ii* $-x + 2, y - 0.5, -z + 1.5$)

(44) Addison, A. W.; Rao, T. N.; Reedijk, J.; van Rijn, J.; Verschoor, G. C. *J. Chem. Soc., Dalton Trans.* **1984**, 1349–1356.

Article

[N13–H 0.880, H···C11ⁱⁱ 2.383, N13···C11ⁱⁱ 3.149 Å, N13–H···C11ⁱⁱ 145.67°] is evident in the crystal structure as well.

In the complex **HL**^{5b} acts as a neutral tridentate ligand coordinating to copper(II) through the azepine ring nitrogen atom N5 [Cu–N5 = 2.022(15) Å], hydrazine nitrogen atom N14 [Cu–N14 = 1.9787(15) Å], and pyridine nitrogen atom N17 [Cu–N17 = 2.0466(15) Å]. The copper(II) atom is five-coordinate, the remaining binding sites being occupied by two chlorido ligands [Cu–Cl1 = 2.4681(5) Å; Cu–Cl2 = 2.2461(5) Å]. The τ descriptor for five-coordinate complexes, expressed as the difference between the angles N5–Cu–N17, 156.85(6)°, and Cl2–Cu–N14, 153.96(5)°, divided by 60, gives a value of 0.05, which is very close to the ideal one for a square pyramid (0).⁴⁴ A similar value (0.10) was reported for a closely related complex [Cu(**HL**^{6a})Cl₂].¹⁸ It is noteworthy that the interatomic bond distances Cu–N5 and Cu–N17 in **5b** are significantly shorter than in [Cu(**HL**^{6a})Cl₂],¹⁸ whereas both Cu–Cl bonds in **5b** are longer.

The conformation of the coordinated ligand **HL**^{5b} in **5b** differs slightly from that adopted by the metal-free ligand (Figure 3). The angle of 74.34(4)° between the mean plane of the indole moiety and the pyridine ring in **5** is very close to that reported for [Cu(**HL**^{6a})Cl₂] (78.6°).¹⁸ The bond distances N5–C6 = 1.359(3), C6–N13 = 1.329(3) and N13–N14 = 1.382(3) Å in **HL**^{5b} are altered by the coordination to copper(II). Whereas the N5–C6 and N13–N14 bonds are shorter in **5b** [1.298(2) Å and 1.358(2) Å, correspondingly], the bond C6–N13 = 1.362(2) Å is longer, indicating the configurational change from an exocyclic C⁶=N¹³ double bond in **HL**^{5b} to an endocyclic N⁵=C⁶ double bond in complex **5b**.

Stability Studies. The kinetic stability of complexes **1a**, **1b**, **4a**, **4b**, and **5b** in aqueous solution with a dimethyl-sulfoxide content of 1% v/v was studied by UV–vis spectroscopy over 24 h. Coordination of the corresponding ligands to copper(II) via the pyridine nitrogen atom, the hydrazine nitrogen, and the pyridine ring or azepine ring nitrogen atom alters significantly the conjugated π systems of the yellow-colored ligands **HL**^{1a}, **HL**^{1b}, **HL**^{4a}, **HL**^{4b}, and **HL**^{5b}, resulting in significantly different electronic absorption spectra. As a result, solutions of **1a**, **1b**, **4a**, **4b**, and **5b** show significant absorption in the visible region, namely, a broad charge-transfer band with a maximum at 461, 453, 461, 456, and 422 nm, respectively (Supporting Information, Figures S7–S9). A small decrease in absorption (ca. 5%) was observed for **1a**, **1b**, and **5b** over the first 4 h, with no further changes over the next 20 h, indicating that the coordination sphere of copper(II) remained intact. These results are in accord with those reported previously for complexes [Cu(**HL**^{6a})Cl₂] and [Cu(**HL**^{6b})Cl₂].¹⁸ For complexes **4a** and **4b** the decrease in absorption over the first 4 h is slightly higher (ca. 7%), with no further changes over the next 20 h.

Cytotoxicity in Cancer Cells. The cytotoxicity of the copper(II) complexes was determined by means of a colorimetric microculture assay (MTT) in three human cancer cell lines (A549, CH1, SW480), yielding IC₅₀ values in the 10^{–8} to 10^{–6} M range (Table 2). Note that the IC₅₀ values for cisplatin, carboplatin, and oxaliplatin in SW480 cells are at 4.5 ± 1.7, 61 ± 10, and 0.30 ±

Inorganic Chemistry, Vol. 49, No. 23, 2010 11093

Table 2. Cytotoxicity of Copper(II) Complexes with Indoloquinoline- (**1a–4b**) or Paullone-Based (**5b**, **6a**, **6b**) Ligands in Three Human Cancer Cell Lines

compound	IC ₅₀ (μM), 96 h ^a		
	A549	SW480	CH1
1a	1.72 ± 0.03	1.3 ± 0.1	0.40 ± 0.07
1b	0.18 ± 0.04	0.024 ± 0.001	0.030 ± 0.005
2a	1.7 ± 0.1	0.75 ± 0.04	0.33 ± 0.07
2b	0.14 ± 0.01	0.024 ± 0.002	0.026 ± 0.006
3a	1.4 ± 0.3	0.64 ± 0.11	0.41 ± 0.05
3b	0.23 ± 0.01	0.049 ± 0.003	0.065 ± 0.012
4a	1.6 ± 0.1	0.47 ± 0.03	0.36 ± 0.03
4b	0.20 ± 0.03	0.032 ± 0.004	0.052 ± 0.008
5b	0.67 ± 0.15	0.21 ± 0.04	0.064 ± 0.015
6a	1.28 ± 0.03	0.40 ± 0.04	0.28 ± 0.03
6b	0.43 ± 0.03	0.18 ± 0.02	0.080 ± 0.005

^a 50% inhibitory concentrations (means ± standard deviation from at least three independent experiments), as obtained by the MTT assay using exposure times of 96 h.

0.08 μM.⁴⁵ A549, a generally more chemoresistant cell line, is the least sensitive to all the tested compounds, whereas IC₅₀ values in CH1 and SW480 cells are up to ten and seven times lower, respectively. The corresponding uncomplexed ligands could not be tested because of insufficient solubility in biocompatible media.

Comparison of the copper(II) complexes reveals the following structure–activity relationships: methyl (**2a**), chloro (**3a**), or bromo (**4a**) substitution at position 8 has nearly no impact on cytotoxicity compared to **1a** lacking a substituent in this position. In contrast, a methyl group in position 14 results in a dramatic enhancement of cytotoxicity, with about 10 times lower IC₅₀ values in A549 and CH1 and about 50 times lower IC₅₀ values in SW480 cells in the case of compound **1b** (Figure 4A–C). Likewise, IC₅₀ values of **2b**, **3b**, and **4b** are 1 order of magnitude lower than those of the analogues **2a**, **3a**, and **4a**, confirming the impact of this methyl substitution as well as the irrelevance of electron-releasing or electron-withdrawing substituents at position 8.

For comparison, complexes with paullone ligands (**5b**, **6a**, **6b**) closely related to the indoloquinoline complexes **1b**, **4a**, and **4b**, but containing a folded seven-membered azepine ring instead of a flat six-membered pyridine ring were also tested. In contrast to a previously reported comparison of indoloquinoline versus paullone complexes of ruthenium(II) and osmium(II) that yielded differences of mostly 1 order of magnitude,¹⁹ differences in cytotoxicity are much less pronounced for the copper(II) complexes reported here. Only in SW480 cells, comparison of **4b** with **6b** and **1b** with **5b** (all bearing a methyl group in position 14 (**1b**, **4b**) or 15 (**5b**, **6b**)) reveals 6 and 9 times higher cytotoxicity of the indoloquinoline complex, respectively (Figure 4D–F), whereas **4a** and **6a** (lacking a substituent in position 14 and 15, correspondingly) are comparably cytotoxic in all three cell lines. A possible reason can be the increased reactivity of the azomethine carbon atom C¹⁴ in **4a** and the conversion of this complex into other species, similar to [Cu(L⁸)₂Cl₂], which may behave similar to **6a**. The reason for the

(45) Mendoza-Ferri, M.-G.; Hartinger, C. G.; Eichinger, R. E.; Stolyarova, N.; Severin, K.; Jakupec, M. A.; Nazarov, A. A.; Keppler, B. K. *Organometallics* **2008**, *27*, 2405–2407.

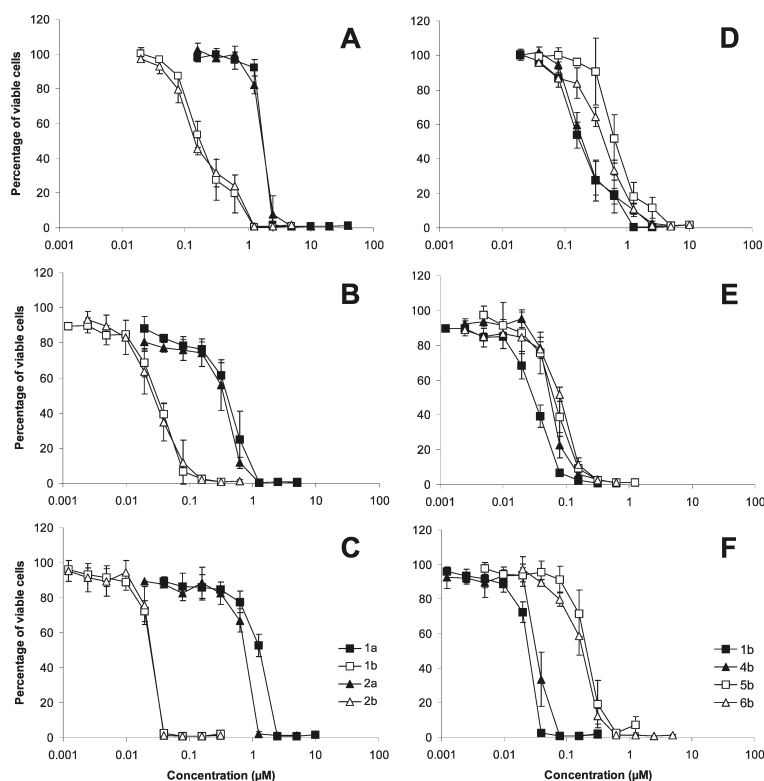


Figure 4. Concentration-effect curves of complexes **1a**, **1b**, **2a**, and **2b** in the human cancer cell lines A549 (A), CH1 (B), SW480 (C), indicating the different impact of methyl substitution depending on the position; and concentration-effect curves of complexes **1b** and **4b** in comparison with the corresponding paullone ligands **5b** and **6b** in the human cancer cell lines A549 (D), CH1 (E), SW480 (F), all determined by the MTT assay using continuous exposure for 96 h.

generally smaller differences as well as the generally higher cytotoxicity of the copper(II) complexes may either be related to the different central metal or to the different metal-binding sites in the ligands and the consequences of coordination to the metal or a combination of both. Comparisons with the uncomplexed ligands were not possible for lack of solubility, but even if the role of the metal for biological activity remains yet unclear, it should be emphasized that metal complexation renders these compounds applicable for biological testing in solution.

Final Remarks

The reported results establish synthetic access to a new class of highly cytotoxic copper(II) complexes. Complexation of copper(II) chloride with potentially tridentate indolo[3,2-*c*]quinolines and indolo[3,2-*d*]benzazepines modified at the lactam function resulted in five-coordinate copper(II) complexes, which practically remain intact in aqueous solution containing 1% DMSO over 24 h. The complexes show

remarkably high antiproliferative activities in human cancer cell lines with IC₅₀ values in the 10⁻⁸ to 10⁻⁶ M concentration range. The effect of copper(II) on cytotoxicity could not be elucidated because of the very low solubility of the metal-free ligands in biocompatible media. Binding to copper(II) improved the solubility of the resulted complexes, enabling them to be tested as potential antitumor agents. The use of 2-acetylpyridine instead of 2-formylpyridine for the synthesis of tridentate indoloquinoline Schiff-bases results in a huge enhancement of cytotoxicity by a factor of 10 to 50. The presence of an electron-releasing group (methyl), or electron-withdrawing substituents (Cl, Br) compared to H in position 8 of the indoloquinoline backbone does not have any effect on cytotoxicity of the corresponding copper(II) complexes. The effect of substitution of the seven-membered azepine ring in copper(II) complexes with modified paullones by a flat six-membered pyridine ring is clearly seen upon comparing the antiproliferative activities of complexes **5b** and **6b** with those of compounds **1b** and **4b**, correspondingly, in SW480 cells, revealing a six- to nine-fold decrease of

Article

IC₅₀ values. Further experiments are in progress to shed light onto the mechanism of action of these compounds, including their DNA-intercalating and DNA-breaking potencies. The ability of copper(II) complexes to cut DNA is well-documented in the literature.^{46–50}

(46) Tan, J.; Wang, B.; Zhu, L. *J. Biol. Inorg. Chem.* **2009**, *14*, 727–739.

(47) Galaris, D.; Evangelou, A. *Crit. Rev. Oncol. Hematol.* **2002**, *42*, 93–103.

(48) Kennedy, L. J.; Moore, K., Jr.; Caulfield, J. L.; Tannenbaum, S. R.; Dedon, P. C. *Chem. Res. Toxicol.* **1997**, *10*, 386–392.

(49) Lloyd, D. R.; Carmichael, P. L.; Phillips, D. H. *Chem. Res. Toxicol.* **1998**, *11*, 420–427.

(50) Barbosa, L. F.; Garcia, C. C. M.; Di Mascio, P.; Gennari de Medeiros, M. H. *Dalton. Trans.* **2009**, *8*, 1450–1459.

Inorganic Chemistry, Vol. 49, No. 23, 2010 11095

Acknowledgment. We would like to thank Mrs. Aliona Luganschi and Mr. Anatolie Dobrov for recording ESI-MS spectra, Prof. Dr. Markus Galanski for collecting NMR data, and Prof. Dr. Peter Lieberzeit for providing the Perkin-Elmer 12 UV–vis spectrophotometer. This work was financially supported by the University of Vienna within the doctoral program, “Initiativkolleg Functional Molecules” (IK 1041–N).

Supporting Information Available: Further details are given in Figures S1–S10 and Table S1, and crystallographic data is given in CIF format. This material is available free of charge via the Internet at <http://pubs.acs.org>.

Simone Göschl

PERSONAL DATA

Date of Birth	September 17 th , 1986
Place of Birth	Klagenfurt
Nationality	Austrian
Place of Living	Vienna
Mail	simone.goeschl@univie.ac.at

WORK EXPERIENCE

since 2010	University of Vienna , Institute of Inorganic Chemistry, Research Associate, Cell biology laboratory Diploma Thesis: „Cellular effects of indoloquinoline complexes and related compounds in human tumor cell lines”
July-August 2008	Donau Chemie AG - Internship
July-August 2007	Donau Chemie AG - Internship
July-August 2006	Landeskrankenhaus Klagenfurt - Internship

EDUCATION

2005-present	Study of Chemistry , University of Vienna
1997-2005	Grammar school , BG/BRG Mössingerstraße, Klagenfurt <i>A-level exam with honors</i> - main subjects: Math, English, German, Chemistry, Physics, Biology, Latin

PERSONAL SKILLS AND COMPETENCES

Language skills

German	native language
English	fluently
Italian	basic knowledge
Japanese	basic knowledge

Computer skills and competences

Good command of Microsoft Office™ tools (Word™, Excel™ and PowerPoint™)
LateX and Adobe Photoshop (beginner)

Social engagement

since 1993	Guide of the Association of Boy Scouts and Girl Guides of Austria
since 2006	Austrian scout leader training
2007-2010	Chair Woman of the Austrian Scout Youth Council
since 2010	International Commissioner of the Carinthian District

HONORS AND AWARDS

2003	3rd place of Austrian Federal Competition in Chemistry (carinthian district)
2003	3rd place of Biology Olympiade (carinthian district)
2004	1st place of Biology Olympiade (carinthian district)
2005	2nd place of Austrian Federal Competition in Chemistry (carinthian district)
2005	Participant of Austrian Federal Competition in Chemistry (Austria)
2005	1st place of Biology Olympiade (carinthian district)

PUBLICATIONS**Structure-Activity Relationships of Highly Cytotoxic Copper(II) Complexes with Modified Indolo[3,2-c]quinoline Ligands**

M. Primik, S. Göschl, M. A. Jakupec, A. Roller, B. K. Keppler, V. B. Arion

Inorganic Chemistry, vol. 49, No. 23, pp. 11084-95, 2010

POSTER PRESENTATIONS**Structure-Activity Relationships of Highly Cytotoxic Copper(II) Complexes with Modified Indolo[3,2-c]quinoline Ligands**

M. Primik, S. Göschl, M. A. Jakupec, A. Roller, B. K. Keppler, V. B. Arion, 15th International Conference on Biological Inorganic Chemistry, Vancouver, CAN, Aug. 7th-12th, 2011

Structure-Activity Relationships of Highly Cytotoxic Copper(II) Complexes with Modified Indolo[3,2-c]benzazepines and Indolo[3,2-c]quinoline Ligands

M. Primik, S. Göschl, M. A. Jakupec, A. Roller, B. K. Keppler, V. B. Arion 14. Österreichische Chemietage, Linz, AUT, Sept. 24.-26., 2011